SPHEROID-ENRICHED CANCER STEM-LIKE CELLS AS A MODEL FOR TARGETED THERAPY IN ORAL CANCER WITH DISTAL 11Q LOSS

by

Hatem Osama Kaseb

MBBCh, Faculty of Medicine, Cairo University, Egypt, 2003

MSc, Clinical & Chemical Pathology, Faculty of Medicine, Cairo University, Egypt, 2009

Submitted to the Graduate Faculty of

the Graduate School of Public Health in partial fulfillment

of the requirements for the degree of

Doctor of Philosophy

University of Pittsburgh

2016

UNIVERSITY OF PITTSBURGH

GRADUATE SCHOOL OF PUBLIC HEALTH

This dissertation was presented

by

Hatem Osama Kaseb

It was defended on

30th June, 2015

and approved by

Zsolt Urban, PhD
Associate Professor, Department of Human Genetics
Graduate School of Public Health, University of Pittsburgh

Eric Lagasse, PharmD, PhD
Associate Professor, Department of Pathology
Director of the Cancer Stem Cell Center at the McGowan Institute
School of Medicine, University of Pittsburgh

Rahul Parikh, MD, PhD
Assistant Professor, Division of Hematology/Oncology, Department of Medicine
School of Medicine, University of Pittsburgh

Dissertation Advisor
Susanne M. Gollin, PhD
Professor, Department of Human Genetics
Graduate School of Public Health, University of Pittsburgh

Susanne M. Gollin, PhD

SPHEROID-ENRICHED CANCER STEM-LIKE CELLS AS A MODEL FOR TARGETED THERAPY IN ORAL CANCER WITH DISTAL 11Q LOSS

Hatem O. Kaseb, PhD

University of Pittsburgh, 2016

ABSTRACT

Oral squamous cell carcinoma (OSCC) has a poor prognosis due to multiple factors including local recurrence, distant metastasis and therapeutic resistance. Our laboratory has demonstrated that the ATR-CHEK1 pathway is a critical modulator of radioresistance in OSCC; we evaluated the effectiveness of targeted CHEK1 inhibition in OSCC cancer stem-like cells (CSLC). To this end, we analyzed CSLC properties and the effect of ionizing radiation (IR) and CHEK1 inhibition on CSLCs isolated from OSCC (parental) cell lines with and without distal 11q loss. The CSLCs, propagated in enriched serum-free medium, demonstrated stem-cell like characteristics including asymmetrical and symmetrical cell division, self-renewal, re-differentiation, colony forming capacity at extreme (limiting) dilutions, and radioresistance.

CHEK1 inhibitors affected the functional CSLC properties, resulting in significant reduction in proliferation, survival, colony initiation, growth, migration. The most drastically affected CSLC property was extracellular matrix migration. As determined by dose-response curves, a drug level ≈100-fold higher than the dose that was effective on parental OSCC cell lines was required to inhibit CSLC migration.

Overall, our results suggest that distal 11q loss may predict radioresistance in CSLC; however, the CSLC response to IR-CHEK1 inhibition is not distal 11q loss-driven. CHEK1 inhibitors increase the radiosensitivity of oral CSLC as they do for OSCC cell lines. Thus, we

propose that CHEK1 inhibition may be a useful adjuvant therapy for advanced and/or metastatic OSCC.

PUBLIC HEALTH SIGNIFICANCE: Our results increased the understanding of cancer stem-like cells in oral cancers and establish these cells as a contributing factor to radioresistance that could be potentially reversed in as many as 25% of cancers by CHEK1 inhibitors.

TABLE OF CONTENTS

LIST OF TABLES

LIST OF FIGURES

ACKNOWLEDGMENT

I am extremely grateful to my advisor, Dr. Susanne M. Gollin for providing me the opportunity to work in her laboratory and for instilling in me the qualities of a good researcher and mentor. I would also like to thank all agencies that funded the project, including the Fulbright Foundation, the Egyptian Ministry for High Education and the Joan G. Gaines Cancer Research Fund at the University of Pittsburgh.

I thank the members of my thesis committee, Drs. Zsolt Urban, Eric Lagasse and Rahul Parikh for their guidance and taking time to answer my questions in spite of their busy schedules. I greatly appreciate the guidance and precious advice from Dr. Eric Lagasse that included experimental design recommendation such as extreme limiting dilution and antibody selection, such as CD133/1, in addition to providing cancer stem cell cells isolated from primary tumors. I greatly appreciate the advice from Dr. Zsolt Urban concerning the double staining experiments and the cluster plotting/analysis of cancer stem-like cell division. Furthermore, I also would like to thank Dr. William Saunders for advice on the cell division experiments and for sharing some cell division antibodies. I would also like to thank Mr. Dale Lewis, who helped train me in experimental design, cell culture techniques and FISH; Mr Dale Lewis also did the CSLC CIN experiments. I would also like to thank the past and present members of the Gollin laboratory for making my experience extremely rewarding. I am grateful for the assistance of, Dr. Paolo Piazza for helping with the flow-cytometry experiments; Dr. Khaled Hemada, research fellow in Mayo

Clinic, Rochester, MI for his statistical advice and for analyzing the survival data; Laura McLean for helping with the phase imaging capturing; Megan Bresky, MSc Student and Samuel Wilshire, undergraduate student who worked at some time points on the project, Imgenex corporation for providing cancer stem cell antibodies, Miltenyi Corporation for providing the new CD133/1 viobright.

I would finally like to dedicate this work to my wife Tammy Novotne, family and friends for supporting and believing in me. Lastly, I would especially like to dedicate the current work to my past mentors, the late Dr Soheir Abdel-latif, Professor of Microbiology, NCI, Cairo University; Dr Amira Khorshid, Professor of Hematology, NCI, Cairo University and Dr Tarek Mansour, Professor of Immunology and Vice Director of Children Cancer Hospital (57357).

1.0 INTRODUCTION

1.1 OVERVIEW

Cancer is the second leading cause of death in the United States of America (USA) despite the major improvements in the management of this disease. Resistance to conventional therapy is a significant cause of recurrence and mortality in cancer patients. Cancer is a very complex disease, with different clinical presentations, molecular types, grades and staging all affecting treatment and overall survival (OS). Cancer has been shown to be driven by genetic defects that accumulate over time. One of the approaches that can be utilized to determine the most effective therapy for a particular cancer is genetic profiling to identify the best treatment for that cancer based on comparative diagnostic biomarkers. Studies have shown that cancer stem-like cells (CSLC) are playing an important role in the therapeutic resistance in many tumors. Our groups' previous studies have shown that a novel biomarker, the loss of distal chromosome 11q is associated with decreased sensitivity to radiation therapy (radioresistance) and better response to combined IR and targeted CHEK1 inhibitors. Understanding the role of distal 11q loss in CSLC is a good first step towards understanding the association between biomarkers and therapeutic resistance.

Molecular biomarkers aid in better selecting the right patients for certain therapeutic interventions, thereby leading to better management of the disease in this population. Molecular

biomarkers also open the door for the era of personalized therapy, in which the right drugs are given to the right patients. For example, a patient whose CSLCs have distal 11q loss may have a poor response to radiation therapy, but may have a favorable response to a combination of conventional radiation therapy and ATR-CHEK1 pathway small molecule inhibitor therapy. In conclusion, supplementing conventional therapy with a targeted inhibitor is expected to improve survival in patient subpopulations. Overall, the expected public health significance of molecular biomarkers and targeted approaches is expected to be substantial.

1.2 EPIDEMIOLOGY OF ORAL SQUAMOUS CELL CARCINOMA

Solid tumors in general and epithelial tumors in particular show clinical, pathological, phenotypical and biological heterogeneity, making the efficient treatment of such tumors difficult (Chen, et al. 2011b). Head and neck squamous cell carcinoma (HNSCC) is an epithelial tumor that is caused by multiple genetic alterations, chronic inflammation, and environmental factors (Gollin 2014) Major risk factors for HNSCC include tobacco smoking, alcohol consumption and HPV infection (Gollin 2014; Leemans, et al. 2011).

HNSCC comprises approximately about 80% of the head and neck cancers seen in patients (Figure 1) (SEER 2015). HNSCC is recognized as the seventh most prevalent cancer worldwide (Gollin 2014). More than 60% of the head and neck cancers are classified as OSCC (Oral Squamous cell Carcinoma) (Siegel, et al. 2014; Siegel, et al. 2015). The estimated number of new cases of OSCC in the US in 2015 is more than 45,000 and the estimated deaths are more than 8,000 (Siegel, et al. 2015). OSCC is currently the eighth most common cancer in males in the USA, having a higher incidence than leukemia and liver tumors (Siegel, et al. 2015). OSCC

can affect any region of the oral cavity, which includes the lining of the cheeks, salivary glands, hard palate, retromolar trigone, floor of mouth, gums and tongue. Prognosis remains poor, with approximately 60% 5-year overall survival (OS) rate (Figure 1) (SEER 2015). This low survival rate is due to a number of factors such as local recurrence, distant metastasis and therapeutic resistance (Figure 1) (Prince, et al. 2007).

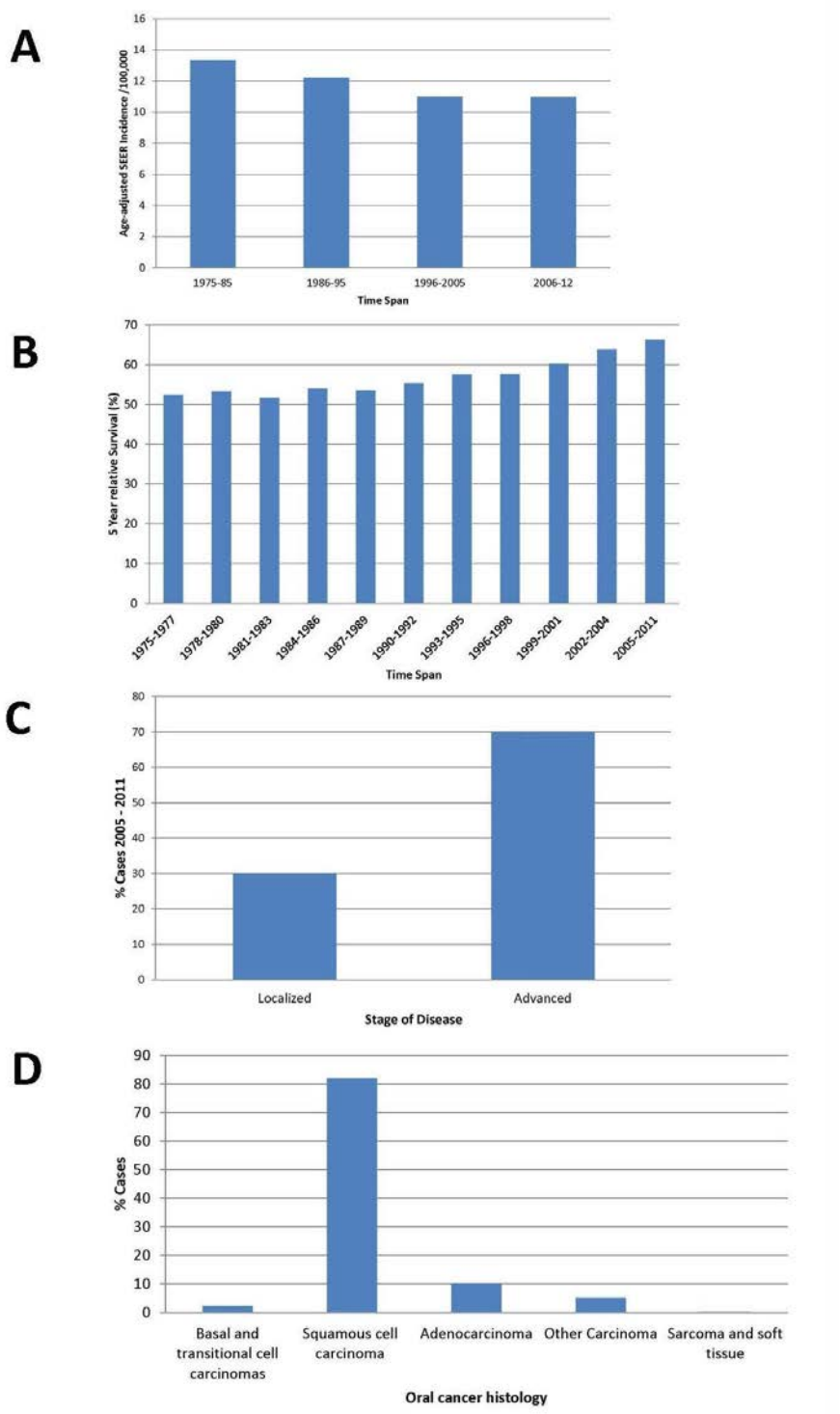

Figure 1. Epidemiological assessment of oral cancer in the US based on SEER data (SEER 2015)

A. Age-adjusted SEER incidence rates per 100,000; age-adjusted to the 2000 US standard population. Data extracted from SEER 9 areas (San Francisco, Connecticut, Detroit, Hawaii, Iowa, New Mexico, Seattle, Utah, and Atlanta).
B. 5-Year relative survival (%) by year of diagnosis. Data extracted from SEER 9 areas (San Francisco, Connecticut, Detroit, Hawaii, Iowa, New Mexico, Seattle, Utah, Atlanta).
C. Disease classification (%) 2005-2011. Data extracted from SEER 18 areas (San Francisco, Connecticut, Detroit, Hawaii, Iowa, New Mexico, Seattle, Utah, Atlanta, San Jose-Monterey, Los Angeles, Alaska Native Registry, Rural Georgia, California excluding SF/SJM/LA, Kentucky, Louisiana, New Jersey and Georgia excluding ATL/RG). Based on follow-up of patients into 2012.
D. Percent distribution histology among histologically confirmed cases, 2008-2012. Data extracted from SEER 18 areas (San Francisco, Connecticut, Detroit, Hawaii, Iowa, New Mexico, Seattle, Utah, Atlanta, San Jose-Monterey, Los Angeles, Alaska Native Registry, Rural Georgia, California excluding SF/SJM/LA, Kentucky, Louisiana, New Jersey and Georgia excluding ATL/RG).

1.3 CHARACTERISTICS OF ORAL CANCER STEM-LIKE CELLS

1.3.1 CSLC Hypothesis

The CSLC hypothesis suggests that a subpopulation of the cells in the tumor possess the potential to self-renew and generate the entire heterogeneous tumor bulk in a unique pattern (Clarke, et al. 2006; Harper, et al. 2007; Prince, et al. 2007) (Figures 2-4). There are two models that explain how CSLC recapitulate the tumor. The first is the ‘stochastic model’ that entails that any cancer cell can acquire stemness properties through clonal evolution acquired through sequential mutations and copy number alterations and the second model is the ‘hierarchic model’, where the CSLC resides on the top of the cell hierarchy and divides symmetrically and asymmetrically in a similar pattern to other stem cells (SC), such as adult SCs (Figures 3, 4) (Odoux, et al. 2008). Many researchers believe that these two models are mutually exclusive, adding even more complexity to the understanding of the biology of these cells (Odoux, et al. 2008). The hierarchic CSLC model is better understood than the stochastic model, and has

gained much support in the past few years. According to the hierarchic CSLC model, CSLC possess the unique ability to divide both asymmetrically to generate differentiated cells and symmetrically to self-renew (Figure 2) (Harper, et al. 2007; Lathia, et al. 2011). The main aspect that remains unanswered concerning CSLCs is the exact origin of these cells. There are two possible explanations for how CSLCs originate, but none has gained compelling supportive evidence; the first being that CSLC form as a result of oncogenic mutations of normal tissue stem cells (Visvader 2011) and the second being that CSLC arise from non-CSLC that have acquired stemness properties (Blagosklonny 2007).

CSLCs were shown first in hematopoietic cancers (Bonnet and Dick 1997) and later in solid tumors, such as gliomas (Bao, et al. 2006; Uchida, et al. 2000), lung cancer (Wang, et al. 2013), hepatocellular carcinoma (Lingala, et al. 2010; Yin, et al. 2007), breast cancer (Al-Hajj, et al. 2003; Grimshaw, et al. 2008; Han and Crowe 2009; Ponti, et al. 2005), colon cancer (Odoux, et al. 2008; Ricci-Vitiani, et al. 2007), HNSCC (Prince, et al. 2007; Wilson, et al. 2013), prostate cancer (Li, et al. 2010; Sheng, et al. 2013; Su, et al. 2010), pancreatic cancer (Bunger, et al. 2012), melanoma (Monzani, et al. 2007), gastric cancer (Tian, et al. 2012), esophageal cancer (Zhao, et al. 2012), and sarcoma (Fujii, et al. 2009). The amount of evidence that supports the hierarchic CSLC model has increased significantly especially in the past few years. Different terminologies have been used to describe these cells, such as cancer stem cells, cancer initiating cells, functional tumor stem cells, tumor initiating cells and cancer stem-like cells (Baumann, et al. 2008).

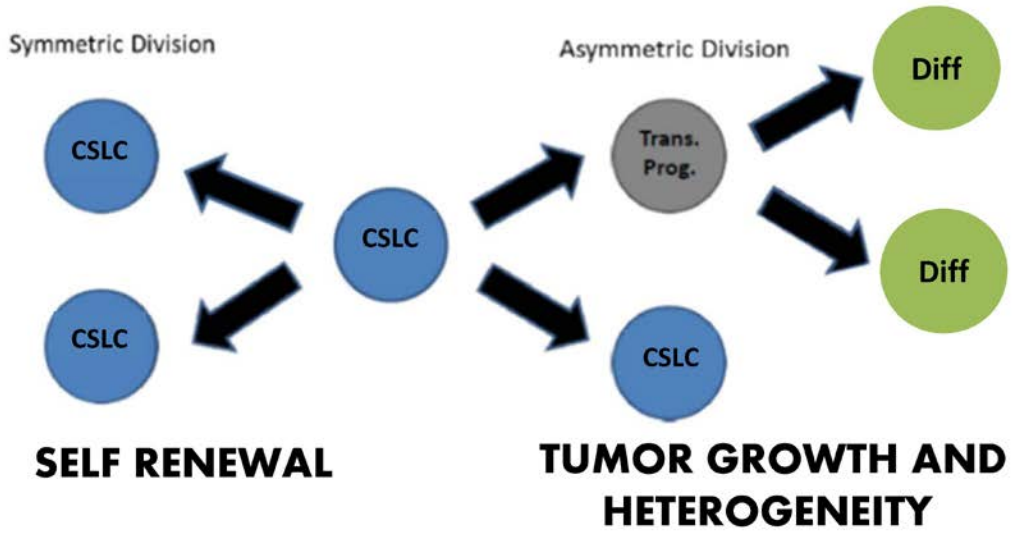

Figure 2. Division patterns of CSLCs and their significance

CSLCs are unique cells that can divide both symmetrically and asymmetrically. On the left, the CSLC (blue) divides symmetrically to produce two CSLC (blue). On the right, the CSLC divide asymmetrically to produce a CSLC (blue) and a transient progenitor (grey); the transient progenitor can divide to produce two differentiated progeny cells (green). (Abbreviations: CSLC, cancer stem-like cell; Trans. Prog., Transient progenitor; Diff, Differentiated progeny cells). Symmetrical division is related to the CSLC trait of "self renewal" and Asymmetrical division is related to the CSLC trait of "Tumor growth initiation and heterogeneity".

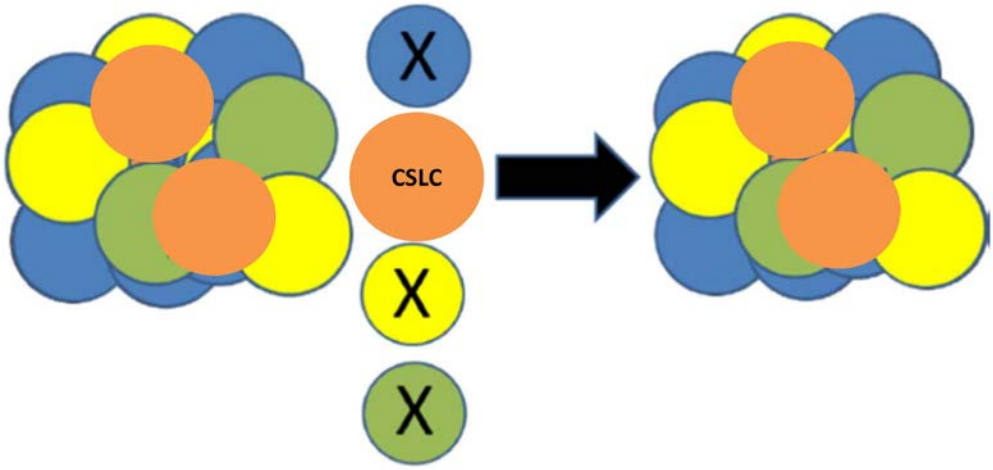

Figure 3. Cancer Stem Cell Hypothesis: Hierarchic Model

Tumors are clonally heterogeneous (left). Each cell can produce more cells of the same clone (yellow, blue and green), only the CSLC (orange) has the ability to divide both symmetrically and asymmetrically to produce the entire heterogeneous tumor pattern (right). The model is referred to as the "Hierarchic Model."

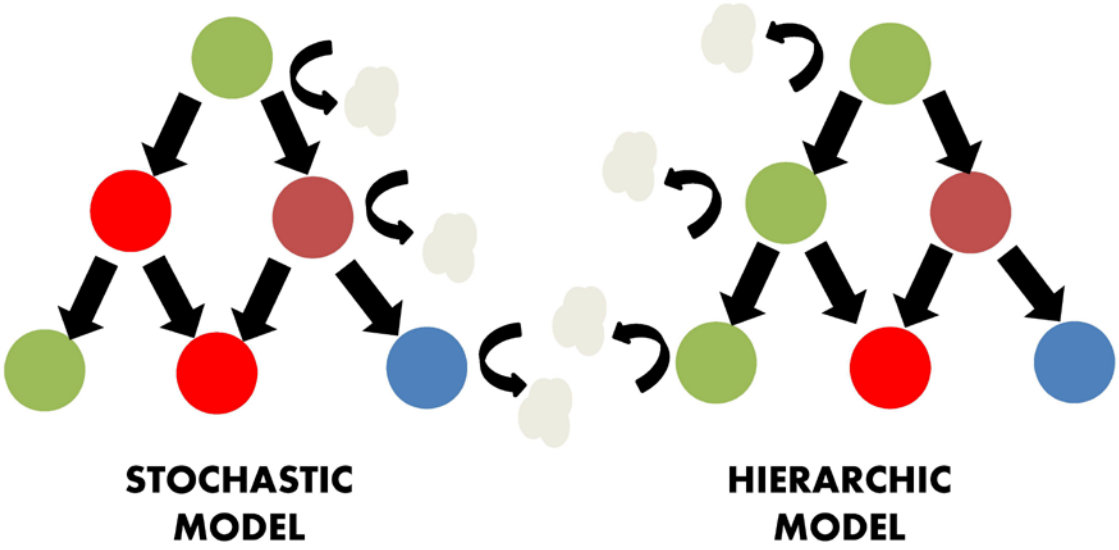

Figure 4. The two models of the CSLC hypothesis: the 'Hierarchic' and 'Stochastic' models

1.3.2 Basic properties of CSLCs

For a subpopulation to be defined as CSLC, it should show four main characteristics. Firstly, it should possess distinctive cell surface markers. Secondly, the homogenous CSLC population should be able to give rise to the phenotypically diverse original tumor. Thirdly, these CSLC should be able to generate tumors in immunodeficient mice from as few as 100-500 cells (Bhaijee, et al. 2012; Sheng, et al. 2013). Lastly, serial transplantation through multiple generations should be proven, thereby showing that these cells possess the ability to self-renew (Odoux, et al. 2008). The American Association for Cancer Research Workshop on Cancer Stem Cells considered successful quantitative orthotopic xerograft tumor transplantation as the most important characteristic proving CSLC (Clarke, et al. 2006). In addition, some researchers believe that selective resistance to radiation therapy and chemotherapy should also be shown. The CSLC – niche interaction regulates many of the properties of CSLC, and consists of both cellular (fibroblasts, endothelial cells) and non-cellular components, and is currently the most promising area of CSLC research.

The unique survival capacity of the CSLC subpopulation has been attributed to multiple factors, such as self-renewal (Tian, et al. 2012), the enhanced ability to remove drugs (Liu, et al. 2012), the ability to repair DNA damage (Bao, et al. 2006), overexpressed anti-apoptotic proteins, and the niche interaction (cellular-extracellular interaction) (Figure 5). The relative quiescence of CSLC is also an important factor that has been correlated to the therapeutic resistance of these cells (Tabor, et al. 2011), because CSLC can switch off their proliferative machinery during therapy, thereby leading to decreased chances of cellular damage. Thus, the CSLC model may explain the resistance patterns of many tumors to conventional therapies (Ponti, et al. 2005). The CSLC model may also explain tumor heterogeneity (Wang, et al. 2012).

Research has shown that as many as 30% of breast cancer patients show micrometastatic seeds in the bone marrow at the time of diagnosis, although fewer than half of these patients develop metastases (Al-Hajj, et al. 2003). The characteristics and associations of CSLC clearly show that these cells are clonal, either tumorigenic or non-tumorigenic; only when tumorigenic cells metastasize do tumors develop (Al-Hajj, et al. 2003). For any treatment regimen to be effective, it must be able to target this unique population of tumorigenic CSLC (Bao, et al. 2006; Damek-Poprawa, et al. 2011).

Studying the CSLC subpopulation within tumors was extremely difficult until the early 2000s (Al-Hajj, et al. 2003; Locke, et al. 2005; Prince, et al. 2007). Important factors that impeded CSLC research include the difficulty of isolation, the inability to propagate CSLC in culture, and the inability to control mechanisms underlying key properties, such as asymmetrical division (Locke, et al. 2005). However, the last few years have shown a dramatic change due to the development of efficient isolation and in vitro propagation techniques, such as spheroid enrichment and flow sorting for cell surface markers (Fujii, et al. 2009; Lim, et al. 2011; Tian, et al. 2012). One of the approaches that have been used to isolate CSLC is flow sorting to identify the side population (SP) cells. SP isolation depends on the characteristic property of CSLC of Hoechst dye effluxion by multi-drug-like transporters (Han and Crowe 2009; Wan, et al. 2010).

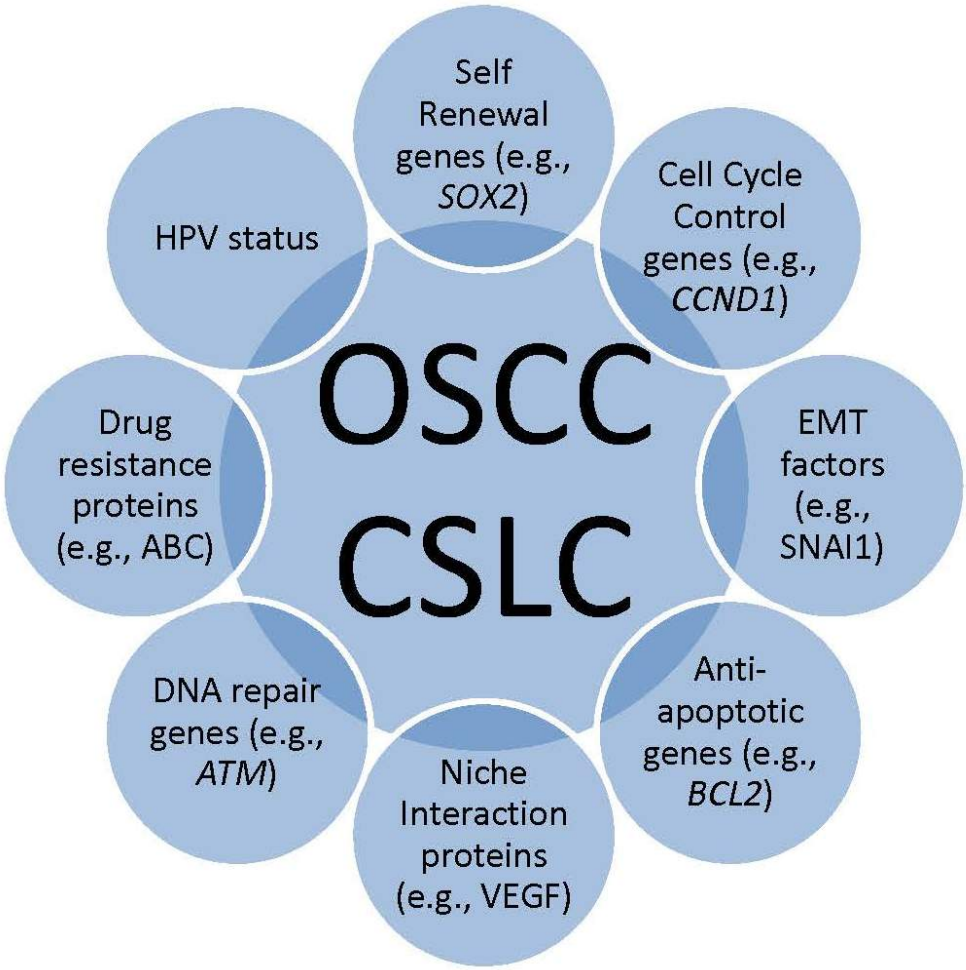

(Adapted from Sayed, et al. 2011).

Figure 5. Factors affecting CSLC survival

The survival capacity of the CSLC subpopulation has been attributed to multiple factors, such as self-renewal, the enhanced ability to remove drugs, the ability to repair DNA damage, overexpressed anti-apoptotic proteins and the niche interaction (cellular-extracellular interaction)(Abbreviations: OSCC CSLC, Oral squamous cell carcinoma cancer stem-like cell; EMT, Epithelial mesenchymal transition).

1.3.3 Isolation and identification of CSLC in HNSCC

Many markers have been used to identify CSLC in epithelial tumors. No single surface marker or method can has been shown to be optimum in regards to identifying CSLC in HNSCC.

However, a number of markers have been replicated by many research groups using CD133, CD44 and ALDH1 enzymatic activity (Table 1). CD44 has been the most controversial of the markers used, CD133 has been shown to be less controversial and ALDH1 is the most promising and the least controversial of the markers used to date (Table 1).

When using patient samples to isolate CSLC it is crucial to eliminate non-epithelial lineage cells, such as normal leukocytes, fibroblasts, endothelial, and mesothelial cells from the tumor specimens using cell surface markers such as CD2, CD3, CD10, CD16, CD18, CD31, CD64, and CD140b (Al-Hajj, et al. 2003; Prince, et al. 2007). The standardization of isolation techniques will certainly be a critical step that will enhance our ability to study this subpopulation. Some researchers recommend double-sorting when there is any suspicion of cell impurity and to confirm that the sorted cells represent CSLC (Prince, et al. 2007). Wilson et al. compared the most common isolation techniques, such as SP, ALDH1, and CD44 expression for HNSCC and concluded that CD44 was the most promising cell-sorting marker in HNSCC (Wilson, et al. 2013).

CD133 is a 120-kDa unique pentaspan membrane glycoprotein marker of CSLC and their early progenitor cells (Damek-Poprawa, et al. 2011; Tirino, et al. 2008). The role of CD133 seems unclear although some researchers believe that it plays a role in the organization of plasma membrane protrusions (Mizrak, et al. 2008). CD133 was one of the earliest markers used to isolate CSLC in hematological and neurological tumors (Fargeas, et al. 2003). It was also shown in hepatocellular carcinoma (Yin, et al. 2007), colon (Ricci-Vitiani, et al. 2007), prostate (Collins, et al. 2005), melanoma (Monzani, et al. 2007) and osteosarcoma (Tirino, et al. 2008). The pioneering work by Bao et al. on glioma tumor cells showed that CD133+ CSLC possess all the characteristics of CSLC (Bao, et al. 2006). The results confirmed that high expression of

CD133 is associated with higher risk of metastases in glioma (Bao, et al. 2006). These results encouraged some groups to use CD133 as a marker for identification and isolation of CSLC in HNSCC (Shrivastava, et al. 2015; Yu, et al. 2014). In laryngeal carcinoma, a subpopulation of around 5% of cells expressing CD133 was identified and analysis of this subpopulation confirmed that they possess CSLC properties (Wei, et al. 2014; Wei, et al. 2009). Chen et al. also successfully isolated CSLC from laryngeal cell line using CD133 and BMI1 (Chen, et al. 2011a). Zhang et al. found 2% - 3% CD133+ cells in a HNSCC cell lines and patient biopsies (Zhang, et al. 2010).

The most well-studied cell surface marker that was used in isolation and characterization of CSLC from HNSCC is CD44 (Harper, et al. 2007; Joshua, et al. 2012; Locke, et al. 2005; Mack and Gires 2008; Prince, et al. 2007; Wilson, et al. 2013). CD44 is a cell surface glycoprotein receptor for hyaluronic acid, encoded by a single gene on chromosome 11p13 (Sayed, et al. 2011). It is involved in aggregation, proliferation, adhesion, migration and metastasis of cancer cells (Rajarajan, et al. 2012; Trapasso and Allegra 2012). CD44 was first identified as a marker of CSLC in lung tumors utilizing immunohistochemistry (Penno, et al. 1994). CD44 has been used to identify and isolate CSLCs from many tumor types, such as breast tumors (Al-Hajj, et al. 2003; Kim, et al. 2012), prostate (Guo, et al. 2012; Sheng, et al. 2013), pancreatic (Bunger, et al. 2012), and head and neck carcinomas (Prince, et al. 2007; Wilson, et al. 2013). In a huge bioinformatics study, increased CD44 expression in HNSCC was found relative to many other tumor tissue types and also normal epithelial tissue (Rajarajan, et al. 2012). In HNSCC, different isoforms, CD44v3 and CD44v6 have also been seen to correlate with overall disease aggressiveness especially radioresistance and metastases (Trapasso and Allegra 2012). Prince et al. was the first to isolate a CSLC subpopulation from HNSCC

specimens using fluorescence-activated cell sorting (FACS) analysis using an antibody against CD44; further analysis showed that the CD44 positive cells highly co-expressed BMI1, another important marker of CSLC (Prince, et al. 2007). Harper et al. compared the expression of CD44, CD29, and CD133 as presumed markers of CSLCs in HNSCC tumors; and found that the CD44 expression showed the highest correlation with tumor clonogenicity (Harper, et al. 2007). Other investigators such as Locke et al. (Locke, et al. 2005), Okamoto et al. (Okamoto, et al. 2009), Wilson et al. (Wilson, et al. 2013) and Su et al. (Su, et al. 2011) used CD44 to isolate and characterize CSLC from HNSCC cell lines. Okamoto et al. focused on the chemoresistance characteristics of this subpopulation, and found that *ABCB1*, *ABCG2*, *CYP2C8*, and *TERT* chemoresistance genes were upregulated in the CD44+ subpopulation (Okamoto, et al. 2009). While Harper et al. focused on the morphological aspects, cell cycle and apoptotic resistance patterns of CSLC (Harper, et al. 2007). Harper et al. also showed that the CD44 CSLC subpopulation showed enhanced chemoresistance and longer G2 phase of the cell cycle (Harper, et al. 2010). Other researchers have shown that CD44+ CSLC were more resistant to paclitaxel (Wilson, et al. 2013), cisplatin and docetaxel treatment (Su, et al. 2011). Some studies showed conflicting results regarding the significance of CD44 expression in head and neck tumors (Joshua, et al. 2012; Mack and Gires 2008). Some researchers argue that CD44s is highly expressed in HNSCC cells, making it a less reliable marker for CSLC identification (Mack and Gires 2008; Wilson, et al. 2013). Furthermore, Oh et al. showed functionally that CD44- cells also possess CSLC properties (Oh, et al. 2013). Overall, these conflicting reports suggest that it would be better to investigate other markers and to use more than one marker for isolation and characterization of CSLC.

ALDH1 enzymatic activity has been used as a marker of CSLC in many tumors, such as breast cancer (Morimoto, et al. 2009). ALDH1 plays a role in early differentiation of stem cells by oxidizing retinol to retinoic acid (Croker, et al. 2009). In HNSCC, ALDH1 was shown to be a successful marker for CSLC by Chen et al. (Chen, et al. 2009) and Clay et al. (Clay, et al. 2010) because it consistently fulfills all the criteria of being rare, recapitulate the tumor heterogeneous structure and shows serial dilution xenotransplantation. Krishnamurthy et al. have shown that the combination of CD44 and ALDH1 expression selects CSLC in HNSCC efficiently using an orthotopic xenograft model (Krishnamurthy, et al. 2010). Based on these promising results, many researchers now use both CD44+ and ALDH1+ to identify the CSLC population (Kiang, et al. 2012).

BMI1 is a polycomb group transcription repressor that mediates gene silencing by regulating chromatin structure (Liu, et al. 2012). In murine SC, in vivo and in vitro functional studies have demonstrated that Bmi-1 is essential for the self-renewal of neural SCs but not for their survival or differentiation. In HNSCC, BMI1 plays a crucial role in the self-renewal of CSLC and has been correlated with the tumor aggressiveness and carcinogenesis of HNSCC (Prince, et al. 2007). BMI1 has been found to be overexpressed in CSLC in HNSCC (Prince, et al. 2007; Tabor, et al. 2011; Zhang, et al. 2010). It has also been shown to be overexpressed in other tumors such as cancer breast (Wang, et al. 2012). The combined isolation and evaluation of CSLC by both BMI1 and another CSLC marker can therefore be helpful in the assessment of the CSLC subpopulation in HNSCC.

SP cells have also been shown to a successful isolation approach for CSLC in HNSCC (Yu, et al. 2012). This technique was first described by Goodell et al. in bone marrow-derived cells using flow-cytometry (Goodell, et al. 1996). The unique drug efflux phenotype of SP cells

is determined by ATP-binding cassette G2 subfamily (ABCG2). This protein superfamily is responsible for the multiple drug-resistant traits shown by these cancers (Liu, et al. 2012). In HNSCC, Wan et al. were the first to isolate CSLC using the SP approach (Wan, et al. 2010).

Overall, the controversy and inconsistency of cell surface markers used in the field of CSLC research has led many researchers to focus on the identification of other cell surface markers that might be more reliable and consistent. Recent promising markers include CD10 (Fukusumi, et al. 2014), CD98 (Rietbergen, et al. 2014), CD163 (He, et al. 2014), CD166 (Yan, et al. 2013), CD200 (Jung, et al. 2015) and CD271 (Murillo-Sauca, et al. 2014).

Table 1. Stem cell markers used in the identification of CSLC in HNSCC

Isolation strategy	Stem Cell Marker	% reported in samples	Region	Reference
FACS/SPH	CD133	≈2	Oral	(Zhang, et al. 2010)
FACS	CD133	≈3	Larynx	(Wu, et al. 2011)
FACS	SP/CD133	≈0.3	Larynx	(Wu, et al. 2011)
FACS	CD133	≈3	Larynx	(Wei, et al. 2014; Wei, et al. 2009)
FACS	CD133	<1	Head and neck	(Harper, et al. 2007)
FACS/SPH	CD133, BMI1	≈3	Larynx	(Chen, et al. 2011a)
FACS	CD44	≈6	Head and neck	(Harper, et al. 2007)
FACS	CD44	<10%	Head and neck	(Prince, et al. 2007)
FACS	CD44	25	Head and neck	(Joshua, et al. 2012)
FACS	CD44	na	Head and neck	(Lim, et al. 2011)
FACS	CD44	≈4	Head and neck	(Harper, et al. 2010)
FACS	CD44	90-100%	Head and neck	(Wilson, et al. 2012)
FACS	CD44+/CD24−	≈37	Head and neck	(Chen, et al. 2009)
FACS	CD44+/CD24− /ALDH+	na	Head and neck	(Chen, et al. 2009)
FACS	CD44/ALDH1	≈2	Head and neck	(Krishnamurthy, et al. 2010)
FACS	CD44/ALDH1	na	Oral	(Chou, et al. 2015)
FACS	CD44/ALDH	na	Head and neck	(Chinn, et al. 2014)
FACS	ALDH1	≈15	Head and neck	(Wilson, et al. 2012)
FACS	ALDH1	≈8	Head and neck	(Chen, et al. 2009)
FACS	ALDH1	≈4	Head and neck	(Clay, et al. 2010)
FACS	SP	≈17	Larynx	(Wu, et al. 2011)
FACS	SP	0.1-6.0	Oral	(Yu, et al. 2014)
FACS	SP	≈14	Larynx	(Wan, et al. 2010)
FACS	SP	≈1	Head and neck	(Tabor, et al. 2011)
FACS	SP	≈1	Head and neck	(Wilson, et al. 2012)
FACS	SP	0.1	Head and neck	(Lim, et al. 2011)
FACS	SP	<1	Head and neck	(Harper, et al. 2007)
SPH	CD44	3	Head and neck	(Okamoto, et al. 2009)
SPH	SOX2	na	Oral	(Chou, et al. 2015)
SPH	β-catenin	na	Head and neck	(Lee, et al. 2014)
SPH	OCT4	na	Head and neck	(Lee, et al. 2014)
SPH	OCT4	na	Oral	(Tsai, et al. 2014)
SPH	na	na	Head and neck	(Shrivastava, et al. 2015)
SPH	na	na	Oral	(Yu, et al. 2014)
SPH	na	na	Oral	(Chen, et al. 2012)
SPH	na	na	Head and neck	(Lim, et al. 2011)
SPH	na	na	Head and neck	(Harper, et al. 2007)
SPH	na	na	Head and neck	(Lim, et al. 2012)

Abbreviations: FACS - Flow cytometry cell sorting, SP – Side population flow sorting, SPH - spheroid enrichment, na - not available

1.3.4 Spheroid enrichment as a model for studying CSLCs

Spheroid enrichment for CSLC is an efficient, economic and reliable approach for studying CSLC. It is used mainly to study the therapeutic response of CSLC. Different approaches have been standardized, making this approach reproducible by researchers (Foty 2011; Friedrich, et al. 2009; Ho, et al. 2012; Vinci, et al. 2013). The three-dimensional (3D) culture of spheroids mimics how metastatic and growing cancer colonies would behave when treated with various chemotherapeutic agents system, adding another advantage to this approach. The 3D spheroid culture model can also be used to understand CSLC properties of invasion and migration, both being crucial properties associated with tumor initiation and subsequent relapse or recurrence (Vinci, et al. 2013).

The main difficulties associated with using spheroids in CSLC research include the necessity of using advanced imaging equipment and that not all cell lines or primary tumors form spheroids in culture (Friedrich, et al. 2009; Woolard and Fine 2009). Furthermore, it is technically difficult to assess the extent of CSLC enrichment in the spheroids or isolate CSLC from the formed spheroids for further experimentation and analysis due to various factors such as high intra-spheroidal cell death and partial differentiation of progeny cells (Perego, et al. 2011; Woolard and Fine 2009). Using adherent systems with CSLC enriched media is rapidly gaining ground as an approach to efficiently grow and/or isolate CSLCs, overcoming much of the technical difficulties faced with non-adherent spheroids (Lim, et al. 2012; Woolard and Fine 2009). The interaction between CSLC and the extracellular matrix components along with the high exposure of adherent CSLCs to the enriched media might be key mechanisms that result in the inhibition of CSLC differentiation and increased CSLC propagation in these adherent CSLC

models (Woolard and Fine 2009). Eventually, a combined spheroid and adherent system might be the best approach for researchers in this field.

1.3.5 Role of CSLC in prognosis

Studying the role of CSLCs in chemo- and radioresistance will lead to new diagnostic and prognostic tests that can aid in patient care. Researchers have shown that the CSLC markers, CD133 (Chiou, et al. 2008), CD44 (Chinn, et al. 2015; Joshua, et al. 2012; Kokko, et al. 2011; Lindquist, et al. 2012), SOX2 (Huang, et al. 2014; Li, et al. 2014), OCT4 (Tsai, et al. 2014) and ALDH1 (Zhou and Sun 2014) can predict tumor behavior, aggressiveness and determine the prognosis of patients (Table 2). However, as reviewed in Table 1, the value of CSLC in HNSCC did not yield consistent results; some researchers showed poor prognosis across all parameters, others showed poor prognosis in some parameters, interestingly few papers even showed favorable prognosis. Overall, these results show that more research is crucial before more major conclusions that could be drawn.

Work by Chinn et al. (Chinn, et al. 2015), Joshua et al. (Joshua, et al. 2012), Kokko et al. (Kokko, et al. 2011) and Lindquist et al. (Lindquist, et al. 2012) all showed that CD44 can be used as a marker of prognosis. In a sample of 40 patients, Chinn et al. found that CD44 high positivity by flow-cytometry was associated with tumor size and stage, but not with metastatic spread or survival (Chinn, et al. 2015). Joshua et al. showed that a flow cytometric measurement of the frequency CD44 CSLCs in human tumors grown in mouse models can correlate with prognosis. A cut-off point of 15.2% discriminates between the good and bad prognostic groups (good prognostic group < 15.2% and the bad prognostic groups > 15.2%) (Joshua, et al. 2012). Using IHC in a sample of 135 patients, Kokko et al. found a strong correlation between CD44

overexpression and poor 5-year OS in patients with HNSCC (Kokko, et al. 2011). Interestingly, the group also found that heavy smoking and not heavy alcohol consumption to be significantly associated with CD44-high positivity in the tumors (Kokko, et al. 2011). Similarly, utilizing IHC, Lindquist et al. also found a strong correlation between CD44-high positivity and shorter OS in a group of 73 patients (Lindquist, et al. 2012). Both Kokko et al. and Lindquist et al. focused not only on the percentages of positive cells, but on the intensity of staining (Kokko, et al. 2011; Lindquist, et al. 2012). These results show that CSLC cell surface markers, such as CD44 can be used to determine the prognosis of patients.

SOX2 is another CSLC that has shown to be an independent prognostic significance in HNSCC (Table 2). In a recent study, Huang, et al. showed that CD44 and SOX2 are useful prognostic marker in a group of 66 oral tumors (Huang, et al. 2014). Another study confirmed this finding and showed that SOX2 expression in OSCC is specifically correlated with lymph node metastasis in 80 oral tumors (Michifuri, et al. 2012). Lee et al. and Chou et al. demonstrated that SOX2 overexpression correlates with decreased OS (Chou, et al. 2015; Lee, et al. 2014). A recent meta-analysis of SOX2 as a prognostic marker in HNSCC showed that SOX2 assessment by IHC was closely correlated with advanced TNM stage and decreased OS (Li, et al. 2014).

A meta-analysis that assessed the value of ALDH1 as a HNSCC prognostic marker, showed that high ALDH1 CSLC was highly correlated with lymph node metastasis, decreased OS and decreased disease-free survival (DFS) (Zhou and Sun 2014). However, ALDH1 expression was not significantly associated with tumor stage.

Table 2. Prognostic significance of CSLC Markers in HNSCC

Stem Cell Marker	Region	Reference	Prognostic significance
CD44	Larynx	(Esteban, et al. 2005)	Favourable
CD44	Oral	(Kosunen, et al. 2007)	Variable
CD44	hypopharynx	(Uwa, et al. 2011)	Variable
CD44	Larynx	(Yuce, et al. 2011)	Variable
CD44	Larynx	(de Jong, et al. 2010)	Variable
CD44	Head and neck	(Mack and Gires 2008)	No
CD44	Head and neck	(Chen et al., 2010)	Variable
CD44	Head and neck	(Joshua, et al. 2012)	Poor
CD44	Head and neck	(Kokko, et al. 2011)	Variable
CD44	Oral	(Lindquist, et al. 2012)	Poor
CD44	Head and neck	(Koukourakis et al.,2012)	Poor
CD44	Head and neck	(Chinn, et al. 2014)	Variable
CD44	Oral	(Huang, et al. 2014)	Poor
CD133	Oral	(Liu et al., 2013)	Poor
CD44/CD44v	Head and neck	(Kawano, et al. 2004)	Variable
CD44v6	Larynx	(Staibano, et al. 2007)	Poor
CD44v6	Larynx	(Guo, et al. 2009)	Poor
CD133	Larynx	(Lu, et al. 2011)	No
SOX2	Oral	(Zullig et al., 2013)	Poor
SOX2	Head and neck	(Schrock et al., 2014)	Poor
SOX2	Hypopharynx	(Ge et al. 2010)	No
SOX2	Salivary	(Dai et al. 2014)	Poor
SOX2	Oral	(Du et al. 2013)	Poor
SOX2	Larynx	(Tang et al. 2011)	Poor
SOX2	Larynx	(Ye et al. 2013)	No
SOX2	Hypopharynx and Larynx	(Gonzalez-Marquez, et al. 2014)	No
SOX2	Oral	(Michifuri et al., 2012)	Variable
SOX2	Oral	(Huang, et al. 2014)	Poor
ALDH1	Head and neck	(Chen et al., 2010)	Poor
ALDH1	Head and neck	(Koukourakis et al.,2012)	Favourable
ALDH1	Head and neck	(Xu et al.,2013)	Variable
ALDH1	Oral	(Liu et al., 2013)	Poor
ALDH1	Oral	(Qian et al., 2013)	Poor
ALDH1	Oral	(Huang et al.,2014)	Poor
ALDH1	Head and neck	(Qian et al., 2014)	Poor
ALDH1	Oral	(Michifuri et al., 2012)	Variable
ALDH1	Oral	(Huang, et al. 2014)	Poor
OCT4	Hypopharynx	(Ge et al. 2010)	Poor
OCT4	Oral	(Huang, et al. 2014)	Poor
OCT4	Head and neck	(Lee, et al. 2014)	Poor
β-catenin	Head and neck	(Lee, et al. 2014)	Poor

1.3.6 Role of CSLC in radioresistance

Radiotherapy is currently an important treatment modality for HNSCC, used either alone or in combination with chemotherapy for primary and recurrent cancers (Strojan, et al. 2015). Radiotherapy will remain a crucial component of therapy for HNSCC because these tumors tend to locally infiltrate important surrounding structure; in addition surgery is often difficult owing to the anatomical location. Research has shown that cell surface markers, CD133 and CD44 could be markers of radioresistance in tumors (Gallmeier, et al. 2011; Piao, et al. 2012; Xiao, et al. 2012). Breast CSLC have been shown to survive various protocols of radiation treatment, and even show higher self-renewal potential on some protocols (Lagadec, et al. 2010). The SP cells from breast cancer cell lines were found to be more resistant to radiation than the non-SP cells (Han and Crowe 2009). Bao et al. showed that CD133-positive glioma CSLCs repaired radiation-induced DNA damage more efficiently than CD133-negative cells, and might be the source of tumor recurrence after radiation therapy (Bao, et al. 2006). CD133-positive non-small cell lung carcinoma (NSCLC) CSLCs are also radioresistant, due to defects in DNA repair which were manifested as decreased phosphorylation of various protein kinases, including ATM and Krüppel-associated protein 1 (KAP1) (Lundholm, et al. 2013). In prostate cancer, CD44-positive CSLCs were radioresistant when compared to parental cancer cells (Cho, et al. 2012), CD44 knockdown was shown to enhance radiosensitivity (Xiao, et al. 2012). Taking a new approach in selecting CSLC, Ghisolfi et al. showed that irradiation enriched CSLCs in tumors, however this approach has not been replicated yet by others (Ghisolfi, et al. 2012).

Few groups have begun working in the field of radioresistance in HNSCC CSLC; showing radioresistance using a number of different markers. Chen et al. found evidence that an ALDH1+ subpopulation exhibited increased radioresistance compared to ALDH- (Chen, et al. 2009). Wan

et al. also showed increased radioresistance of CSLC SP cells isolated from a laryngeal cell lines, AMC-HN-8 and Hep-2 (Wan, et al. 2010). On the other hand, Wilson et al. showed no significant differences in radiosensitivity between HNSCC cell lines using a number of different CSLC isolation techniques (Wilson, et al. 2012). Overall, radioresistance in HNSCC CSLCs is a promising field of research that we and others are exploring.

1.3.7 Targeted approaches against CSLC

Many groups are investigating the potential of certain targeted agents to selectively inhibit HNSCC CSLCs. Approaches include small molecule inhibitors such, a WNT inhibitor (Warrier, et al. 2014); Cucurbitacin I, a STAT3 inhibitor (Chen, et al. 2010); compounds including Salinomycin and Quercetin (Basu, et al. 2011; Chang, et al. 2013); antibodies (Damek-Poprawa, et al. 2011); cell-based immunotherapy (Visus, et al. 2011); humanized monoclonal antibody anti-CD44v6 (bivatuzumab mertansine) (Tijink, et al. 2006); multifunctional experimental nanoparticles (Hermann, et al. 2010); a niche-based approach (Krishnamurthy, et al. 2010), histone deacetylase inhibitors (Giudice, et al. 2013); restoration of microRNA-200c (miR200c) (Lo, et al. 2011); and knockdown of critical stemness genes through small interfering RNA (siRNA)/short hairpin RNA (shRNA) against SNAI1 (Chen, et al. 2009), EZH2, OCT4 (Lo, et al. 2012), SMURF1 (Khammanivong, et al. 2014), and BMI1 (Chen, et al. 2011a).

The results of applying specific anti-CSLC compounds are promising, but comparative analysis against parental cell lines is crucial to verify the sensitivity against CSLC (Basu, et al. 2011; Chang, et al. 2013; Chen, et al. 2010). More research on the mechanisms by which Salinomycin and Quercetin affect CSLC is necessary before major conclusions can be drawn (Basu, et al. 2011; Chang, et al. 2013). Results using Cucurbitacin I look promising, but

replication by other groups and comparison with the current standard of care seem crucial (Chen, et al. 2010)

In a phase 1 clinical trial, bivatuzumab, a humanized monoclonal antibody directed against CD44v6, covalently linked to the cytotoxic agent mertansine showed initial positive results, however serious severe skin reactions led to the discontinuation of any further clinical trials of this therapeutic modality (Tijink, et al. 2006). In an important study, Damek-Poprawa et al. showed that a targeted genotoxin against CD133-positive CSLCs in HNSCC is possible (Damek-Poprawa, et al. 2011). They used an anti-human CD133 monoclonal antibody (MAb) conjugated with a periodontal pathogen to target CD133-positive CSLCs in cell lines; the pathogen being characteristically sensitive against epithelioid-like cells (Damek-Poprawa, et al. 2011). Damek-Poprawa, et al. showed selective inhibition of the proliferative capacity against the CD133+ CSLC subpopulation (Damek-Poprawa, et al. 2011). Visus et al. successfully used an immunotherapeutic cell-based approach in which CD8+ T-cells specifically targeted the CSLC ALDH+ subpopulation within cell lines and fresh specimens (Visus, et al. 2011). They showed that ALDH+ CSLC are more tumorigenic when transplanted in immunodeficient mice at low dilution when compared to ALDH- (Visus, et al. 2011). They confirmed the inhibition of ALDH+ CSLC *in vitro* and *in vivo* using multiple approaches; animal model studies also yielded positive results in terms of increased mice survival (Visus, et al. 2011). In addition, Visus et al. used a novel intra-tumoral injection approach, thus proposing a clinical approach to the proposed therapeutic modality (Visus, et al. 2011). Krishnamurthy et al. used a niche-based approach to decrease signaling between the CSLC and the perivascular niche (Krishnamurthy, et al. 2010). They ablated endothelial cells in the perivascular niche using a caspase-based artificial death switch and this lead to a decrease in the CD44+/ALDH+ cells subpopulation within the tumors.

These important results provide evidence for the potential use of anti-angiogenic drugs, such as bevacizumab in animal models to target CSLC.

Chen et al. used a siRNA against SNAI1 (aliases - SNAIL), a key factor in maintaining CSLC properties through Epithelial Mesenchymal Transition (EMT) and reported that this approach can be used to overcome chemo- and radioresistance (Chen, et al. 2009). Chen et al. used shRNA to knockdown BMI1 and confirmed the critical role of BMI1 in laryngeal CSLC (Chen, et al. 2011a). BMI1 is an oncogene belonging to the Polycomb group (PcG) proteins family and has been shown to play a role in the proliferation of tumors and the self-renewal to CSLCs (Chen, et al. 2011a). Lo et al. used a non-viral gene delivery method to inhibit the CSLC subpopulation in an HNSCC cell line using a siRNA against EZH2 and OCT4 and showed weak inhibition of the ALDH1+/CD44+ CSLC subpopulation properties, such as EMT and radioresistance (Lo, et al. 2012). In addition, EZH2/OCT4 inhibition showed better results over radiation therapy alone in an animal model (Lo, et al. 2012). Some researchers consider this paper to have set the gold standard for the preliminary identification of a potential CSLC-inhibitor because it used a non-viral vector, used an animal model and confirmed the effectiveness of the inhibition using multiple methods, such as cell survival, sphere formation and tumor invasion when compared to existing standard therapy IR (Kiang, et al. 2012).

There are many other promising approaches that can be used to target the stemness self-renewal pathways of CSLC (Lee, et al. 2014; Takahashi-Yanaga and Kahn 2010). Warrier et al. used WNT antagonist in HNSCC and showed enhanced chemosensitivity to cisplatin and decreased spheroid formation which was reversed by the addition of WNT3A (Warrier, et al. 2014). Silencing of SOX2 *in vitro* has been shown to decrease CSLC self-renewal, chemoresistance, invasion capacities and in vivo tumorigenicity in HNSCC (Lee, et al. 2014).

SOX2 overexpression in HNSCC was found to lead to cyclin B1 and SNAI1 overexpression, as probable mechanism that might give these cells a survival advantage (Lee, et al. 2014). Targeting various stemness pathways may provide high therapeutic value; however, the side effects of such interventions, especially the effects on normal SC should be carefully investigated (Kaseb and Gollin 2015). For instance, NOTCH inhibitors have demonstrated marked toxicity affecting the gastrointestinal tract, muscle and immune systems in clinical and preclinical trials (Groth and Fortini 2012; Kaseb and Gollin 2015; Mourikis, et al. 2012). Further, the important role of the NOTCH pathway in regulating squamous epithelial differentiation is consistent with reports of cutaneous disorders and malignancies as side effects of NOTCH inhibitors in an Alzheimer's disease clinical trial and in Notch1 knockout mice (Stransky, et al. 2011). To avoid possibly severe and life-threatening skin or muscle-related side effects, alternative therapeutic approaches should be examined, including intra-tumoral administration of NOTCH inhibitors in preclinical models, as suggested by Pickering et al. (Pickering, et al. 2013). Another approach may be to develop alternative small molecule inhibitors or antibodies to inhibit specific NOTCH receptors, their activating ligands, or other components of the NOTCH pathway in tumor cells (Fouillade, et al. 2012; Kaseb and Gollin 2015). For example, Wu et al. generated antibodies that can specifically target murine and human Notch receptors; short-term administration (2–3 weeks) showed fewer and less severe side effects compared to other Notch inhibitors (Wu, et al. 2010). Similarly, SOX2 targeting approaches have also been investigated. For instance, SOX2 inhibition through a zinc finger-based artificial transcription factor approach has been successful in breast cancer cells (Stolzenburg, et al. 2012); Furthermore, a novel inhibitor of SOX2 DNA binding has been identified (Narasimhan, et al. 2011). Overall, these results and others clearly show that more research concerning the effects and side effects of inhibiting the stemness

pathway in normal cells and tumor cells is crucial before targeted therapeutic approaches against the stemness pathway are further implemented (Kaseb and Gollin 2015)

1.4 CHARACTERISTICS OF ORAL SQUAMOUS CELL CARCINOMA

1.4.1 Genetic Heterogeneity

OSCC is a result of multiple genetic aberrations, which includes the inactivation of genes by deletion or mutations or the up-regulation of genes as a consequence of point mutation, amplification or other cytogenetic changes (Mitelman, et al. 2007). Sequencing studies in OSCC and other solid tumors have shown that these tumors possess two types of genetic mutations. The first group is the ‘driver genes’ (usually around 5-10 per tumor) and mutations in these genes tend to initiate and drive the cancerous transformation of the cell. Driver gene mutations are important because they might determine the prognosis of the patient. The second group is called ‘passenger gene' mutations and these occur from exposure to various environmental factors and defects caused by ‘driver' mutations (Lord and Ashworth 2012). In OSCC, four different critical driver pathways (mitogenic signaling, NOTCH, cell cycle, and TP53) were identified (Pickering, et al. 2013). Sequencing studies have confirmed that mutations in *FAT1, CASP8, TP53, CDKN2A, PTEN, PIK3CA, HRAS, NOTCH1, IRF6, and TP63* are possible driver mutations in OSCC (Pickering, et al. 2013; Stransky, et al. 2011).

The karyotypes of OSCC are usually complex, near-triploid, with various numerical and structural chromosome alterations abnormalities (Gollin 2014; Martin, et al. 2008). OSCC have been found to harbor more than 400 different chromosomal aberrations (Gollin 2014; Mitelman,

et al. 2014). The most common chromosomal abnormalities in OSCC are gains of 5p14-15, 8q11-12, and 20q12-13, gains/amplifications of 3q26, 7p11, 8q24, and 11q13, and losses of 3p, 4q35, 5q12, 8p23, 9p21-24, 11q14-23, 13q12-14, 18q23, and 21q22 (Gollin 2014). Using genetic expression profiles, researchers have classified OSCC into categories that aid in predicting prognosis in patients. Chung et al. proposed a classification for OSCC that categorized OSCC into four entities. The first group shows upregulation of transforming growth factor alpha and epidermal growth factor receptor (EGFR) pathway, and overall poor prognosis; The second group shows a strong mesenchymal cell signature, and poor prognosis possibly due to the higher risk of metastasis possibly due to EMT; the third group were biologically similar to normal squamous epithelial cells; and the last group showed an expression pattern unique to cigarette smoke exposure (Chung, et al. 2004). A more recent study validated and proposed a similar classification strategy, with types 1 through 4 being: basal, mesenchymal, atypical (often HPV+), and classical, respectively, based on the unique high genetic expression in each category (Walter, et al. 2013).

CSLC regulatory genes, such as *SOX2* and *NOTCH1* have been found to be dysregulated in a proportion of OSCC patients. *SOX2* gain has been shown to contribute to oncogenesis in OSCC; driving EMT an important characteristic of metastatic cells (Freier, et al. 2010; Lechner, et al. 2013). On the other hand, *NOTCH* gene mutations have been found in approximately 15% of head and neck tumors; and are usually complex, being associated with loss of-function, gain-of-function, or both (Gaykalova, et al. 2014; Stransky, et al. 2011). Functional studies suggest that *NOTCH1* may act as a tumor suppressor gene in HNSCC (Pickering, et al. 2013).

1.4.2 Chromosomal Instability and Segregation Defects

Chromosomal instability (CIN) is a one of the important features of cancer cells. It refers to the gain or loss of entire or segments of chromosomes at a higher rate in a subpopulation of cells (Ha and Califano 2002). CIN is the result of multiple aberrations in multiple processes, including chromosomal segregation defects, cellular checkpoint abrogation, telomere instability, and DNA damage response (DDR) defects (Gollin 2005). The high prevalence of genetic alterations especially in solid tumors as they progress implies that CIN is both the cause and an effect of carcinogenic evolution (Lord and Ashworth 2012; Mitelman, et al. 2007). Although many of the processes/pathways involved in CIN are unrelated, they are interconnected at some points; adding complexity to CIN (Gollin 2005; Gollin 2014). CIN is indeed a double-edged weapon; defects in DDR can drive cancer cell resistance or evolution, on the other hand, CIN is the basis of many cancer therapeutic approaches such as IR and DNA crosslinking agents (Lord and Ashworth 2012). Chemotherapeutic agents, such as cisplatin induce covalent crosslinks between DNA bases that lead to DNA damage and apoptosis

CIN can be in the form of structural or numerical alterations and may result in a change of the gene expression of the respective cells including oncogenes and tumor suppressor genes thereby driving carcinogenesis. CIN can also lead to a major dysfunction of normal cellular machinery including cell cycle regulation and DNA damage repair (Gollin 2005; Hanahan and Weinberg 2011; Shiloh 2003; Shiloh 2006). Overall, the net result is the evolution of cancer cells that will eventually lead to cancer growth and progression (Albertson 2006; Hanahan and Weinberg 2011). Structural CIN usually results from multiple breakage-fusion-bridge (BFB) cycles (Gollin 2005). Another important cause of CIN is chromosomal segregation defects (CSD). These defects in chromosomal segregation can lead to aneuploidy because of the

abnormal distribution of chromosomes to daughter cells (Gollin 2005; Reing, et al. 2004; Saunders, et al. 2000). The occurrence of CSD in OSCC was found to be an intrinsic and heritable property that occurs in primary tumors and cancer cell lines passages (Minhas, et al. 2003; Reing, et al. 2004; Reshmi, et al. 2004; Saunders, et al. 2000).

Defects in DNA double-strand breaks (DSB) repair are also an important cause of CIN because it results in genetic mutations, gene amplification, and chromosomal aberrations, which can drive carcinogenic evolution (Shiloh 2006; Shiloh 2014). However, the various interconnections between the DDR genes and CIN is not entirely clear (Gollin 2005). Cell cycle disturbances are also an important cause of CIN. In HNSCC, defects in the spindle assembly checkpoint have been shown to be a contributing factor to CIN (Minhas, et al. 2003).

In colorectal cancer, CIN has been shown to be crucial in precancerous development as well as cancerous evolution of these tumors (Draviam, et al. 2004). Siebers et al. showed that CIN assessed in pre-malignant oral lesions might aid in predicting malignant transformation in these lesions and in monitoring prognosis in malignant oral lesions (Siebers, et al. 2013). Understanding CIN in OSCC CSLC is one of the objectives of our current work.

1.4.3 11q13 amplification

Amplification of chromosomal band 11q13 is a common event in human cancer and it follows 11q loss. Amplification increases the gene dosage and results in up-regulation of most of the distal genes (Huang, et al. 2006). 11q13 amplification was observed in ≈ 61% of OSCC patients (Gollin 2014; Huang, et al. 2006). 11q13 amplification in OSCC plays a role in early pre-oncogenic transformation, enabling progression from moderate to severe dysplasia (Noutomi, et al. 2006; Salahshourifar, et al. 2014). Our group has shown previously that the 11q13

amplification in OSCC occurs by the BFB mechanism and that the loss of the distal part of chromosome 11q is an early step in this process (Reshmi, et al. 2007). The poor clinical correlation with 11q13 amplification was attributed specifically to amplification and overexpression of *CCND1* and *EMS1* (Schuuring 1995; Schuuring, et al. 1998). Other important genes amplified include, *ORAOV1, ANO1 and FADD* (Huang, et al. 2006; Wilkerson and Reis-Filho 2013). *CCND1* plays a crucial role in the regulation of the G1/S checkpoint and drives tumor growth in OSCC (Huang, et al. 2006). *EMS1* encodes human cortactin, an actin binding protein possibly involved in the organization of the cellular cytoskeleton and cell adhesion structures (Wilkerson and Reis-Filho 2013)

1.4.4 Distal 11q Loss and Therapeutic Resistance

Research has shown that distal 11q deletion is the first step in the 11q13 amplification process in OSCC (Reshmi, et al. 2007). Loss of chromosomal material from 11q14-11q23 has been shown to occur in ~50% of the HNSCC tumors examined (Gollin 2014; Martin, et al. 2008). Distal 11q loss has been shown to occur early in tumor intiation; in the transition of the tumor from carcinoma in situ (Califano, et al. 2000). The loss of distal 11q, where the DDR genes, *MRE11A, ATM,* and *H2AFX* are located, contributes to tumor development and progression (Parikh, et al. 2007). Research has proven that haploinsufficiency of specific DDR genes (*ATM, H2AFX, and MRE11A*) is associated with CIN (Bassing, et al. 2003). Our group has shown that distal 11q loss occurs in a subset of tumors and can be used as a biomarker for prediction of radiosensitivity in HNSCC, lung and ovarian cancer cell lines and a companion diagnostic biomarker for combination therapy with ATR/CHEK1 pathway inhibitors (Parikh, et al. 2007; Sankunny, et al. 2014). One of the important genes that plays a role in OSCC radioresistance is *ATM* (Sankunny,

et al. 2014). The *ATM* (ataxia-telangiectasia mutated) gene, located at 11q22.3 is a master regulator of DDR induced by agents such as IR. The sensor multiprotein complex MRE11A-RAD50-NBN (MRN) complex activates ATM (Dai and Grant 2010). After ATM activation, ATM kinase activates a number of signaling pathways that leads to cell cycle arrest, apoptosis, and DNA repair (Jiang, et al. 2009). ATM activates these different pathways by phosphorylating its substrates, ABL1, TP53, NBN, BRCA1, and CHEK2 proteins (Shiloh 2014). ATM modulates DSB repair via nonhomologous end joining (NHEJ) in G1-phase, and via homologous recombination (HR) in S-phase and G2-phase (Branzei and Foiani 2008). Repair via HR is mediated through a vast collection of proteins that are phosphorylated downstream (Shiloh 2014). Researchers have found it extremely difficult to define which of its downstream targets mediates the increased sensitivity to IR. The histone H2AX, is one of the critical substrates of ATM. ATM activates H2AX specifically at the DSB regions, activating it through phosphorylation into γH2AX; γH2AX, then directs the recruitment of different DNA damage response proteins to the damaged site (Sankunny, et al. 2014; Stucki, et al. 2005).

Ataxia Telangiectasia and Rad3-related (ATR) is a PI3K family protein involved mainly in the repair of stalled replication forks and maintenance of genetic integrity during S phase (Byun, et al. 2005). The ATR pathway regulates the DDR response primarily to ultraviolet radiation (UV) and agents that stall replication fork progression, such as aphidicolin and hydroxyurea (Gollin 2014). The ATR pathway is also interconnected with the ATM pathway. The interaction between ATR, ATR interacting protein (ATRIP) and replication protein A (RPA) plays an important role in the maintenance of chromosomal integrity (Sankunny, et al. 2014). The crucial role of ATR in the maintenance of genomic integrity was shown through loss of function experiments; where inhibition of ATR function led to CIN as a result of overexpression

of common fragile sites (Casper, et al. 2002). ATR phosphorylates a number of downstream proteins that includes BRCA1, CHEK1, MCM2, RAD17, RPA2, SMC1 and TP53, which activates cell cycle checkpoints as well as DNA repair and apoptosis pathways (Gollin 2014; Pruitt, et al. 2014). Overall, the various DDR pathways and networks are highly interconnected. The selective sensitivity of cancer cells to DNA-damaging IR suggests that interconnections between cell cycle checkpoint and survival pathways are altered in tumors. These pathway defects could be used to specifically enhance the killing of tumor cells.

Our current study was designed to understand whether distal 11q loss plays a role in the response of OSCC CSLCs to radiation therapy. We used enriched tumorosphere assays which mimic the in vivo environment of cancers. This approach has also been shown to better predict radioresistance both on the short- and long-terms than standard clonogenic survival analysis (Bartucci, et al. 2012; Cho, et al. 2012). We used a CHEK1 inhibitor in conjunction with IR to study the effect of this combination on OSCC CSLCs. We hypothesized that the CHEK1 small molecule inhibitor (SMI) would reverse the radioresistance of our cell lines in a biomarker-specific manner. Our group has shown previously that radioresistance in OSCC cell lines with distal 11q loss can be reversed by ATR-CHEK1 pathway inhibitors; whereas in OSCC cell lines without distal 11q loss, radiosensitivity is unaffected by ATR-CHEK1 pathway inhibition (Parikh, et al. 2013; Parikh, et al. 2007; Sankunny, et al. 2014).

1.5 THE DNA DAMAGE RESPONSE (DDR)

1.5.1 Overview of the DDR

The DNA damage response is a complex integrated system that maintains the genomic integrity of cells (Shiloh 2014). DNA damage can be a result of multiple causes that include UV, IR, hypoxia or environmental mutagens. DDR components interact with the cell cycle checkpoint and chromosome segregation machinery to repair DNA before the onset of mitosis (Warmerdam and Kanaar 2010).

The cell cycle has three checkpoints that can be delayed to repair DNA damage before the onset of mitosis (Figure 5). These checkpoints are the G1-S, S phase, and the G2-M checkpoints. The G1-S checkpoint, the first of these checkpoints, is TP53-dependent and is regulated by ATM (Massague 2004). Unfortunately, the G1-S checkpoint is commonly dysregulated in OSCC and many other solid tumors (Michalides, et al. 2002). The S phase checkpoint is activated in response to DNA replication errors and DNA damage occurring during the S phase; ATR is one of the main regulators of this checkpoint (Sorensen, et al. 2003). Defects of the S phase checkpoint leads to premature mitosis, premature chromatin condensation (PCC), and mitotic apoptosis (Nghiem, et al. 2001). The aim of the G2-M checkpoint, the last checkpoint before the initiation of mitosis is to prevent cells with DNA damage or replication errors from initiating mitosis. This checkpoint is regulated by ATM/CHEK2 that phosphorylate CDC25A and prevent the activation of cyclin E/CDK2 (Figure 6) (Bucher and Britten 2008). In cells with defective G1-S and S phase checkpoints, targeting the G2M checkpoint with drugs that inhibit ATM/CHEK2, ATR/CHEK1 or CDC25 results in cell death by mitotic catastrophe and is a promising targeted anti-cancer therapeutic approach.

One type of DNA damage is the DSB, usually leads to a cascade of cellular DDR events that result in repair of the damage or cell death (Shiloh 2006; Shiloh 2014). DSB is induced by IR and oxygen free radicals (Shaheen, et al. 2011). Cells repair DSBs via either NHEJ or HR (Figure 6) (Abraham 2004). HR occurs after DNA replication, in the S and/or G2M cell-cycle phases, whereas NHEJ is occurs in G0/G1. HR is an accurate process because it uses the homologous template to repair the DSB; NHEJ on the other hand, is less accurate and utilizes end trimming (Shaheen, et al. 2011)

DSB response can be divided into a three-tiered signaling cascade (Figure 7). 'Sensor' proteins detect and identify the damaged DNA and transmit signals to regulator 'transducers' that in turn transmit the signal switching on/off different 'effector' proteins. Important DNA damage sensor proteins include the MRE11A-RAD50-NBN (MRN) complex, TP53BP1 and MDC1 (Shiloh 2003; Shiloh 2006). One of the primary transducer proteins of the DSB cascade is the protein kinase ATM, which is a member of the PIKK family (Abraham 2004). The PIKK family consists of six members: ATM, ATR, PRKDC (protein kinase, DNA-activated, catalytic polypeptide), MTOR (mammalian target of rapamycin), SMG1 (suppressor of morphogenesis in genitalia-1) and TRRAP (transformation/transcription domain-associated protein) (Shiloh 2003). PRKDC, ATM, ATR and SMG1 play important roles in the DDR; ATM and PRKDC play a major role in the DSB cascade (Helt, et al. 2005). ATR, on the other hand, acts as a protein transducer in response to UV damage and stalled replication forks. Despite the fact that ATM and ATR have different functional roles in the DSB cascade, they are interconnected (Figure 6) (Shiloh 2006).

Defects in the DDR have shown to be a cause of a variety of diseases including constitutional, inherited and somatic disorders. Defects in the DDR have been implicated directly

in familial predisposition to forms of cancer such as hereditary breast and ovarian cancer; the cause being loss of function mutations in HR genes, including *BRCA1* and *BRCA2* (Moynahan and Jasin 2010). Congenital inherited disorders, such as Ataxia telangiectasia (AT), Li-Fraumeni and Fanconi anemia have been shown to harbor defects in the DDR pathways. The DDR has also been found to be markedly elevated in some precancerous lesions, as identified by a marker of DSBs, such as nuclear γH2AX foci (Bartkova, et al. 2006).

Alterations in the DDR are crucial to the survival of CSLCs and tumor regrowth (Lord and Ashworth 2012). The pioneering work by Bao et al. showed that CSLCs have a more robust DDR and DNA repair activity when compared to non-CSLCs in gliomas (Bao, et al. 2006). They also showed that a DDR-targeted drug, such as a combined CHEK1/CHEK2 inhibitor, enhanced the killing of CSLCs induced by IR. Inhibition of these DDR proteins using targeted therapies is currently an important field of anti-cancer research (Table 3) (Hosoya and Miyagawa 2014). If such drugs can prevent cancer cells from repairing their damaged DNA, these cancer cells would lose their genetic integrity and die at an increased frequency in response to conventional therapies. Currently, more work is being done to investigate the appropriate dosing and scheduling of these inhibitors to decrease the side effects that have been observed in preclinical and clinical trials (Shaheen, et al. 2011).

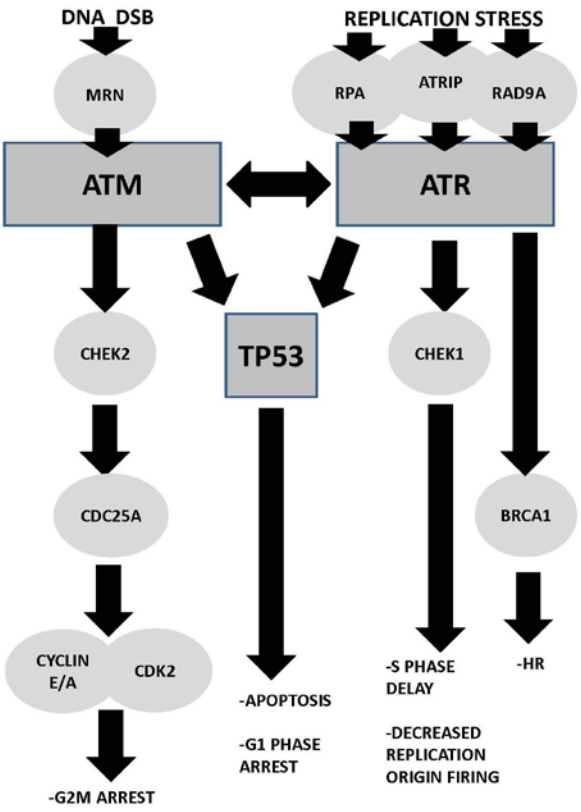

Figure 6. Schematic representation of the roles of ATM and ATR in the DDR signaling cascade

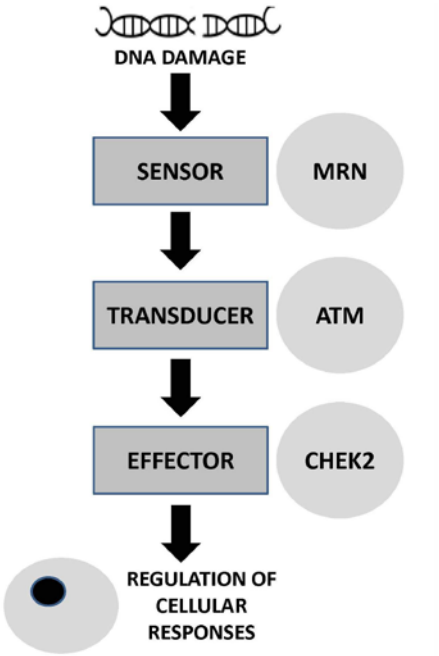

Figure 7. Schematic representation of the DDR signaling cascade

Table 3. DDR Inhibitors in Clinical Use, Clinical Trials or under Development[a]

In Clinical Use
Topoisomerase I inhibitor Topoisomerase II inhibitor
In Clinical Trials
CHEK1 inhibitor Combined CHEK1/CHEK2 inhibitor DNA-PK /mTOR inhibitor PARP inhibitor APE1 inhibitor MGMT inhibitor
Under Development
DNA protein kinase inhibitor MRE11 inhibitor ATM inhibitor ATR inhibitor CHEK2 inhibitor RAD51 inhibitor Telomerase inhibitor
For current status and information of clinical trials, please refer to http://clinicaltrials.gov/, a service of the US National Institutes of Health.

[a] Adapted from Hosoya and Miyagawa 2014

1.5.2 DNA Damage Repair Machinery

As discussed earlier, the causes of DNA damage are numerous and complex; to counteract this complexity, eukaryotic cells possess multiple complex DDR repair machinery comprised of multiple pathways (Table 4) (Lord and Ashworth 2012). Currently, there are more than 150 different human proteins that play a role in DNA repair (Li, et al. 2012). Collectively, the five major DNA repair pathways can be subdivided into two categories. The first category of pathways repairs DSB and is comprised of the NHEJ and HR pathways. The second category repairs single strand breaks (SSB) and contains the nucleotide excision repair (NER), base excision repair (BER) and mismatch repair (MMR) pathways (Lord and Ashworth 2012; Shaheen, et al. 2011). BER repairs oxidative lesions, alkylation, small base adducts, and SSBs,

while NER repairs DNA helix disruptions caused by bulky adducts. MMR repairs dNTP misinsertions and 'insertion and deletion' loops that form during DNA replication. As discussed earlier, HR and NHEJ are involved in repairing DSBs and interstrand crosslinks (Shaheen, et al. 2011).

Table 4. Major DNA Repair Pathways

Repair Pathway	Lesion	Key Proteins
NHEJ	Interstrand crosslink, DSB	KU70/80, PRKDC
HR	Interstrand crosslink, DSB	BRCA1, BRCA2, RAD51, ATM, ATR, CHEK1, CHEK2
NER	Bulky adducts, SSB	ERCC1, ERCC4
BER	Uracil, Abasic site, SSB	PARP1, XRCC1, LIG3
MMR	A-G mismatch, T-C mismatch, insertion, deletion, SSB	MSH2, MLH1

1.6 CHEK1 INHIBITION AS A TARGETED CANCER THERAPY

1.6.1 TARGETED CANCER THERAPY

Targeted therapy against cancer has made substantial progress in the past decade. Specific gene mutations in cancer can lead to defects that can be targeted by drugs. The identification of genetic alterations as the cause of cancer has led to a major shift in cancer drug development. The aim of this evolution was to better target cancer cells, decreasing death of normal cells and eventually decreasing side effects.

Targeted cancer strategies can be divided into two major categories. The direct 'conventional' anticancer approaches that aims to inhibit or neutralize signaling pathways and 'synthetic lethality' that aims to exploit the complex genetic defects of tumor cells (Ferrari, et al. 2010). Conventional targeted approaches were launched in hematological cancers, such as CML where a distinct, unique *BCR-ABL1* gene fusion is the driving cause of malignant growth (Druker, et al. 1996). Following the success of targeted therapy in CML and other hematological cancers, other targeted approaches were developed. Targeting the downstream effector proteins in cancer cells was also developed for use when direct inhibition is impossible. Examples of this approach include the targeting of the downstream effectors, KRAS, MEK in breast cancer and BRAF in melanoma (Garon, et al. 2010; Solit, et al. 2006).

Cetuximab, an anti-EGFR targeted agent, is the only FDA-approved targeted therapy used in patients with OSCC (Simpson, et al. 2015). Cetuximab is used as an adjuvant therapy in primary or relapsed patients; especially patients who cannot tolerate platinum-based agents (Bonner, et al. 2010; Vermorken, et al. 2008). Cetuximab use in patients can be guided by *EGFR* expression studies, because patients with EGFR overexpression tend to have low OS (Ang, et al.

2002). Development of resistance to EGFR therapy is a major obstacle that needs to be addressed either through the development of other agents against EGFR or its downstream interacting targets, such as the PI3K pathway (Simpson, et al. 2015). Overall, it is clear that the development of other novel targeting approaches to OSCC is crucial.

One of the promising targeted approaches that can be used in OSCC is agents that cause 'synthetic lethality.' Synthetic lethality refers to the interaction of two genes, where a single genetic mutation is compatible with viability, but a combined genetic mutation is lethal (Ferrari, et al. 2010; Shaheen, et al. 2011). Synthetic lethality was first identified in yeast mutation screens, where the targeting of two mutations leads to an additive negative effect that compromises cellular function (Hannon 2002; Timmons 2006; Tong, et al. 2001). This unconventional targeted approach has a number of advantages. It spares normal cells because these cells do not have genetic mutations. It can also target the tumor cells if they have acquired either loss-of-function or gain-of-function mutations. Furthermore, it aids in the discovery of novel biomarkers and can be valuable in targeting cancer cells with 'non-druggable' pathway defects (Ferrari, et al. 2010). Disadvantages of synthetic lethality include the possibility of increasing the side effects of other cancer drugs and an increased risk of a shortened lifespan of effectiveness because of the development of resistance through other adaptation mechanisms (Shaheen, et al. 2011).

The concept of synthetic lethality was shown to be extremely valuable in the manipulation of both the DDR and the cell cycle response. Cancer cells, unlike normal cells, acquire more genetic alterations and DNA damage post-therapy; this necessitates stopping at major cell cycle checkpoints to repair their DNA (Origanti, et al. 2013; Shaheen, et al. 2011). Most cancer cells lack an effective G1-S checkpoint and must arrest at the G2M checkpoint to

repair their genomes prior to cell division. Without efficient genomic repair at the G2M checkpoint, these cells would enter mitosis with damaged genomes and undergo 'mitotic catastrophe' (MC) (Shaheen, et al. 2011). Adding an agent that induces synthetic lethality through the abrogation of the G2M checkpoint would therefore spare normal cells which have a normal G1 checkpoint, which protects them against DNA damage-induced cell death (Origanti, et al. 2013). The concept of applying synthetic lethality in human tumor cells with defective DDR machinery was first shown in *BRCA1*- and *BRCA2*-deficient cells, where the defective HR caused by DSB made these cells susceptible to PARP1 inhibition (Bryant, et al. 2005; Farmer, et al. 2005). Overall, it is clear that targeted cancer approaches are gradually gaining more ground as possible adjuvant and neo-adjuvant therapeutic modalities in various cancers.

1.6.2 CHEK1 INHIBITION

Checkpoint kinase 1 (CHEK1), is an important downstream protein of ATR and is an important contributor to all of the cell cycle checkpoints, including the G1/S, intra-S-phase, G2/M, and the mitotic spindle checkpoint (Dai and Grant 2010). CHEK1 is activated through phosphorylation at Ser317/Ser345 (Sankunny, et al. 2014). Unlike CHEK2, CHEK1 is activated by diverse stimuli that cause SSB in the DNA (e.g., UV, replication stresses, and DNA-damaging agents) through both ATR and ATM. On the other hand, CHEK2 activation is largely restricted to DSBs through ATM. In addition to the role of CHEK1 in cell cycle regulation, CHEK1 also regulates apoptosis independently of TP53, BCL2, and CASP3 (Sidi, et al. 2008). CHEK1 is also involved in the repair of mitotic defects through association with the kinetochores and phosphorylation at non-canonical sites in AURKB, thus enhancing its catalytic activity (Peddibhotla, et al. 2009). Given the important roles of CHEK1 in cell cycle regulation, maintenance of genomic integrity,

as a backup for CHEK2, mitotic defect repair and apoptosis; knocking out CHEK1 is a promising approach to cancer cell eradication (Bartek and Lukas 2003).

The genes encoding components of the ATM/CHEK2 and the ATR/CHEK1 pathways are subject to frequent copy number loss in OSCC. This makes manipulation of the DDR to cause selective tumor cell death through MC partially effective in these tumors. Knocking out the G2M checkpoint using targeted CHEK1 inhibitors has been shown to cause 'synthetic lethality' because these cells would enter mitosis with damaged genomes and undergo MC (Origanti, et al. 2013; Parikh, et al. 2007). CHEK1 inhibitors have been successfully combined with DNA damaging agents in studies both *in vitro* and *in vivo*. The combination of CHEK1 inhibitors and IR (Borst, et al. 2013; Ma, et al. 2012; Parikh, et al. 2013; Parikh, et al. 2007; Riesterer, et al. 2011; Sankunny, et al. 2014) or chemotherapy (Blasina, et al. 2008) has been shown to be effective in a variety of carcinomas. PF-00477736 is a CHEK1 small molecule inhibitor (SMI) developed by Pfizer that our group has used successfully to potentiate the effect of IR (Sankunny, et al. 2014). PF-00477736 also shows a synergistic effect when combined with inhibitors of the DNA repair enzyme, poly (ADP-ribose) polymerase (PARP) in a number of breast and pancreatic cancer cell lines (Mitchell, et al. 2010). Recent results have shown different effectiveness as regards to the combination of gemcitabine and CHEK1 inhibitors in CSLC in from NSCLC (Bartucci, et al. 2012; Fang, et al. 2013). Studying the effects of CHEK1 inhibitors on OSCC CSLCs is a new promising focus of research and is one of the main objectives of our project.

2.0 MATERIALS AND METHODS

2.1 CELL CULTURE

2.1.1 OSCC cell lines

In order to study CSLC markers in OSCC, low passage (<20) UPCI:SCC cell lines: UPCI:SCC029B, SCC040, SCC056, SCC066, SCC078, SCC084, SCC099, SCC103, SCC104, SCC114, SCC116, SCC122, SCC125, SCC131, SCC136, SCC143, SCC172, SCC182 were cultured. We then selected nine OSCC cell lines with or without distal 11q loss for additional studies: UPCI:SCC029B, SCC040, SCC104, SCC066, SCC081, SCC116, SCC122, SCC125 and SCC131. The entire set of UPCI:SCC cell lines was established previously in our laboratory (White, et al. 2007). The UPCI:SCC oral cell lines were cultured in M10 medium comprised of Minimal Essential Medium (MEM) supplemented with 1% non-essential amino acids (NEAA), 1% L-glutamine, 0.05 mg/ml gentamicin and 10% fetal bovine serum (FBS) (all from GIBCO Invitrogen, Grand Island, NY). For subculturing OSCC, adherent cells were detached from the flask surface by trypsinizing with 0.05% trypsin/0.02% EDTA (Irvine Scientific) for 3–5 min at 37^{o}C in a humidified 5% CO_2 incubator. An equal amount of M10 medium was used to inhibit trypsin activity following detachment and cells were replated.

2.1.2 Control cell line

TERT-transfected human oral keratinocytes (OKF6/TERT-1 cells), a gift from Dr. James Rheinwald, Brigham and Women's Hospital, Harvard Institutes of Medicine (Dickson, et al. 2000) were cultured in Keratinocyte-SFM supplemented with 25 µg/ml bovine pituitary extract, 0.2 ng/ml EGF, 0.3 mM $CaCl_2$, and penicillin-streptomycin (GIBCO Invitrogen).

2.1.3 CSLC cell cultures

In order to study CIN in CSLC, CSLC cell cultures HNSCC#13 and HNSCC13 (E8) kindly provided by Dr. Eric Lagasse were used. CSLCs were plated on a stromal monolayer of previously irradiated (80 Gy) rodent epithelial feeder cells (Odoux, et al. 2008) or Matrigel™ - coated plates (BD, Franklin Lakes, NJ).

2.2 FLUORESCENCE IN SITU HYBRIDIZATION (FISH)

2.2.1 Assessment of *ATM* copy number alterations

In order to study the copy number status of *ATM*, and to classify cell lines as 'distal 11q loss' or 'No distal 11q loss' FISH was done. A single colony of *E. coli* carrying the individual BAC (mapping to *ATM;* BAC ID: CTD2047A4) was incubated overnight at 37^{o}C in 5 ml of Luria–Bertani (LB) medium with 50 µg/ml Chloramphenicol. The bacteria were centrifuged at 10,000 x g for 30s. The bacteria were resuspended in 100 µl of STET (8% sucrose, 5% Triton X100,

50mM EDTA, 50 mM Tris pH 8.0). Freshly prepared alkaline SDS (0.2 M NaOH, 1% SDS) was added to lyse the bacteria and the solution was incubated at 24^{o}C for 2 min. Cold ammonium acetate (4^{o}C) was added and the solution was incubated for 5 min on ice. Following this step, the bacteria were centrifuged at 4^{o}C for 15 min at 16,000 x g. Equal amounts of phenol and chloroform were added to the supernatant to extract the DNA. The top layer of the mixture was treated with 0.6 x volume of isopropanol and centrifuged at 4^{o}C for 15 min at 16,000 x g. The supernatant was drained and the pellet washed with 70% ethanol and air dried. The DNA was resuspended in 100– 200 µl of Tris–EDTA (TE) buffer (QIAGEN, Valencia, CA) and stored at 4^{o}C. In order to prepare mitotic cells for FISH analyses, OSCC cells were harvested following 5 hr of 0.1µg/ml Colcemid™ (Irvine Scientific, Santa Ana, CA) treatment, hypotonic KCl (0.075 M) treatment for 15 min and fixation in 3:1 methanol:glacial acetic acid. For FISH analysis, cells were harvested, dropped onto slides, treated with RNase/2xSSC (saline sodium citrate), and dehydrated using serial treatments with 70%, 80% and 100% ethanol. Chromatin was denatured with 70% formamide and dehydrated in 70%, 80% and 100% ethanol. The *ATM* BAC probe clone for FISH, was obtained from Children's Hospital of Oakland Research Institute (CHORI, Oakland, CA) and labelled with Spectrum Orange^{TM}. Using a nick translation kit from Vysis, Inc. (Abbott molecular Inc, Des Plaines, IL), extracted DNA was precipitated with ethanol, resuspended in hybridization buffer, centromere enumeration probe for chromosome 11 labelled with Spectrum Green^{TM} (Abbott Molecular Inc., Des Plaines, IL.), and allowed to pre-anneal for 1-2 h at 37^{o}C. The probe was hybridized to the slides for 16 h at 37^{o}C, after which slides were washed with SSC/Tween-20. Slides were counterstained with 4',6-diamidino-2-phenylindole (DAPI, 160 ng/ml 2xSSC) and mounted with antifade (comprised of 1 mg/ml 1,4-phenylene-diamine (Sigma-Aldrich, St. Louis, MO) prior to analysis. All FISH analyses were carried out

using an Olympus BX61 epiflorescence microscope (Olympus Microscopes, Melville, NY). An Applied Imaging CytoVision workstation with Genus v3.6 software was used for image capture and analysis (Leica Microsystems, San Jose, CA).

2.2.2 Assessment of Chromosomal Instability in CSLC

In order to study the copy number status of different chromosomes (Chromosomes 4, 6, 7, 9 and 20), FISH was done on CSLC isolated from HNSCC#13 and HNSCC#13 (Clone E8). These experiments were done by DL and analyzed by HK. Centromere enumeration probes for chromosomes: chromosome 4 (p4n1/4), chromosome 6 (pEDZ6), chromosome 7 (pZ7.5), chromosome 9 (pMR9A) and chromosome 20 (pZ20) were purchased from Vysis, Inc. (Abbott molecular Inc, Des Plaines, IL). Centromeric probes were labelled with the following the fluorochromes, Chromosome 4 spectrum orange (SO), Chromosome 6 spectrum green (SG), Chromosome 7 (SG), Chromosome 9 (SG), Chromosome 17 (SO) and Chromosome 20 (SO). FISH was done as previously described.

2.3 IMMUNOFISH

To study *ATM* copy number status in CSLC (CD133+) and non-CSLC (CD133-) from OSCC cell lines immuno-FISH was done. Slides were stained with CD133 (1:200, 19898, Abcam) (as described in the IF section) prior to FISH hybridization. Coverslips were removed and washed with 2xSCC 15 min at RT (room temperature) followed by dehydration in a graded series of 70%, 85% and 100% ethanol to dehydrate them. The FISH probe that localizes to the *ATM*

region of chromosome 11 labelled with Spectrum Orange and CEP11 labelled with Spectrum Green (Abbott Molecular Inc, Des Plaines, IL) were mixed with 70% hybridization buffer. The probe set was pre-denatured at 75° C for 5 minutes and preannealed at 37° C for 15 minutes. The probe mixture was applied to the slide, coverslipped and codenatured at 75°C for 5 minutes. The slide was allowed to hybridize in a humidified chamber at 39°C overnight. The following day, the slide was washed free of the unbound probe with a 2xSSC/0.1% Tween-20, stained with DAPI, and mounted with ProLong Gold Antifade Reagent (P10144, Life Technologies Carlsbad, CA). All immuno-FISH analyses were carried out using an Olympus BX61 epifluoresence microscope (Olympus Microscopes, Melville, NY). An Applied Imaging CytoVision workstation with Genus v3.6 software was used for image capture and analysis (Leica Microsystems, San Jose, CA).

2.4 SPHEROID ENRICHMENT ASSAYS

To study the different CSLC properties, spheroid enrichment was used. Two approaches were used for enrichment, an adherent and a non-adherent approach. For the adherent approach, enriched CSLC were grown on Matrigel™ -coated plates (BD, Franklin Lakes, NJ). For the non-adherent (suspension) approach spheroids were grown in ultra-low attachment six-well plates (Corning, NY). OSCC cell lines were dissociated with accutase (A11105-01, Life Technologies Carlsbad, CA) and pipetted with a 10 ml pipette, cell aggregates were washed twice with phosphate buffered saline (PBS), centrifuged and dissociated by pipetting into a single cell suspension. The single cell suspension was placed under stem cell suspension culture conditions, which consisted of serum-free Dulbecco's minimum essential (DMEM/F12) medium

supplemented with N2 supplement (17502-048, GIBCO, Grand Island, NY), B27 (17504-044, GIBCO), L-glutamine (25030-149, GIBCO), Gentamicin (20 mg/ml, GIBCO), human recombinant epidermal growth factor (EGF; 20 ng/ml, Sigma-Aldrich), and human basic fibroblast growth factor (bFGF; 20 ng/ml Sigma-Aldrich) (Lim, et al. 2011).

2.5 SPHEROID SELF-RENEWAL ASSESSMENT

Primary/secondary spheroid enrichment comparative analysis was done to assess the self-renewal capacity of the enriched CSLC. Equal numbers of cells derived from OSCC cell lines (primary) and enriched spheroids (secondary) were suspended in SC medium (as described earlier). Individual primary non-adherent spheroids were selected using a 37 µm Reversible Strainer (Stem cell technologies, BC, Canada), centrifuged at 1400 rpm for 4 min, and then mechanically dissociated and re-plated (Molofsky, et al. 2003). Large spheroids (more than 100 cells) were counted and photographed on a phase contrast microscope (Leica Microsystems, Germany).

2.6 SPHEROID SURVIVAL ASSAY

To assess the radioresistance of CSLC from OSCC cell lines with and without distal 11q loss, spheroid survival was carried out. $5*10^4$ cells were plated in triplicate in ultra-low attachment six-well plates in spheroid enrichment medium. After 7–11 days in culture, colonies with >50 cells were counted. For IR-induced damage studies, cells were then treated with 2.5 or 5 Gy

doses of γ-irradiation from a Gammacell 1,000 Elite Irradiator (Nordion International, Ottawa, Canada) with a ^{137}Cs source at a dose rate of 2.83 Gy/min. All experiments were performed in triplicate. Results were reported as the 'Surviving Fraction' which is the ratio of the number of spheroids observed at a particular dose to that observed in the untreated control, represented as a percentage. It is calculated using the following formula:

Surviving Fraction, SF = (spheroids counted in treated / spheroids counted in untreated) * 100

2.7 SPHEROID GROWTH ASSAY

To assess the effect of IR on spheroid growth, spheroid growth was assessed. 2000 cells were plated in agarose-coated 96-well plates. Post-IR, the wells were imaged using a phase contrast microscope (Leica Microsystems, Germany) and spheroids were analyzed using ImageJ for size differences in response to IR (NIH, Bethesda, MD).

2.8 SPHEROID MIGRATION ZONE ASSESSMENT

To determine the effect of IR and combined IR and CHEK1 SMI on spheroids, the spheroid migration zone was assessed. Spheroid migration zone assessment was modified from that described by Vinci et al. (Vinci, et al. 2013). A fixed endpoint (96 hrs post-plating) was utilized. Non-adherent spheroids were grown as described previously. Plates were coated with Matrigel™ (BD, Franklin Lakes, NJ) for at least 2 hr before use. The spheroids were grown in enriched SC medium and then centrifuged at 900xg for 30 minutes and allowed to attach on Matrigel-coated

plates overnight. Four days post-treatment, plates were fixed with 70% ethanol and stained with Giemsa (Sigma, St. Louis, MO). Plates were then photographed (Leica Microsystems, Germany) and spheroid migration zone analysis was carried out using ImageJ (NIH, Bethesda, MD). The area covered by the spheroids at t= 0 hr and the area covered by the cells that have migrated from the spheroids at t = 96 hr was determined. Data were normalized to the original spheroid recorded using the following formula:

$$\% \text{ migration} = (\text{migrated area } (t = 96 \text{ hr}) / \text{original spheroid } (t = 0 \text{ hr})) \times 100.$$

2.9 CLONOGENIC COLONY SURVIVAL ASSAY

Clonogenic survival assays were carried out to determine cell survival in response to treatment as standardized previously in our lab (Parikh, et al. 2007). Two thousand cells were seeded in 60 mm Petri dishes and allowed to adhere overnight. Cells were then treated with increasing doses of γ-irradiation at 2.5 and 5 Gy using Gammacell 1000 Elite irradiator (Nordion International, Inc., Ottawa, Canada) with a ^{137}Cs source at a dose rate of 2.83 Gy/min. The culture medium was replaced at the end of 7th day. Untreated cells cultured in parallel were used to determine relative plating efficiency and to standardize the treatment plates. After 10-14 days, the plates were fixed with 70% ethanol and stained with Giemsa (Sigma, St. Louis, MO) and the number of colonies was counted. A colony was defined as a cluster of ≥50 cells, having formed from a single cell. All experiments were performed in triplicate, and the error reported as one standard deviation from the mean.

2.10 IMMUNOFLUORESCENCE (IF)

2.10.1 Adherent IF

IF was used to determine whether cells in OSCC cell lines express CSLC markers. $75*10^3$ cells were cultured on square (25mm) coverslips (Thermofisher Scientific, MA) in order to reach a confluency of 75%. The coverslips were then rinsed with 1xPBS and fixed in 4% paraformaldehyde (PF)/1x PBS for 15 minutes in RT. For nuclear/cytoplasmic staining, coverslips were washed with 0.2% Triton X-100/1x PBS; for membrane staining, coverslips were washed with 1xPBS. Cells were then blocked with blocking buffer (1% Bovine serum albumin (BSA) or 3% Rabbit serum, 0.2 M Glycine or Image iT FX signal enhancer (Life Technologies) for 30 - 60 min. Immunostaining with antibodies against CD44 (1:100, 550392, BD), CD133 (1:200, 19898, Abcam), CD133/1(AC133) (1:10, 130-090-422, Miltenyi Biotec), BMI1 (1:400, 6362A, Imgenex), BMI1 (1:400, 14389, Abcam), SOX2 (1:400, 6507A, Imgenex), NESTIN (1:400, 6492A, Imgenex) was carried out at RT for 1 hr. After washing, cells were incubated with secondary antibodies, Goat antimouse Alexa Fluor 488 (1:500, A-11001, Life Technologies) and/or Goat Anti-Rabbit Alexa Fluor 546 (1:500, A-11010, Life Technologies). Nuclei were counterstained with DAPI and mounted with ProLong Gold Antifade Reagent (P10144, Life technologies). Slides were photographed using a confocal fluorescence microscope (Leica Microsystems, Germany).

2.10.2 Suspension IF

Suspension IF was used to assess CSLC in non-adherent spheroids. Spheroids were enriched as described earlier. The spheroid suspension was transferred into a microcentrifuge tube and centrifuged at 800 xg for 3 min and re-suspended in 1 ml PBS. The spheroid suspension was centrifuged at 800 xg for 3 min, and the supernatant was then discarded. The spheroid pellets were re-suspended in 160 µl 1xPBS/20 µl 37% PF for 10 min. Spheroid suspensions were centrifuged, PF was then discarded, and the pellet was re-suspended in 1 ml 1xPBS. The spheroid pellet was permeabilized with 0.3% Triton X-100/1x PBS for 10 min, centrifuged at 800 xg for 3 min, and the supernatant was then discarded. The spheroid pellet was blocked with blocking buffer (1% Bovine serum albumin (BSA) or 3% Rabbit serum, 0.2 M Glycine or Image iT FX signal enhancer (Life Technologies) for 30 - 60 min at RT. The spheroid suspension was centrifuged at 800 xg, the supernatant was then discarded, and the pellet was mixed with 100 µl primary antibody ((CD44 (1:100, 550392, BD), CD133 (1:200, 19898, Abcam), BMI1 (1:400, 6362A, Imgenex) or SOX2 (1:400, 6507A, Imgenex)), thermo-mixed for 30 sec, and then incubated at RT for 1 hr. The spheroid suspension was centrifuged at 800 xg, the supernatant was then discarded and the pellet was washed three times with 1xPBS. 100 µl secondary antibody, Goat antimouse Alexa Fluor 488 (1:500, A-11001, Life Technologies) or Goat Anti-Rabbit Alexa Fluor 546 (1:500, A-11010, Life technologies) was added to the spheroid pellet and themo-mixed for 30 sec and then incubated at RT for 1 hr. The spheroid suspension was centrifuged at 800 xg, the supernatant was then discarded, and the pellet was washed three times with 1xPBS. Cells were counterstained with DAPI for 5 min at RT. Spheroid suspension was centrifuged at 800 xg, supernatant was then discarded and the pellet was mounted with ProLong

Gold Antifade Reagent (P10144, Life Technologies). Slides were photographed using a confocal fluorescence microscope (Leica Microsystems, Germany).

2.11 IMMUNOFLUORESCENCE ASSESSMENT

The intensity of fluorescence was scored as follows: 0-50% as 1 (+), 50-80% as 2 (++) and >80% as 3 (+++); negative staining was scored as 0. CSLC were identified as the 3 (+++) subpopulation in the sample. Random slides were scored by a second researcher, MB; and more than 85% correlation was observed.

2.12 IMMUNOFLUORESCENCE ASSESSMENT OF GAMMA-H2AX, KU70 AND P-CHEK1 FOCI

IF staining for H2AX, KU70 and pCHEK1 foci was used to assess the DDR in CSLC. Foci were analyzed 1 hr after exposure to 2.5 Gy IR using Gammacell 1,000 Elite Irradiator (Nordion International, Ottawa, Canada) with a ^{137}Cs source at a dose rate of 2.83 Gy/min. Dissociated CSLC from enriched spheroids or adherent enriched CSLC were attached to coverslips prior to treatment with IR. Control slides, which were untreated (0 Gy), were prepared for each cell line. Following exposure to IR, the cells were washed with 1x HBSS (Corning, New York), the medium replaced, and the coverslips incubated under standard culture conditions for 1 hr to allow for repair. After 1 hr, the cells were washed with 1x PBS, fixed with 4% PFA (Sigma, St. Louis, MO) for 30 min and permeabilized with 0.2% Tritonx100/1x PBS. Following

permeabilization, cells were blocked with 2% BSA and incubated with anti-gamma-H2AX primary antibody (1:1000, 22551, Abcam), KU70 (1:100, 611892, BD) or p-CHEK1 (1:100, 2348S, Cell Signaling) for 1 hr. The secondary antibody used was a Goat Anti-Rabbit Alexa Fluor 546 (1:500, A-11010 , Life Technologies) or antimouse Alexa Fluor 488 (1:500, A-11001, Life Technologies) for 1 hr. Cells were then washed, counterstained with DAPI, mounted using ProLong Gold Antifade Reagent (P10144, Life Technologies), and analyzed under an epiflorescence/confocal microscope as described earlier. A minimum of 500 cells were scored from control and IR-treated coverslips for each of the cell lines.

2.13 FLOW CYTOMETRY FOR CELL SURFACE MARKER ASSESSMENT

Flow cytometry was used to study CSLC surface markers in OSCC cell lines. Cells were harvested, counted and suspended in ice cold PBS, 10% FCS, 1% sodium azide at 1.5 x 10^6 cells/ml per well in 96 well round bottomed microtiter plates (100 µl/well). Plates were centrifuged at 400 xg for 5 minutes and washed with monoclonal wash (Hanks, 2% FGS and 0.1% sodium Azide). Cells were stained with conjugated monoclonal antibodies: CD44 Mouse monoclonal CD44 FITC (BD, Franklin Lakes, NJ) or CD133/1 (AC133)-PE (Miltenyi Biotec, Bergisch Gladbach, Germany) prepared in ice cold reagents/sodium azide, at the appropriate dilution (Appendix B) for 30 minutes. Unstained controls were prepared by omitting the staining step. Dead cells were detected with propidium iodide (10 µg/mL). The cells were washed twice by centrifugation at 400 xg for 5 minutes and re-suspended in 500 µl to 1 ml of ice cold PBS, 10% FBS, 1% sodium azide. The cells were kept in the dark on ice or at 4°C in a refrigerator until the scheduled time for analysis. For extended storage, cells were fixed in 4% PF to prevent

deterioration. Post-acquisition analysis of the fluorescence-activated cell sorting data and desktop publishing were accomplished using the third-party flow cytometry software FlowJo (Tree star, Ashland, Oregon).

2.14 DIFFERENTIATION ASSAY

To determine the differentiation potential of enriched CSLC cells, spheroids were dissociated by pipetting and cultured in M10 medium on Matrigel™ -coated plates without supplemental growth factors (GF) in the presence of 10% serum (Ricci-Vitiani, et al. 2007).

2.15 CELL CLONING BY SERIAL DILUTION

Serial dilution was used to isolate clones from OSCC cell lines that originated from a single cell per well. These experiments were done by HK and MB. For this study, the cell line UPCI:SCC125 was used to isolate cell clones with and without distal 11q loss. UPCI:SCC125 is a unique cell line showing approximately 50% 11q loss (Parikh, et al. 2007). Serial dilution was done in a 96-well plate, single colonies were then dissociated and transferred sequentially to 12-well plates, 6-well plates and T25 flasks. The clones were then assessed by FISH for *ATM* status.

2.16 EXTREME LIMITING DILUTION ASSESSMENT

The aim of extreme limiting dilution assessment is to study the SC frequency in cultures and to determine the clonogenic potential of CSLC in response to therapeutic interventions. 96-well plates coated with agarose as described by Friedrich et al. (Friedrich, et al. 2009) and spheroid medium were used. A 2 ml cell suspension containing 20,000 viable cells was prepared. 200 µl/well were loaded in row A (columns 1-12) and 100 µl was loaded in other well row B-H (columns 1-12). Serial dilution was done down row B through to row H. Plates were assessed for spheroid formation in 7-10 days post plating. Analysis of CSLC was done using CSLC analysis software (Hu and Smyth 2009).

2.17 MITOTIC CELL COLLECTION AND ANALYSIS

To assess mitotic cell division, slides were prepared using the following approach. A method increasing the mitotic division was used modified from that described previously by Lathia et al. was used (Lathia, et al. 2011). Adherent cultures grown on Matrigel™-coated coverslips in M10 medium were enriched with 2mM thymidine for 48 hr. Cells were then cultured for 12 hr in M10 medium without thymidine. After washing with 1x PBS, mitotic cells were shaken off the plates by vortexing for 30 s. Detached cells were collected and settled onto Matrigel™-coated coverslips at the bottom of the 6-well plates using centrifugation at 200 xg. for 15 min at RT (room temperature). Cells were then stained with DAPI or an IF marker as described previously. Fluorescence images were acquired using a confocal microscope (Leica Microsystems, Germany); images were processed and assembled using ImageJ (NIH, Bethesda, MD). To

quantify the degree of asymmetric:symmetric distribution of the CSLC marker between the two daughter cells, the intensity of fluorescence was assessed for each daughter cell. Images of intermediate/late anaphase to telophase were collected for assessment. The dividing daughter cells were defined by the condensed DNA detected by DAPI staining. Each identified daughter cell in a dividing pair was marked with the freehand tool, and the fluorescent signals of the defined daughter cells were determined for the CSLC markers. In order to classify the division type, percentage (%) difference was calculated as follows: F= (F1-F2/F1+F2)*100; where F1 and F2 represent the fluorescent values of a given stain for two dividing daughter cells. The asymmetric cutoff was set based on the evaluation of a cluster analysis as in similar previous studies (Lathia, et al. 2011).

2.18 CHROMOSOMAL SEGREGATION DEFECTS ASSESSMENT

CSD assessment was used to assess the segregation defects post-IR in CSLC (SOX2+) and non-CSLC (SOX2-). We analyzed mitotic defects in OSCC cell lines grown on Matrigel™-coated coverslips. Cells were either untreated or treated with 2.5 Gy and then grown for 36 hours. At the end of the 36 hours, the cells were fixed with 4%PF/1xPBS, dried, and IF stained with SOX2 as previously described. Coverslips were mounted onto slides with ProLong Gold Antifade Reagent. More than 1000 cells were analyzed from each cell line. The frequencies of anaphase and interphase bridges, unclassifiable defects and micronuclei were recorded. The values for cell lines were averaged and grouped into two categories, ‘CSLC’ and ‘Non-CSLC.’

2.19 CELL VIABILITY ASSAY

Cell survival/viability assays assessed the survival of CSLC post-intervention. Two methods were used, the first using a Live/Dead Viability/Cytotoxicity Kit and the second involved using trypan blue exclusion.

2.19.1 Live/Dead Viability/Cytotoxicity Kit

Viability assays were done using the LIVE/DEAD Reduced Biohazard Viability/Cytotoxicity Kit L-7013 (Thermo Fisher Scientific, Carlsbad, CA). Cells were attached to sterile glass coverslips, treated with IR, and stained 72 hrs after the treatment. Culture medium was removed and cells were washed with HBSS. A mixture of SYTO 10 green fluorescent nucleic acid stain (Component A) and ethidium homodimer-2 nucleic acid stain (Component B) were diluted in HBSS (1:500 dilution of each). 200 µL was applied to each coverslip, and then incubated in the dark for 15 minutes. Coverslips were then washed twice with HBSS. Coverslips were then incubated with 4% Paraformaldehyde for 30 minutes. Coverslips were then mounted to slides using ProLong Gold Antifade Reagent, and analyzed under a epiflorescence/confocal microscope (Leica Microsystems, Germany).

2.19.2 Cell viability Assay using Trypan Blue Exclusion

Equal volumes of cell suspension and 0.4% trypan blue (15250-061, Life Technologies) were thoroughly mixed and assessed using a hemacytometer. Cell viability was calculated as the number of viable cells divided by the total number of cells within the grids on the

hemacytometer. If cells stained blue due to uptake of trypan blue, they were considered non-viable.

2.20 STATISTICAL METHODS

2.20.1 General statistical methods

All studies were done in triplicate and results compared by the most appropriate statistical methods. A biostatistician was consulted to verify the methods used in the analysis. Most data are presented as the mean ± SEM, unless otherwise specified. Any p value < 0.05 was considered statistically significant.

2.20.2 Assessment of prognostic significance of CSLC markers in OSCC

Correlation of CSLC markers with various prognostic factors was done to investigate the possible role of CSLC in OSCC prognosis. To assess the prognostic significance of CSLC markers (CD44, CD133, SOX2 and BMI1), patients were grouped based on clinical covariates of interest as categorical variables (histological grade, T, N and TNM staging, smoking, HPV and *TP53*) and CSLC expression (high/low). Fisher's exact test was used to assess the statistical significance within the two groups based on the sample size; p values < 0.05 were considered statistically significant. Statistical analyses were performed using the SAS System for Windows, Version 9.2 (SAS Institute Inc., Cary, NC). Tumor size and CSLC marker expression were analyzed as continuous values. Pearson's correlation was then used to calculate the correlation

coefficient between tumor size and CSLC marker positive group. For survival analysis, CSLC expression of CD44, CD133, SOX2 and BMI1 was grouped into CSLC high and CSLC low groups. Kaplan–Meier survival statistics were used to evaluate OS (time from definitive cancer treatment to death of any cause) among CSLC high and low. Any p value < 0.05 was considered statistically significant.

3.0 RESULTS

3.1 CSLC MARKERS IN OSCC CELL LINES

3.1.1 CSLC markers in OSCC cell lines

To determine the expression of CSLC markers in a group of 18 OSCC cell lines we utilized IF (Table 5); our main objective was to assess which markers could be further used in investigating the properties of CSLC and to assess the prognostic significance of CSLC markers. The OSCC cell lines expressed CSLC markers variably, suggesting the possible role of these markers in prognosis (Figures 8-16). There was no statistical difference between OSCC cell lines with distal 11q loss (UPCI:SCC029B and SCC040) and no distal 11q loss (UPCI:SCC066 and SCC116) based of CSLC marker (Figure 9). Positive (+++) CD44 and BMI1 were expressed at higher rates (23 and 16% respectively) when compared to CD133/1 and SOX2 (6 and 6% respectively). Flow cytometric analyses of four OSCC cell lines revealed that the proportion of CD44+ cells was uniformly high; CD133/1 was inconsistent on replication (Figure 16). Double IF staining with different CSLC markers demonstrated that only ≈1-3% of the cells co-express the CSLC marker (Figures 13, 14). Assessing CSLC markers in a normal oral epithelial cell line (OKF6) showed that CD133/1, SOX2 and BMI1 are not expressed; only CD44 was expressed (Figures

12, 13). Overall, our results suggest that CSLC markers (CD133/1, SOX2 and BMI1) are overexpressed in a cancer cells. Furthermore, double IF of OSCC with CSLC markers has yielded high correlative evidence that a subpopulation of cells exists in our cell lines with SC potential (Figures 14, 15). Our results have also indicated that CD133/1 and SOX2 may be promising CSLC markers in OSCC.

Table 5. Measures of Central Tendency of CSLC-Positive (+++) Cells in UPCI:SCC Cell lines* as assessed by IF

	MEAN	MODE	MEDIAN
CD44	23.11111	15	21
CD133$^{/1}$	6.444444	9	5.5
SOX2	6.8125	6	6
BMI1	16.27778	16	14.5

* UPCI:SCC cell lines investigated: UPCI:SCC029B, SCC040, SCC056, SCC066, SCC078, SCC084, SCC099, SCC103, SCC104, SCC114, SCC116, SCC122, SCC125, SCC131, SCC136, SCC143, SCC172, SCC182.

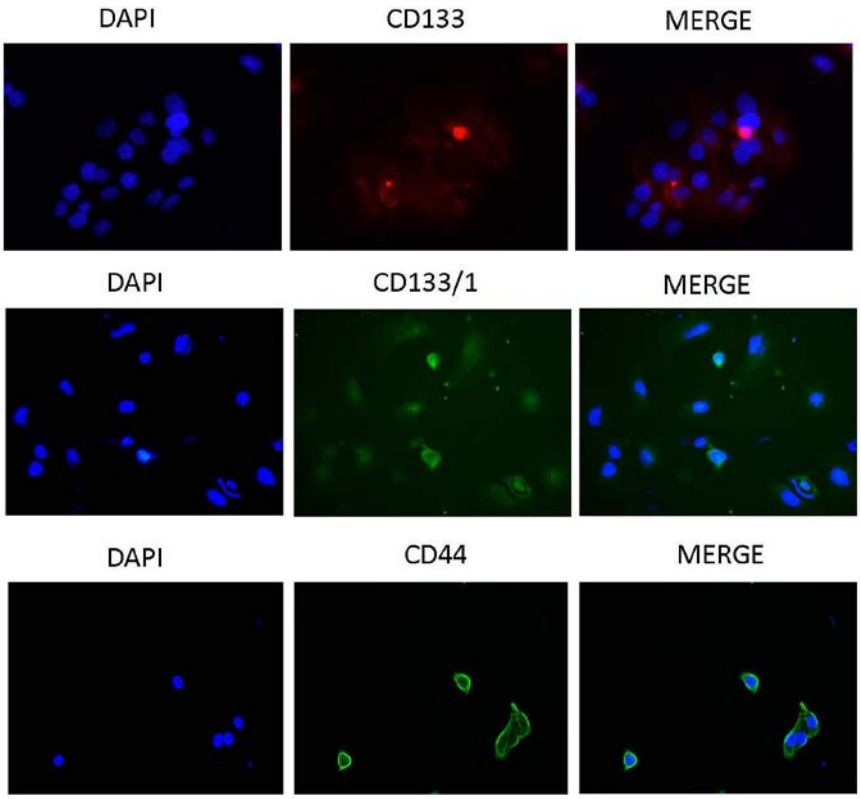

Figure 8. IF staining of UPCI:SCC029B with CSLC surface markers

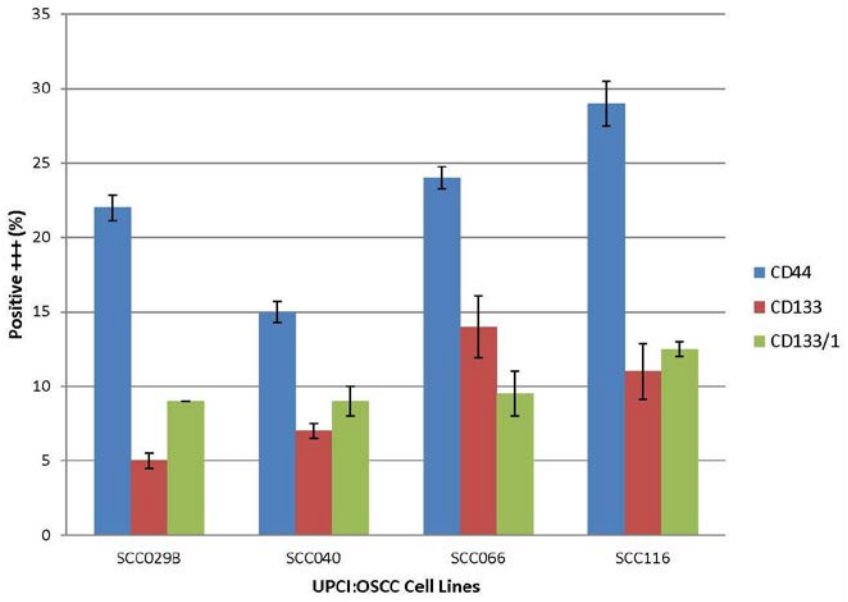

Figure 9. Frequencies of positive cells as assessed by CSLC surface markers

No statistically significant difference is observed in the frequency of cells positive for CSLC markers between OSCC with distal 11q loss (UPCI:SCC029B and SCC040) and without distal 11q loss (UPCI:SCC066 and SCC116).

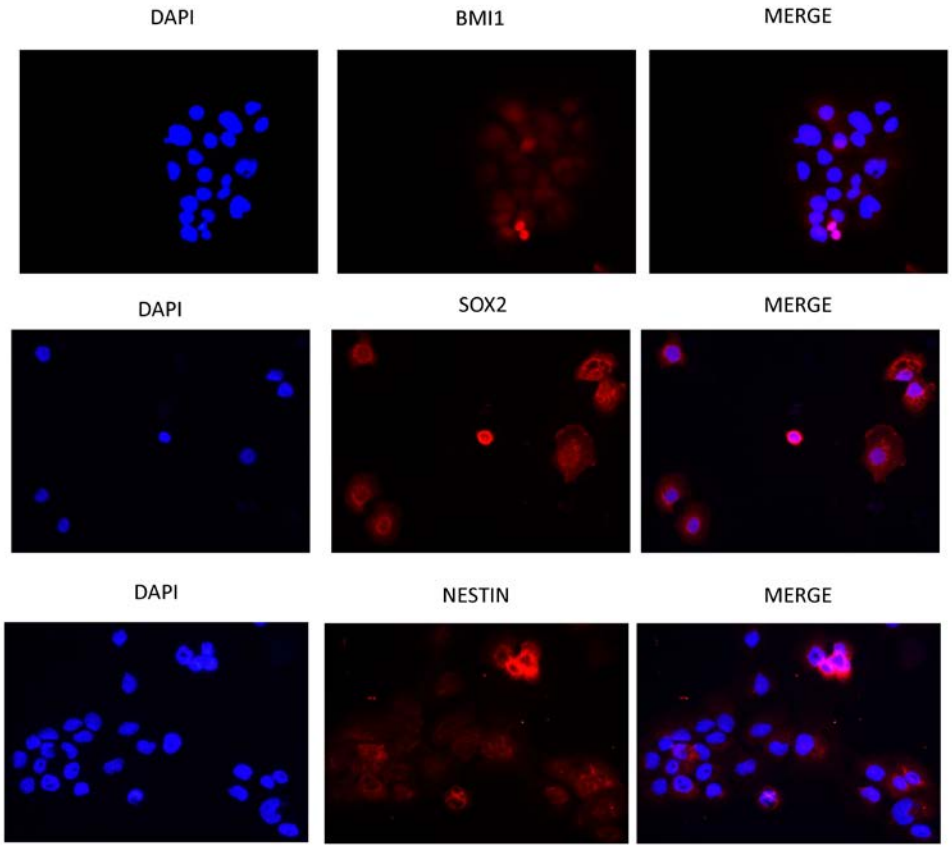

Figure 10. IF staining of UPCI:SCC029B with CSLC markers

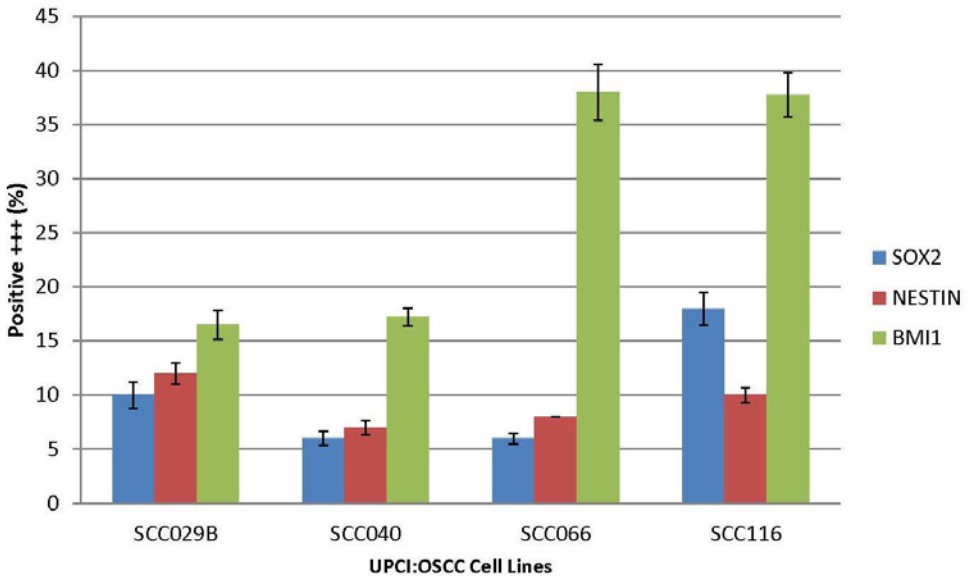

Figure 11. Frequencies of positive cells as assessed by CSLC markers

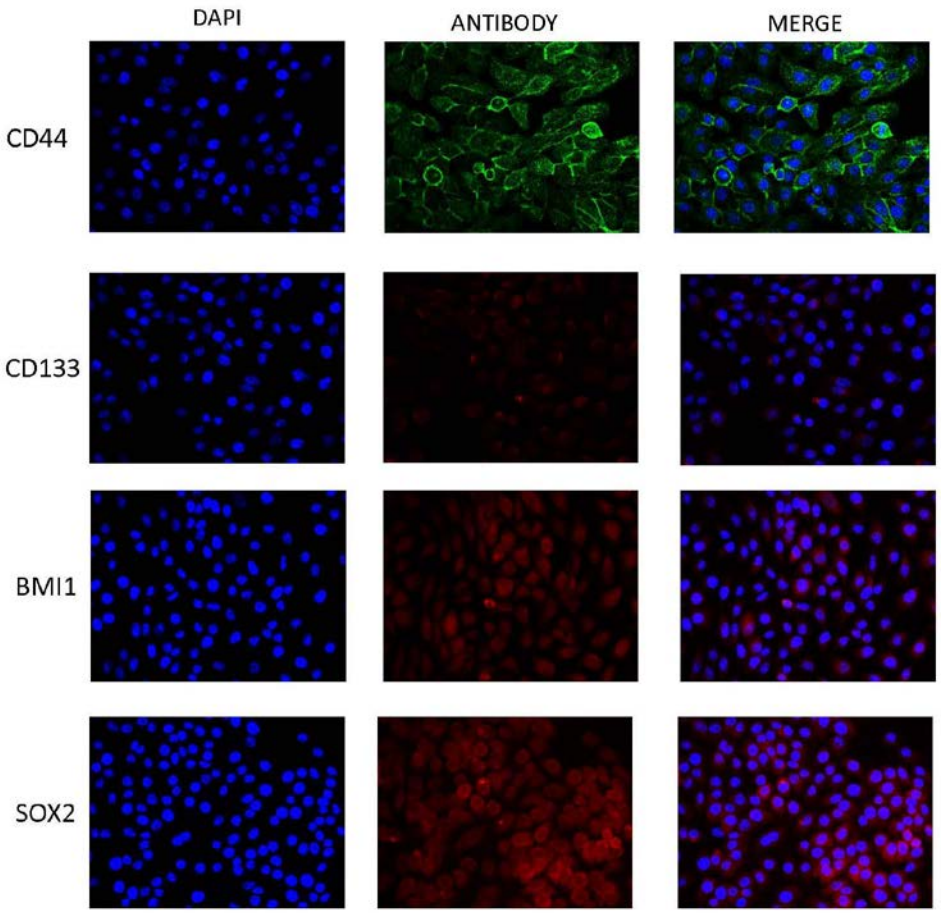

Figure 12. IF of the control cell line, OKF6 with CSLC markers

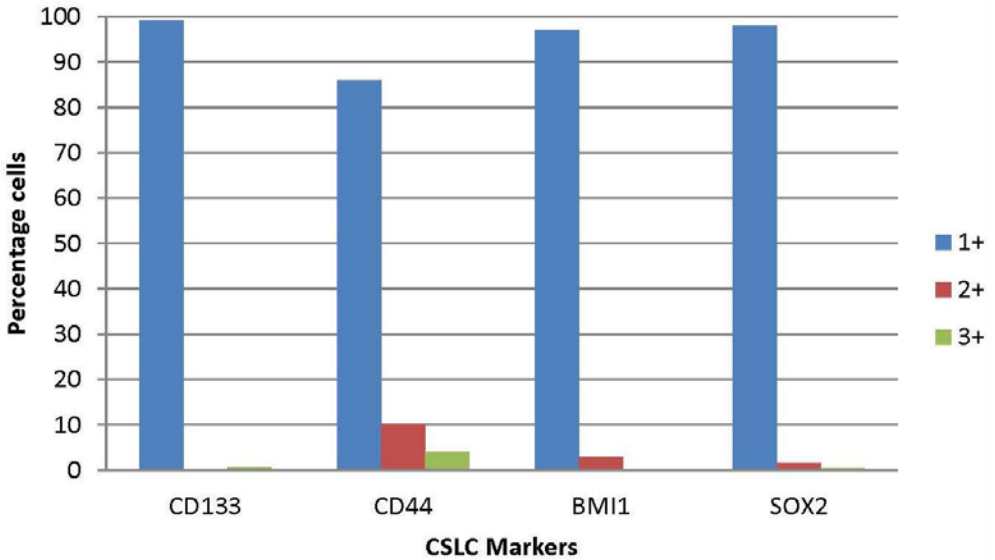

Figure 13. Frequencies of positive cells as assessed by CSLC markers in the control cell line, OKF6

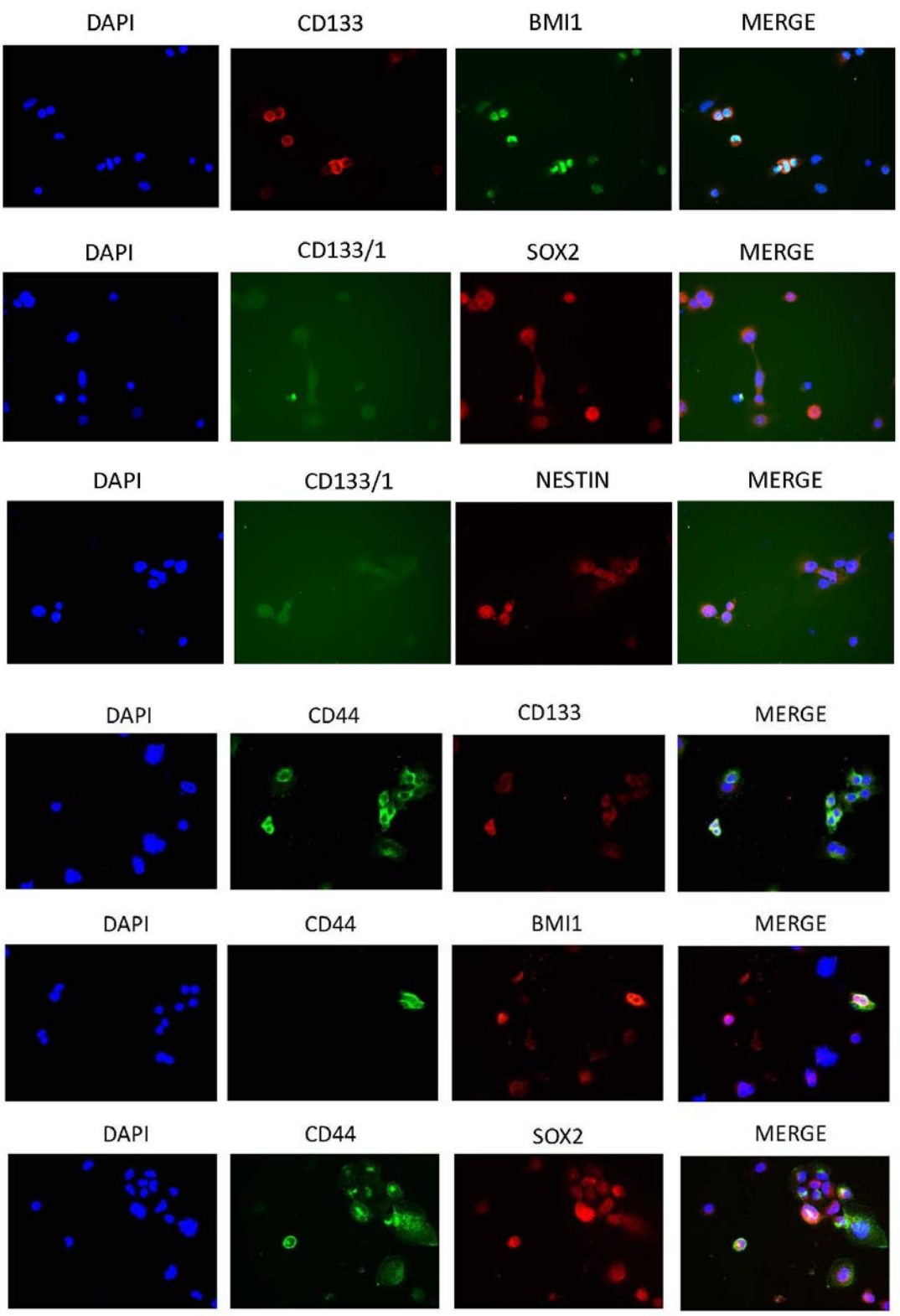

Figure 14. Double IF staining of UPCI:SCC029B with CSLC markers

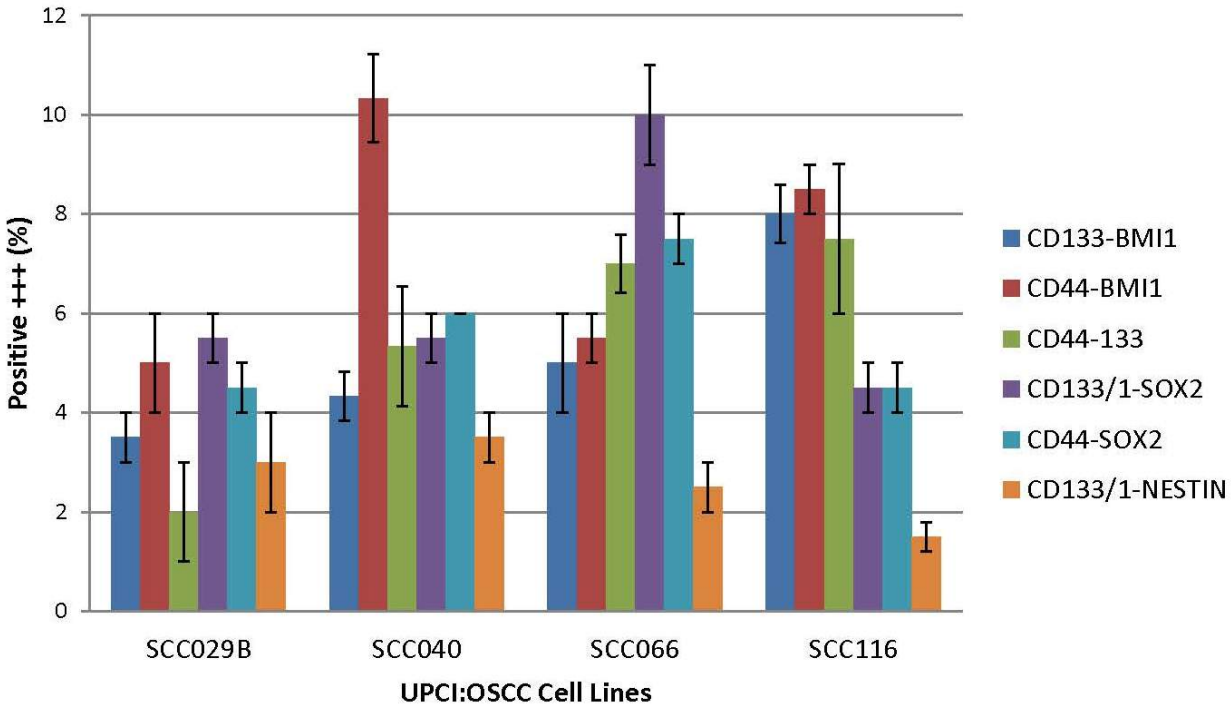

Figure 15. Double IF staining of OSCC cell lines utilizing CSLC marker combinations

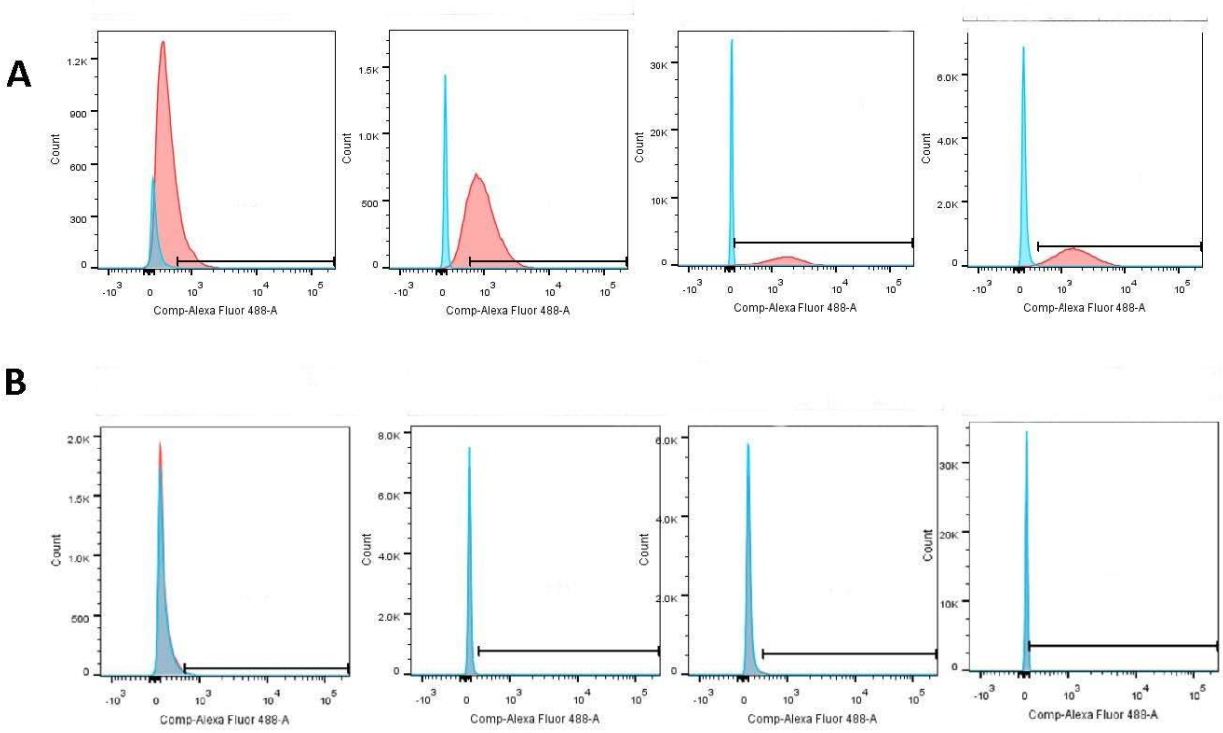

C

Flow cytometric analyses		
Population	CD44	CD133/1
UPCI:SCC029B	HT	IN
UPCI:SCC040	HM	IN
UPCI:SCC066	HM	IN
UPCI:SCC116	HM	IN

Figure 16. Flow cytometric analysis of OSCC tumor cells isolated and cultured under identical conditions

A. Change in fluorescence intensity was measured by flow cytometry for unlabeled cells (blue peaks) and cells labeled with CD44 (red peaks). Gated runs were analyzed with FlowJo modeling software (Left to Right: UPCI:SCC029B, UPCI:SCC040, UPCI:SCC066 and UPCI:SCC116).
B. Change in fluorescence intensity was measured by flow cytometry for unlabeled cells (blue peaks) and cells labeled with CD133/1(red peaks). Gated runs were analyzed with FlowJo modeling software (Left to Right: UPCI:SCC029B, UPCI:SCC040, UPCI:SCC066 and UPCI:SCC116).

C. Table showing the summarized results of flow cytometric analyses of each cell line (HM, Homogenous high staining; HT, two distinct population; N, Negative for the marker; IN, determined inconsistent among the replicates studied).

3.1.2 Prognostic significance of CSLC markers in OSCC cell lines

We assessed the prognostic significance of CSLC markers (CD44, CD133/1, SOX2 and BMI1) by IF in a panel of 18 OSCC low passage cell lines, previously established in our Lab (White, et al. 2007). Cut-offs for CD44, CD133/1, SOX2 and BMI1 in all 18 OSCC specimens were estimated based on previous literature (Chinn, et al. 2015; Joshua, et al. 2012) and the median for each marker (23%, 5%, 5% and 16%, respectively; Table 5) and categorized as high or low based on the frequency of positive cells (+++). Tumor grading was classified as early (stages I/II) or advanced stage tumors (stages III/IV). Lymph node staging was classified as negative (N0) or positive (N1, N2). Histological differentiation was classified as differentiated, moderately differentiated or poorly differentiated. Smoking and HPV status were each classified as positive or negative.

We did not find prognostic significance between CSLC marker and tumor grade, LN positivity, histological differentiation, recurrence/relapse, smoking, HPV status, tumor size and *TP53* status ($p>0.05$)(Table 6). Tumor specimens were analyzed for association between CSLC marker and recurrence/relapse. Patients who developed recurrence/relapse had higher CD44-high compared to patients with CD44-low cell lines; however, this was not statistically significant (CD44: 58% vs 50%; $p>0.05$). CD133/1-high, SOX2-high and BMI1-high did not show a statistically significant relationship with recurrence or relapse (CD133/1: 67% vs 67%, $p>0.05$; SOX2: 58% vs 60%, $p>0.05$; BMI1: 42% vs 67%, $p>0.05$)

Analysis of patient survival outcomes relative to CSLC markers was performed (Figure 17). There was no difference in OS (CD44 p>0.05; CD133/1 p>0.05; SOX2, p>0.05; BMI1, p>0.05) between patients with CSLC high compared to those with CSLC low.

Table 6. Prognostic significance of CSLC marker in a group of 18 OSCC cell lines[a]

	CD44		SOX2		BMI1		CD133	
Range	2-63%		2-18%		2-39%		2-12%	
Characters	High positive cases (%)	P value	High positive cases (%)	P value	High positive cases (%)	P value	High positive cases (%)	P value
T grade								
T1/T2	4/11(36%)	p > 0.05	5/11(45%)	p > 0.05	4/11 (36%)	p > 0.05	6/11 (55%)	p > 0.05
T3/T4	4/7 (57%)		5/6(83%)		5/7 (71%)		6/7 (86%)	
N grade								
N0	5/9 (56%)	p > 0.05	5/9(56%)	p > 0.05	4/9 (44%)	p > 0.05	5/9 (56%)	p > 0.05
N1/2	2/5 (40%)		4/7(57%)		5/8 (63%)		7/8 (88%)	
Histology								
Well	1/2 (50%)	p > 0.05	1/2(50%)	p > 0.05	1/2 (50%)	p > 0.05	1/2 (50%)	p > 0.05
Moderate	7/12 (58%)		7/11(64%)		6/12 (50%)		9/12 (75%)	
Poor	1/2 (50%)		1/2(50%)		2/2 (100%)		1/2 (50%)	
Tumor size								
	0.4264	p > 0.05	0.2331	p > 0.05	0.1835	p > 0.05	0.2334	p > 0.05
		Weak +ve correl[b]		Weak +ve correl[b]		Weak +ve correl[b]		Weak +ve correl[b]
Recc/rel[c]								
N0	3/6 (50%)	p > 0.05	3/5(60%)	p > 0.05	4/6 (67%)	p > 0.05	4/6 (67%)	p > 0.05
YES	7/12 (58%)		7/12(58%)		5/12 (42%)		8/12 (67%)	
Smoking[d]								
N0	1/2 (50%)	p > 0.05	1/2(50%)	p > 0.05	1/2 (50%)	p > 0.05	2/2 (100%)	p > 0.05
YES	8/15 (53%)		8/14(57%)		7/15 (47%)		9/15 (60%)	
HPV[d]								
N0	9/17 (53%)	p > 0.05	9/16(56%)	p > 0.05	8/17 (47%)	p > 0.05	11/17 (65%)	p > 0.05
YES	1/1 (100%)		1/1(100%)		1/1 (100%)		1/1 (100%)	
TP53 status[e]								
Wild	1/5(20%)	p > 0.05	4/5(80%)	p > 0.05	3/5(60%)	p > 0.05	3/5(60%)	p > 0.05
Mutant	7/13(54%)		6/12(50%)		6/13(46%)		9/13(69%)	

[a] - UPCI:SCC cell lines investigated: UPCI:SCC029B, SCC040, SCC056, SCC066, SCC078, SCC084, SCC099, SCC103, SCC104, SCC114, SCC116, SCC122, SCC125, SCC131, SCC136, SCC143, SCC172, SCC182.
[b]- Weak positive correlation.
[c]- Recurrence/relapse.
[d]- Data extracted from (White, et al. 2007).
[e]- Data extracted from (Telmer, et al. 2003; White, et al. 2007).

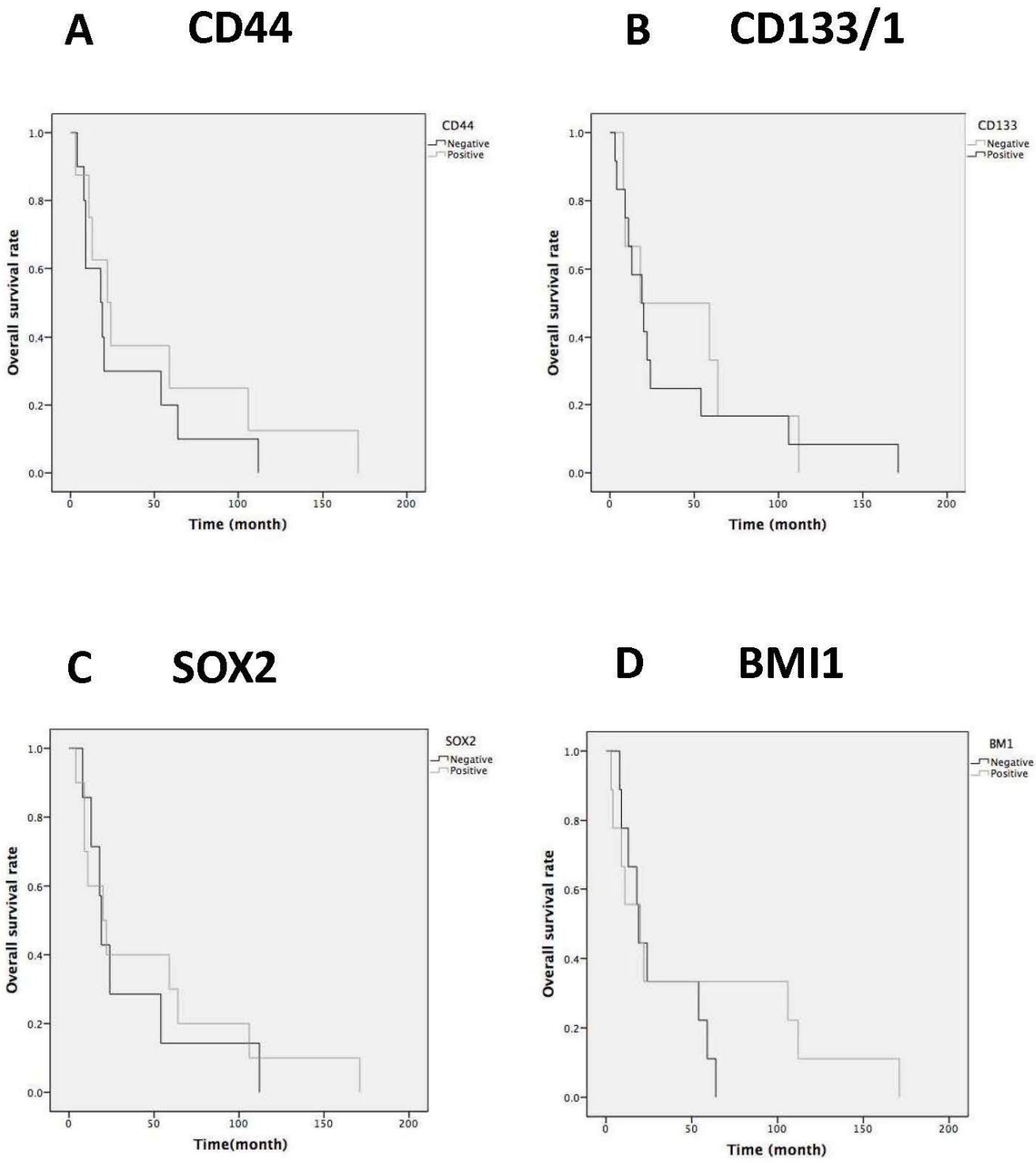

Figure 17. Kaplan-Meier survival analysis of CSLC (high) in 18 OSCC cell lines

A. CD44 **B.** CD133/1 **C.** SOX2 **D.** BMI1.

3.2 DIVISION PATTERNS OF CSLC IN OSCC CELL LINES

3.2.1 Division patterns of CSLC in OSCC cell lines

To evaluate the division patterns of CSLC, we used IF staining, intensity mitotic pair analysis and size mitotic pair analysis utilizing a panel of CSLC markers (CD44, CD133/1, NESTIN, BMI1 and SOX2) in OSCC cell lines. Cluster analysis based on the intensity mitotic pair analysis was carried out (Figure 18); using a modification of the method described by Lathia et al. (Lathia, et al. 2011). Based on our cluster analysis results, symmetrical division was defined when the percentage difference of the stained marker is less than 20% and asymmetrical when the percentage difference is more than 20% (Figure 18). We found that only SOX2 showed significant equal and unequal distribution during mitosis as assessed by cluster analysis (Figure 18). CD133/1 staining was faint, and was therefore not analyzed; CD44, NESTIN and BMI1 showed some intensity variability (Figure 22); however the cluster and mitotic pair analysis (not shown) was not statistically significant.

Under standard serum rich culture conditions, three distinct modes of cell division based on SOX2 were observed, Symmetric SOX2 self-renewing division (positive/positive pair), symmetric non-SOX2 differentiating division (negative/negative pair) and asymmetric SOX2 self-renewing/differentiating division (positive/negative pair) (Figure 18). Analysis of the division patterns of SOX2+ mitotic pairs reveals that the main mode of division observed is symmetric division (≈ 75%), which leads to expansion of the CSLC population (Figure 18). Further assessment of the mitotic pair analysis based on SOX2 intensity shows that SOX2 begins

to be detected in early stages of cell division such as metaphase. In later stages of mitosis, SOX2 is distinct in the mitotic pair (Figure 22). This might indicate that the specification of cell fate starts early in mitosis and gets determined all through the mitotic stages.

We further assessed SOX2 staining during cell division by size mitotic pair analysis (Figures 18, 19). For this objective, we analyzed all the asymmetrical mitotic pairs based on size difference that we observed. As shown in Figure 19, some mitotic pairs (≈ 40%) showed size differences as well as intensity difference that we noted earlier. The sample mitotic pair shown in Figure 19 showed that one of the daughter cells (cell 2) was double the size of the other daughter cell (cell 1). Our size mitotic pair analysis adds further evidence supporting the presence of asymmetrical divisions in our cell lines.

Furthermore, to confirm that the SOX2 mitotic division patterns we observed are not an artifact, dual IF staining with α-tubulin and phospho-Histone H3 was carried out (Figure 21). SOX2/α-tubulin dual staining confirmed that SOX2 determination exists in the dividing mitotic pair, during both symmetrical and asymmetrical cell division as evidenced by presence of cleavage furrows (Figure 22) (Lathia, et al. 2011). Similarly, phospho-Histone H3, a marker of mitotic division also showed equal symmetrical staining of the chromatin regardless of SOX2 distribution (Figure 21). Overall, our results demonstrate that SOX2+ cells are capable of utilizing both symmetrical and asymmetrical cell division to maintain a SOX2+ population, this property being a characteristic of CSLC.

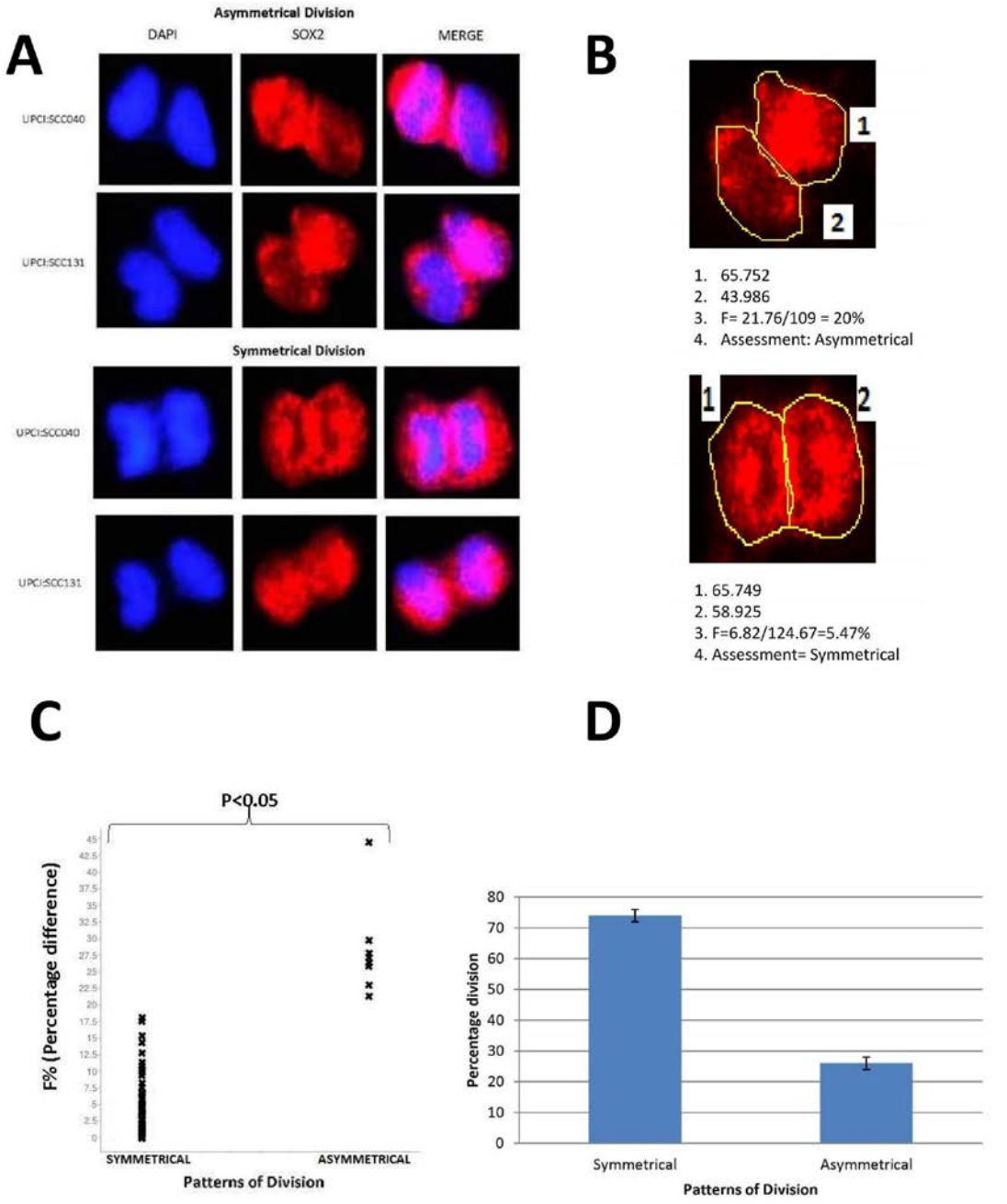

Figure 18. SOX2 as a marker of CSLC division

A. SOX2 staining showing symmetrical and asymmetrical divisions of OSCC. **B.** Mitotic Pair analysis of the cell lines UPCI:SCC040 and UPCI:SCC131 using image analysis software (Image J). **C.** Cluster Plot of Mitotic Pair analysis of the cell lines UPCI:SCC040 and UPCI:SCC131 stained with SOX2 (n=63). Data were analyzed for statistical significance using the student's t test. **D.** Percentage of symmetrical to asymmetrical divisions in OSCC cell lines UPCI:SCC040 and UPCI:SCC131.

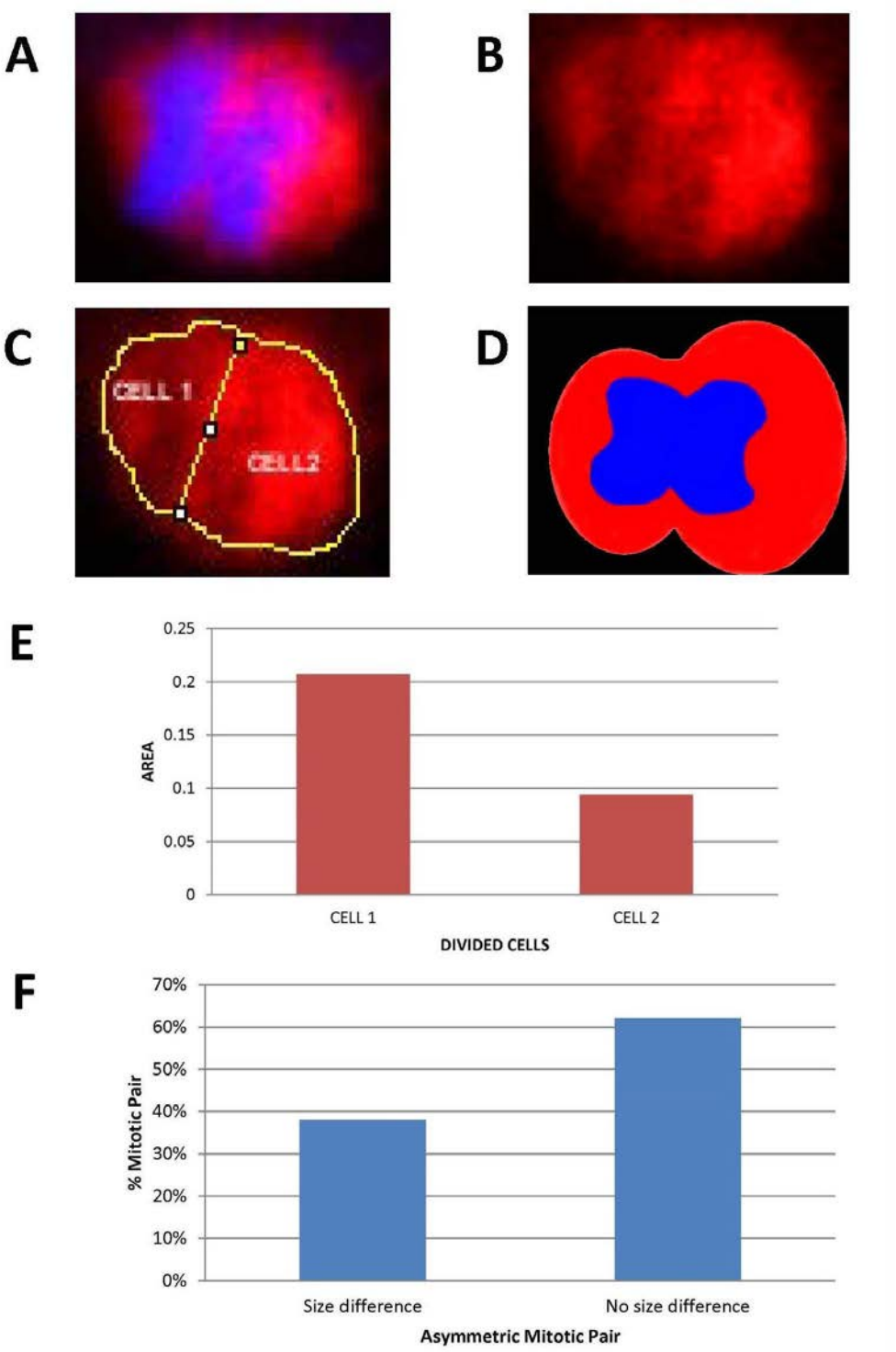

Figure 19. Mitotic Pair analysis of a representative image from the cell line, UPCI:SCC131 showing significant differences in cell size

A. SOX2/DAPI stain merged **B.** SOX2 immunostaining **C.** Demarcated cell pair **D.** Artistic representative image of the size difference of the mitotic pair **E.** Histogram showing the size differences between the mitotic pairs **F.** Histogram showing the percentage of asymmetric mitotic pairs based on size difference.

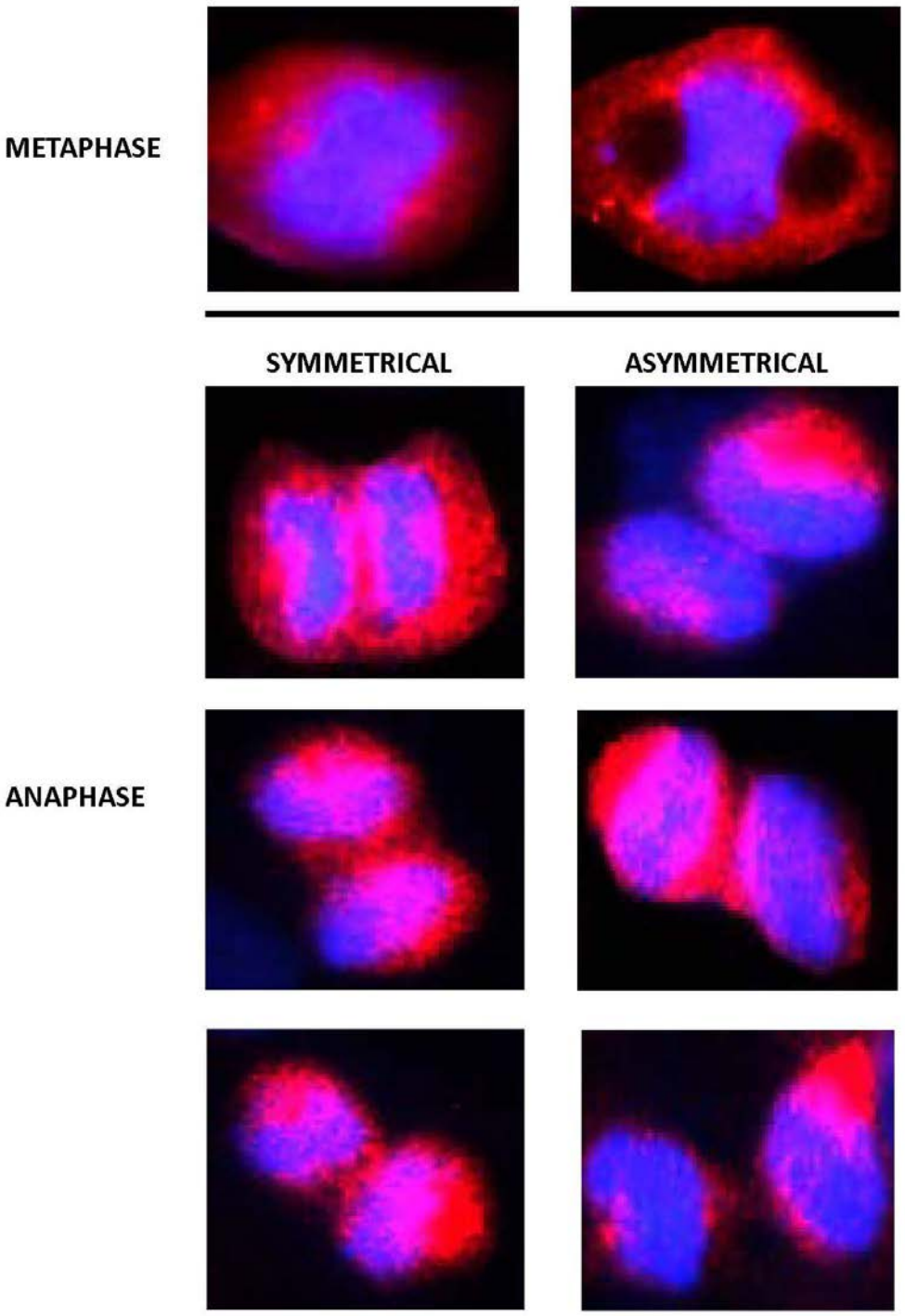

Figure 20. Mitotic Pair analysis of representative images of the cell line UPCI:SCC131 in different stages of division

In metaphase, SOX2 appears in the dividing cells; in anaphase, SOX2 immunostaining can be clearly identified in the mitotic pair.

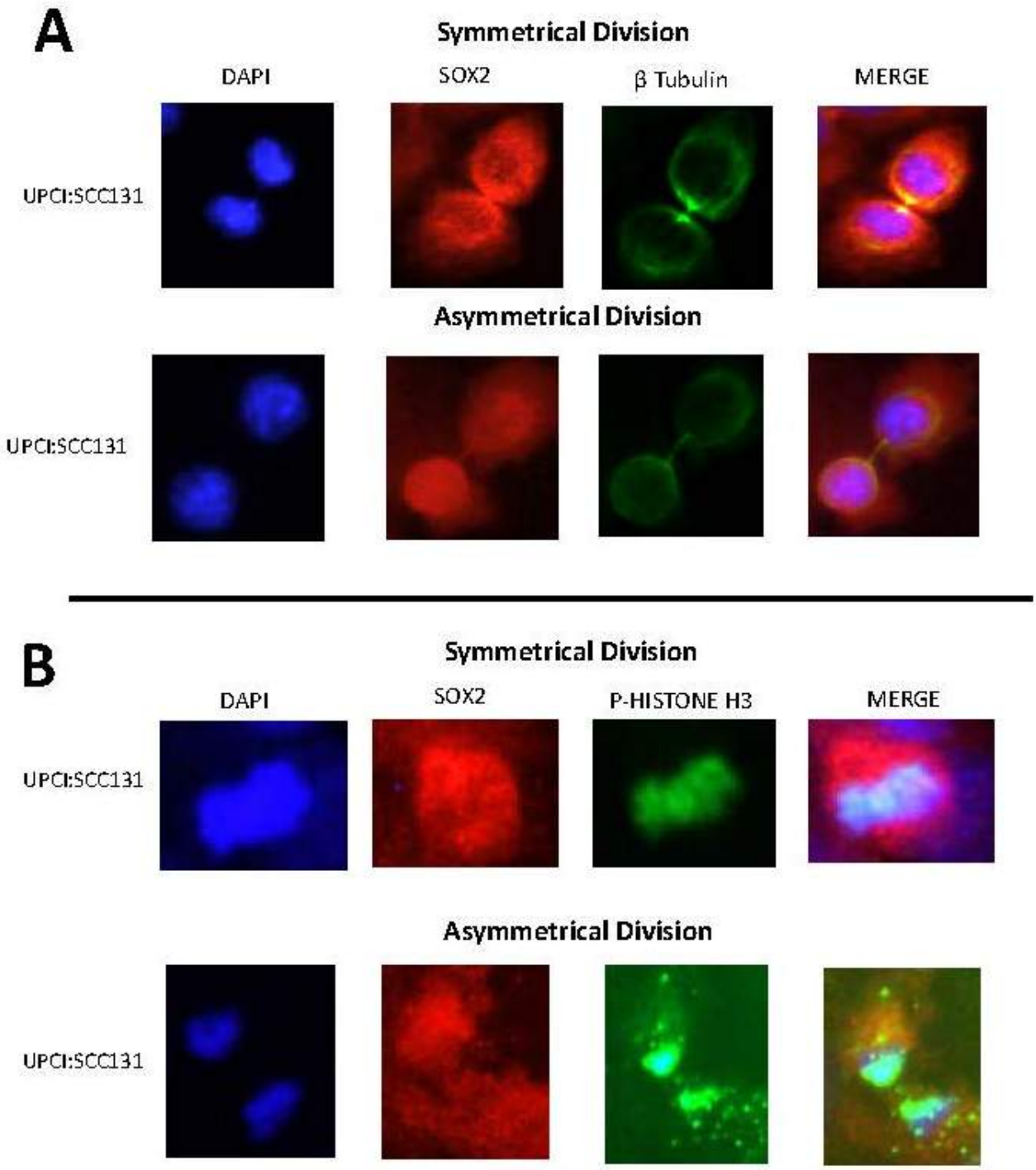

Figure 21. Double immunofluorescence staining of SOX2+ CSLC with markers of cell division α-tubulin and phospho-Histone H3

Double IF staining of SOX2+ CSLC with markers of cell division α-tubulin and phospho-Histone H3 shows mitotic division and SOX2 redistribution during both symmetrical and asymmetrical division.

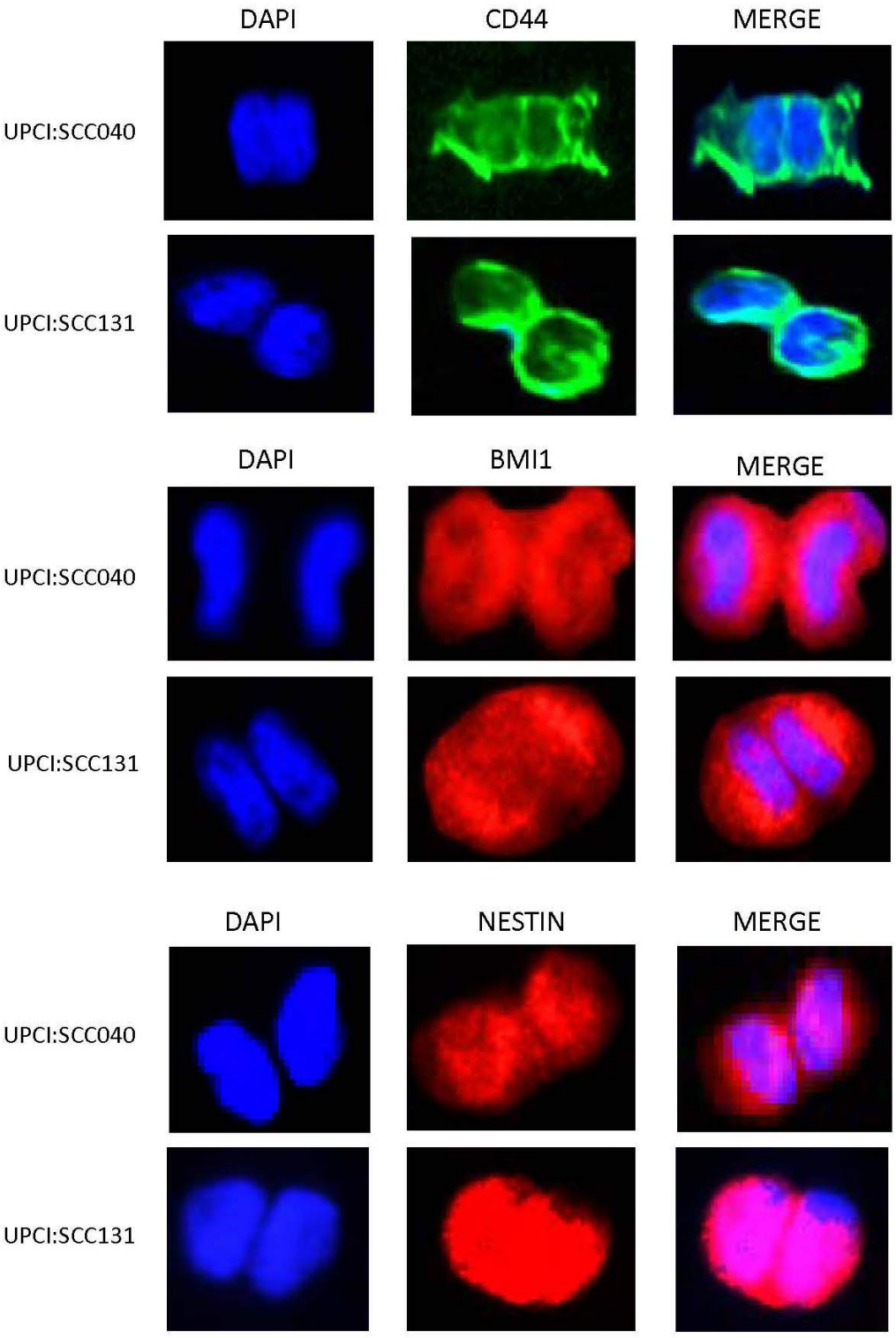

Figure 22. Immunofluorescence staining of CSLC markers in OSCC cell lines during cell division

IF staining with markers of CSLC, CD44, BMI1 and NESTIN shows symmetrical division and no asymmetrical division as confirmed by mitotic pair analysis.

3.2.2 Division patterns in response to IR and enriched spheroid medium

To assess the possible changes in cell division patterns of SOX2+ CSLC in response to external environmental changes, we cultured OSCC cell lines on Matrigel™-coated plates and exposed the cells to IR regimens or enriched SC medium (Figure 23). We expected the dynamics of the division to change in response to the changes in the external environment owing to the central role of CSLC in disease progression. Our results show that the division pattern did not change in response to IR (2.5 Gy*3) and (2.5 Gy*6) as shown in Figure 23. On the other hand, when enriched medium was added to the culture, we observed a decrease in asymmetrical SC division (Figure 23).

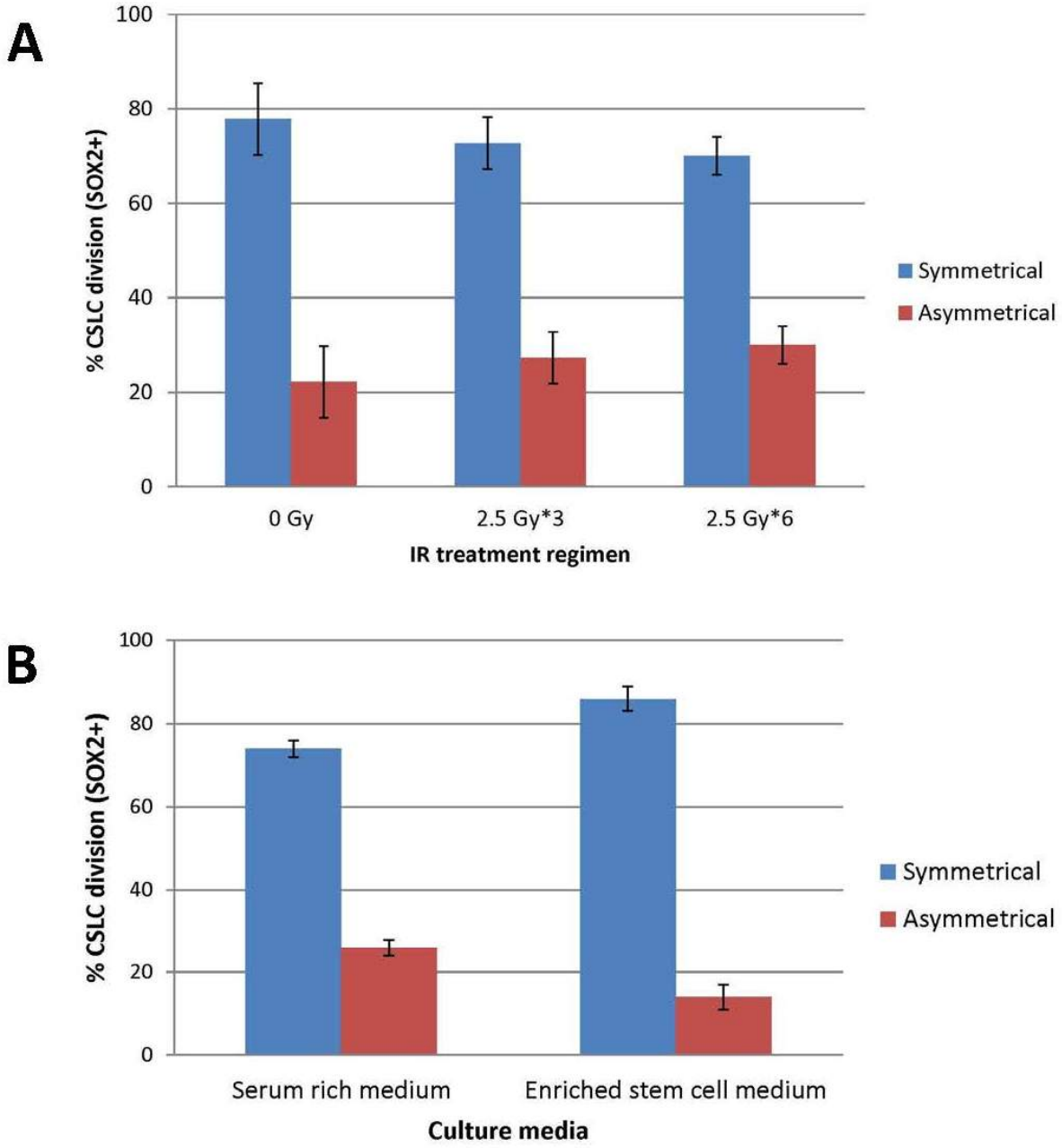

Figure 23. SOX2+ CSLC division in response to IR and enriched SC medium

A. Division patterns of SOX2+ CSLC in response to IR regimens; after three doses of 2.5 Gy and after six doses of 2.5 Gy. **B.** Division patterns of SOX2+ CSLC in response to enriched SC medium (Error bars +/- SEM).

3.2.3 Chromosomal Segregation Defects in CSLC in OSCC cell lines

To assess CSD in CSLC and non-CLSC, we used SOX2 to mark CSLCs in OSCC cell lines in response 2.5 Gy IR (36 hrs post-IR). Assessment of CSD have been previously standardized in our lab; and based on our previous results, we chose UPCI:SCC040 and 131 for our study (Sankunny, et al. 2014; Saunders, et al. 2000). Based on our observation that SOX2 shows high correlation with other CSLC markers in dual-staining and that SOX2 was the only marker that showed symmetrical and asymmetrical division patterns, we choose SOX2 as a marker of CSLC. We then measured the frequencies of micronuclei, anaphase bridges, interphase chromosome bridges, and unclassifiable defects which are caused by misrepaired DNA and chromosomes and/or defective chromosomal segregation (Fenech, et al. 2011).

The frequencies of CSDs in CSLC (SOX2+) and non-CSLC (SOX2-) are shown in Figures 23 and 24. Non-CSLC (SOX2-) had more than 20-fold higher frequency of CSDs when compared to CSLC (SOX2+). Interestingly, the segregation defects observed in CSLC were more frequently associated with symmetrical divisions than asymmetrical divisions (Figure 24). Furthermore, the types of segregation defects observed in CSLC (SOX2+) and non-CSLC (SOX2-) were different (Figures 24, 25). Anaphase bridges were predominant in CSLC (SOX2+) and micronuclei were predominant in non-CSLC (SOX2-). The difference in CSD between CSLC (SOX2+) and non-CSLC (SOX2-) might be due to some form of mitotic arrest by CSLC for repair of DNA defects or other causes. On the other hand, non-CSLC (SOX2-) seem to continue the cell cycle, resolving anaphase bridges into aberrant nuclear chromosomes, micronuclei, and/or interphase bridges. Overall, our results provide additional support to the proposition that CSLC have enhanced DNA repair machinery; further studies are warranted.

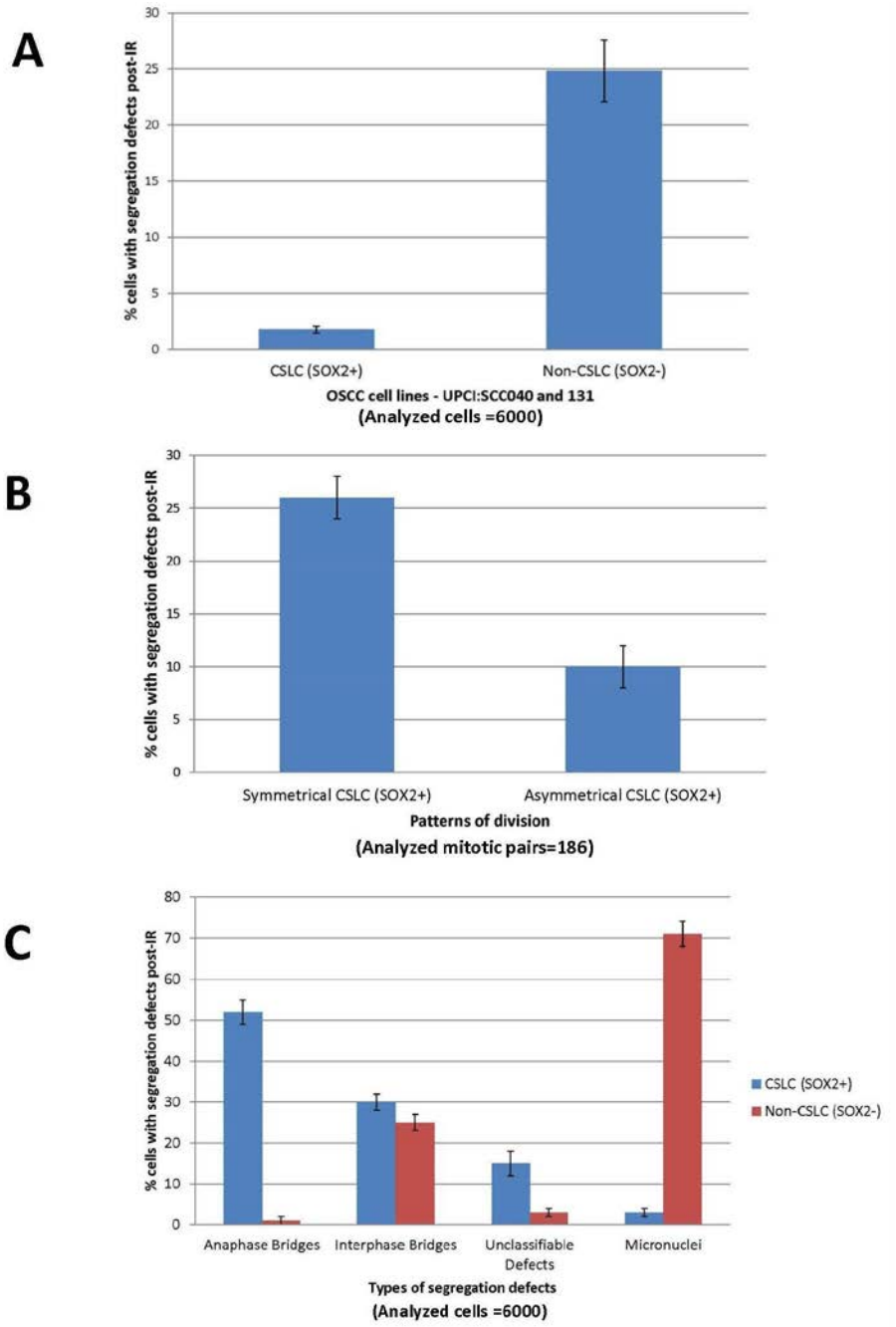

Figure 24. Chromosomal segregation defects in CSLC (SOX2+) CSLC and non-CSLC (SOX2-) 36 hrs after 2.5 Gy IR in OSCC cell lines (UPCI:SCC040 and 131)

A. Percentage frequency of segregation defects in CSLC (SOX2+) and non-CSLC (SOX2-) (+/- SEM).
B. Percentage frequency of segregation defects in symmetrical and asymmetrical CSLC (SOX2+) (+/- SEM).
C. Types of segregation defects observed in CSLC (SOX2+) and non-CSLC (SOX2-) (+/- SEM).

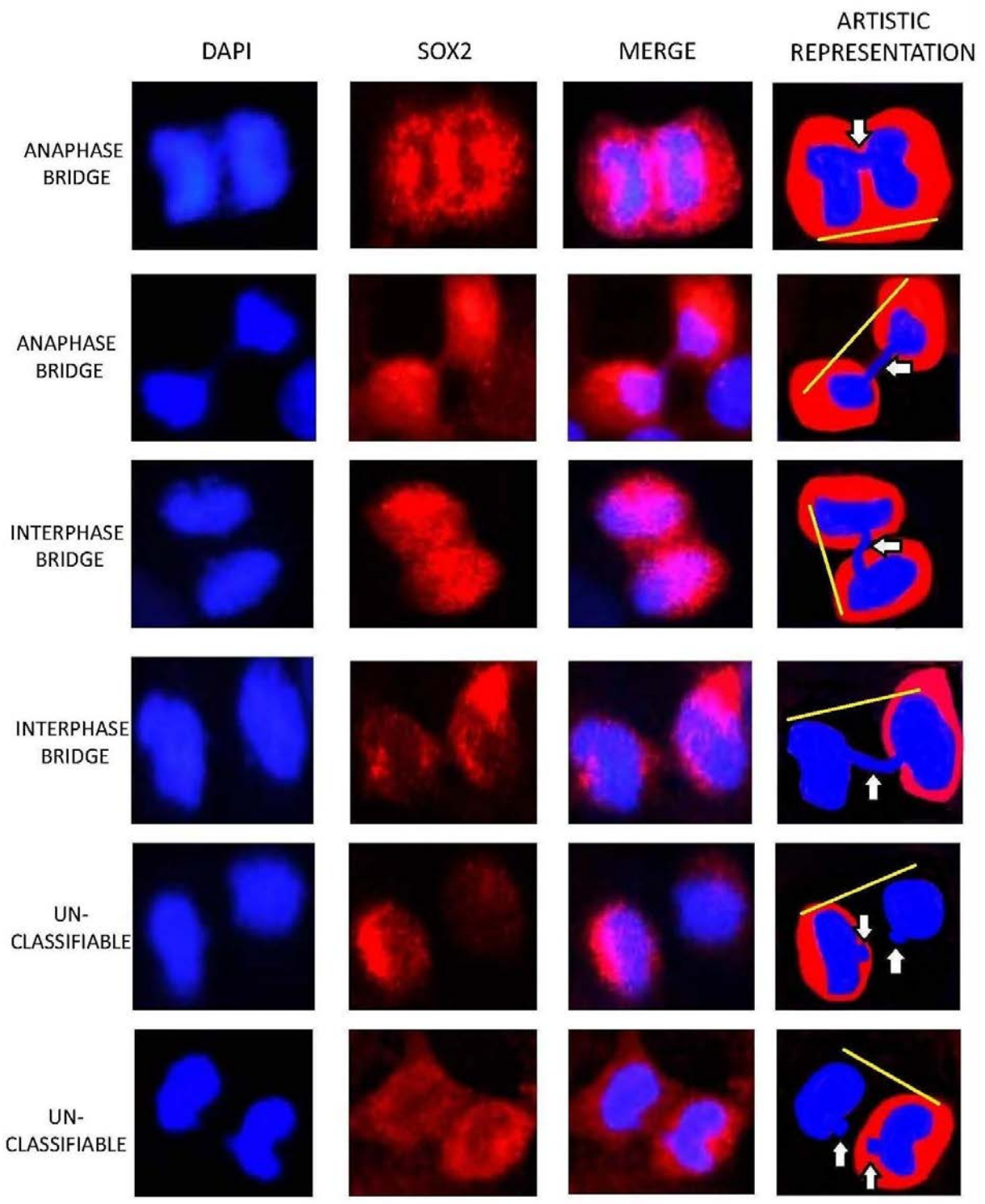

Figure 25. Chromosomal segregation defects in CSLC (SOX2+) 36 hrs after 2.5 Gy IR

Chromosomal segregation defects in CSLC SOX2+ (red) showing the main forms observed, including anaphase bridges, interphase bridges, and unclassifiable defects. Representative images of the defects are marked by arrows and the axis of division is indicated by a yellow line.

3.3 IMMUNOFISH OF CSLC IN OSCC CELL LINES

To understand the role of copy number alterations and CIN in CSLC we did immune-FISH to compare CSLC (CD133+) and non-CSLC (CD133-) in OSCC cell lines, based on the marker CD133. Previous research has shown that CD133 is an important OSCC CSLC cell surface marker. Furthermore, our dual IF staining of CD133 with other CSLC markers showed high positive correlation. We used BAC FISH probe to enumerate *ATM*, since our group had previously shown that copy number loss of *ATM* is associated with radioresistance and enhanced response to combined therapy with IR and a CHEK1 SMI (Parikh, et al. 2007; Sankunny, et al. 2014). Our results (Table 7; Figure 26) showed that the CSLC (CD133+) and non-CSLC (CD133-) expressed similar copy number loss or gain of *ATM*. Overall, our results suggest that loss of *ATM* can occur in CSLC.

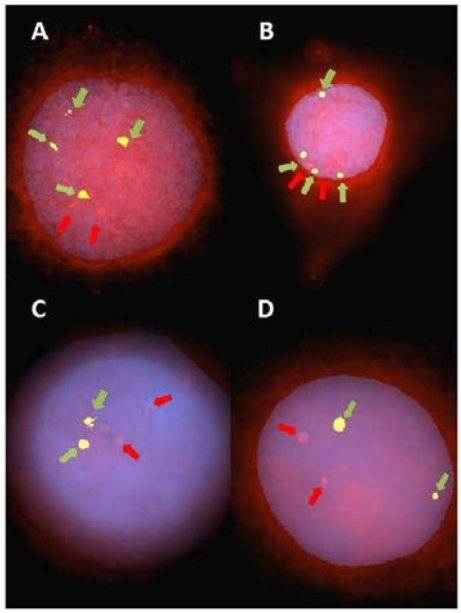

Figure 26. Immuno-FISH results showing *ATM* copy number alterations in OSCC cell lines with and without distal 11q loss

IF: CD133, **FISH:** Green: Cep11, Orange: *ATM*. CD133 Positive: **A**:UPCI:SCC29B, **B**:UPCI:SCC040; CD133 Negative: **C**:UPCI:SCC066, **D**:UPCI:SCC116. The results assessment is shown in Table 7.

Table 7. Immuno-FISH results of UPCI:SCC cell lines*

SCC040	%	
IF	11q Loss	No 11q Loss
1 +/2+	81.88	10.12
3 +	7.36	0.64

SCC029B	%	
IF	11q Loss	No 11q Loss
1 +/2+	87	6
3 +	7	0

SCC066	%	
IF	11q Loss	No 11q Loss
1 +/2+	14.21	74.64
3 +	0.94	10.81

SCC116	%	
IF	11q Loss	No 11q Loss
1 +/2+	4.11	84.74
3 +	2.12	9.64

*IF: CD133/ FISH: *ATM* copy number status. The results show that the copy number alterations in cancer cells is similar to CSLC.

3.4 CHROMOSOMAL INSTABILITY IN CSLC FROM HNSCC AND OSCC CELL LINES

We investigated the CSC stochastic model and CIN in CSLC derived from HNSCC CSLC cell cultures, kindly provided by Dr. Eric Lagasse. Copy number alterations in HNSCC#13 and clonally derived tumor clone HNSCC#13(E8) were assessed by six different centromeric FISH probes (experiments done by DL and analyzed by HK). Our results show that the HNSCC#13 and HNSCC#13(E8) had chromosomal copy number alterations across all six chromosomes investigated (Figure 27). Our results thereby confirm that multiple copy number alterations developed in CSLC from the clone HNSCC#13(E8) CSLCs supporting the stochastic model of CSLC in HNSCC (Figure 27).

In order to further investigate the possibility of a stochastic CSLC model, we generated clones from the cell line UPCI:SCC125, and then propagated these cloned cell lines (clones A, B, C and F6) in enriched SC media to investigate whether *ATM* copy number alterations are carried in the CSLC as suggested by the stochastic CSLC model (Table 8; Figure 28). All of the clones showed variation in *ATM* copy number, confirming that CSLCs express copy number alterations as proposed by the stochastic CSC model and as previously shown by Odoux et al. in metastatic colorectal cancers (Odoux, et al. 2008).

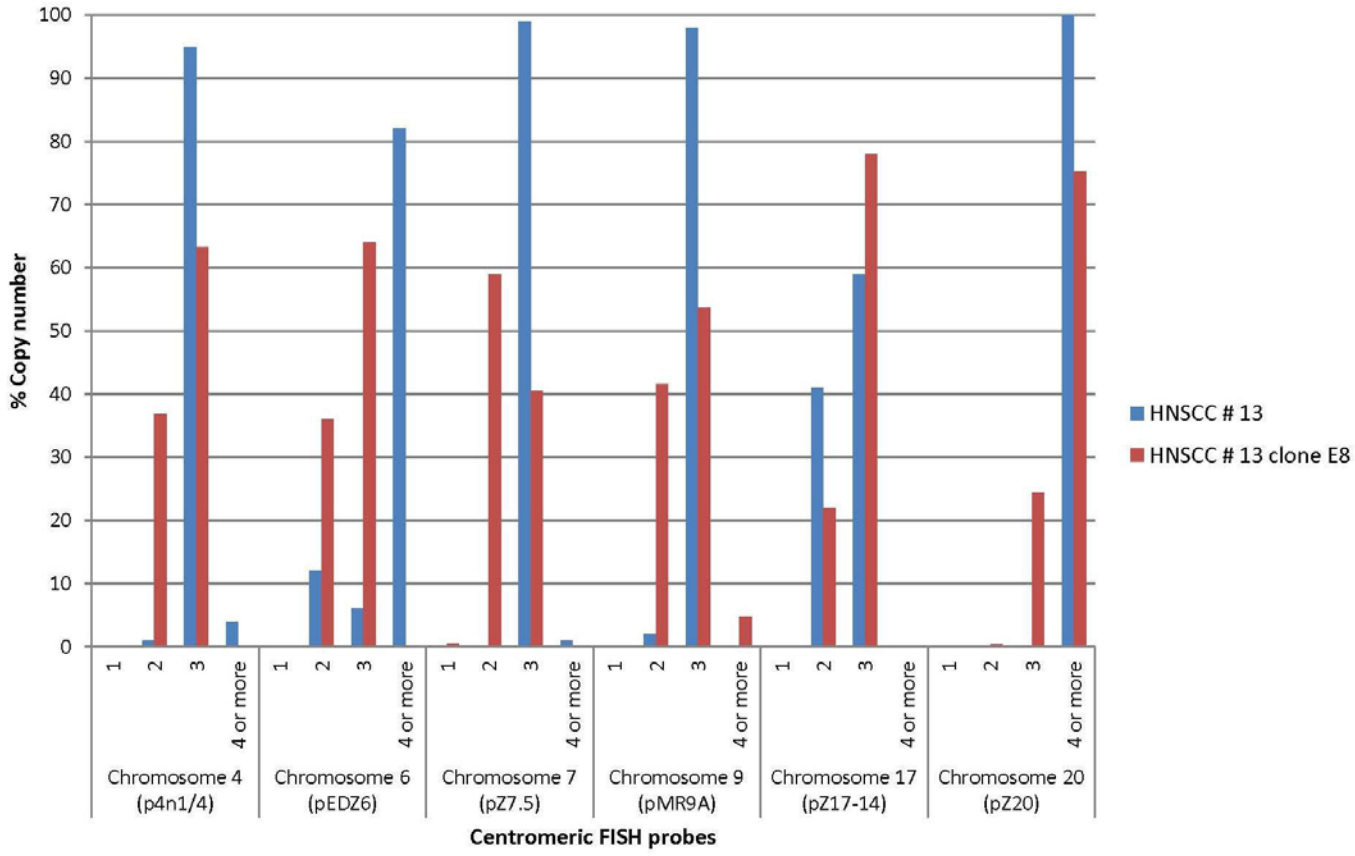

Figure 27. FISH analyses of CSLC isolated from HNSCC#13 and clone HNSCC#13 E8

HNSCC#13 and HNSCC#13 (E8) CSLC cell lines showed variable number of chromosome copies across the six chromosomes assessed, supporting the stochastic model in HNSCC.

Table 8. FISH analysis of *ATM* copy number status in UPCI:SCC125 and derived clones

Cell line/culture	Percentage CSLC with loss of *ATM* 11q22.3	Percentage CSLC with no loss of *ATM* 11q22.3
UPCI:SCC125	54	46
UPCI:SCC125 (Clone A)	12	88
UPCI:SCC125 (Clone B)	25	75
UPCI:SCC125 (Clone C)	10	90
UPCI:SCC125 (Clone F6)	91	9
HNSCC #13	5	95
HNSCC #13 (Clone E8)	60	40

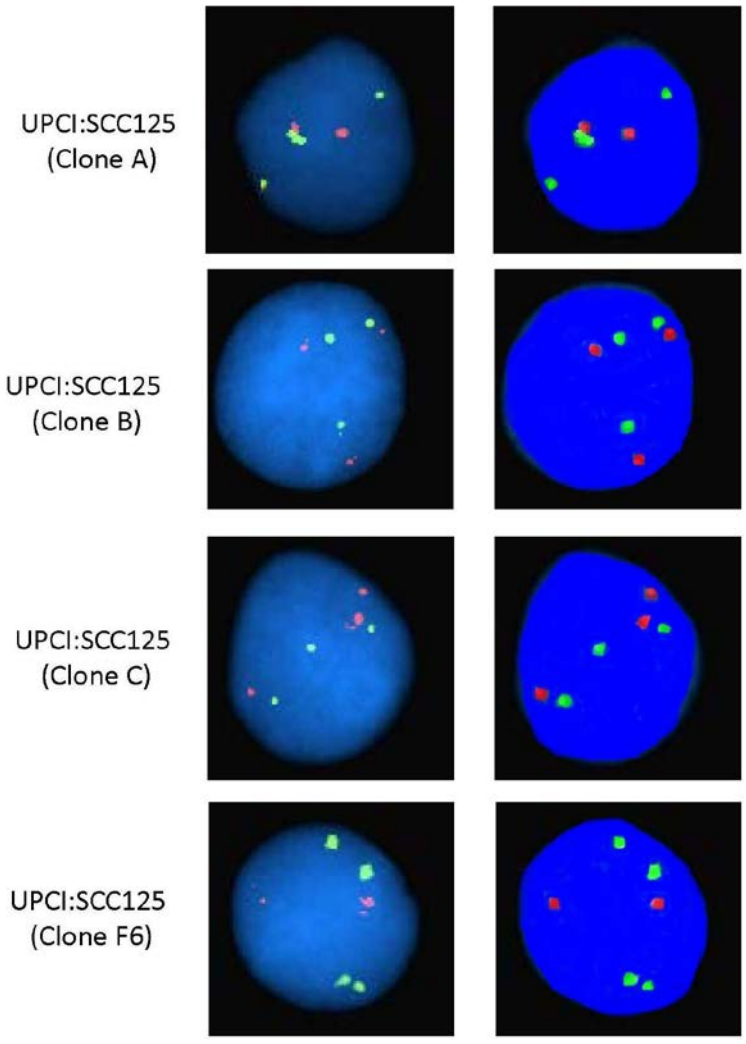

Figure 28. FISH images of CSLC derived from UPCI:SCC125 and UPCI:SCC125 clones showing *ATM* copy number alterations

FISH: Green: Cep11, Orange: *ATM*. UPCI:SCC125 cell line and UPCI:SCC125 cell line clones A, B, C and F6 show different *ATM* copy numbers in CSLC.

3.5 SPHEROID ENRICHMENT IN OSCC CELL LINES

Most human epithelial cell lines with CSLCs can form spheroids in enriched suspension culture. In order to assess the CSLC potential in UPCI:SCC cell lines, we cultured these cells on ultra-low attachment plates in SC-enriched media. All of our cell lines in the study formed spheroids (sphere–like or grape-like) in enriched suspension culture (Figure 29). The ability to form spheroids *in vitro* depends on the presence of self-renewing CSLCs within the population. To confirm the self-renewal potential of these cells, we tested a single cell suspension derived from primary spheroids for spheroid formation. There was a statistically significant difference between primary and secondary spheroids confirming our hypothesis (Figures 29, 30). Correlation analysis between CD133, CD44 and spheroid-forming capacity showed that CD133 has a high correlation with spheroid forming capacity, unlike CD44 (Figure 31, 32). Further, suspension IF staining of the spheroids using stemness markers (CD44, CD133, SOX2 and BMI1) showed variable increases in positive (+++) cells expressing the marker especially in the spherical or grape-like structures; dispersed cell clusters were largely negative to the markers (Figure 33). Our results suggest that spheroid enrichment increases CLSC variably (Perego, et al. 2011), confirming the heterogeneity of OSCC and the high likelihood of asymmetrical division in these cultures. To investigate the tumorigenic potential of single CSLCs from OSCC cell lines, we performed extreme limiting dilution assessment (ELDA) (Odoux, et al. 2008; Uchida, et al. 2000). The ability to form colonies after extreme dilution is a unique and characteristic property of CSLC. Colony formation was observed ≈ 10 days after plating of OSCC cells in SC-enriched media. The estimation of spheroid forming efficiency (SFE) through extreme limiting dilution was 0.005-0.01% (Figure 34), which is similar to the results obtained by other groups using this experimental methodology (Odoux, et al. 2008; Tosoni, et al. 2012). All cell lines studied

showed a statistically significant single hit hypothesis on stem cell analysis (Figure 34). To study the differentiation potential of CSLC, we transferred a single cell CSLC suspension derived from spheroids into Matrigel™-coated plates in serum-rich culture medium to test whether they could grow and differentiate into colonies (holoclones, paraclones and meroclones). Locke et al. previously described the clonal heterogeneity of OSCC cell lines as being 'holoclones' 'paraclone' and 'meroclones' (Locke, et al. 2005); we observed similar trends in our cell lines as described earlier (Locke, et al. 2005). All dissociated spheroids differentiated into colonies with specific characteristics (holoclones, paraclones and meroclones) with cells that demonstrated variability in cell size, shape and nuclear cytoplasmic ratio (Figure 35). Overall, the primary/secondary spheroid, ELDA, spheroid suspension IF staining and differentiation assay all confirmed that CSLC isolated from OSCC cell lines show properties of CSLC including self-renewal, CSLC markers, colony forming capacity at extremely low dilutions, and differentiation potential in serum-rich media.

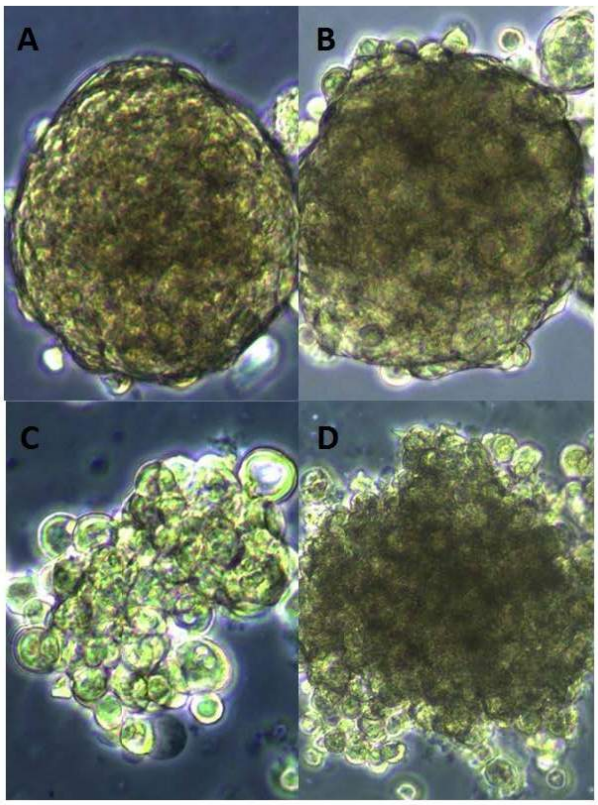

Figure 29. Phase contrast images of spheroids derived from UPCI:SCC cell lines

Enriched spheroids showing sphere-like shape and grape-like shape in UPCI:SCC cell lines; A: UPCI:SCC029B; B: UPCI:SCC040; C: UPCISCC066; D: UPCI:SCC116; cell lines with distal 11q loss (UPCI:SCC029B and 040) and cell lines without distal 11q loss cell lines (UPCI:SCC066 and 116).

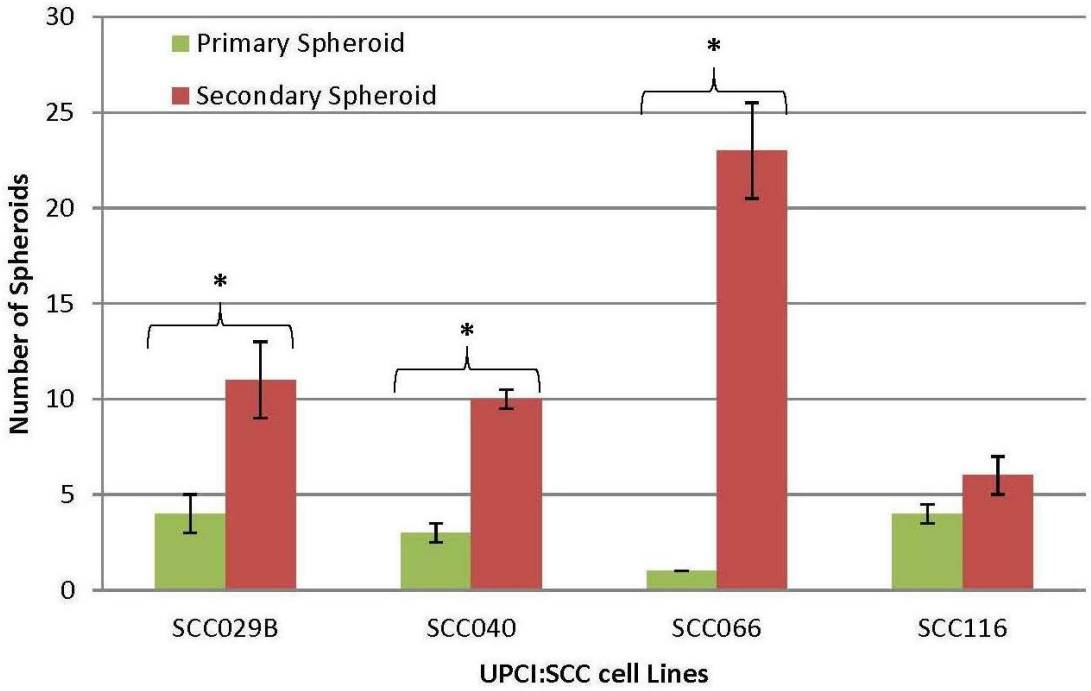

Figure 30. Primary and secondary spheroid formation in UPCI:SCC cell lines

UPCI:SCC029B, 040 and 066 showed a statistically significant increases in formation of secondary spheroids compared to primary spheroids (* $p<0.05$); UPCI:SCC116 showed an increase that was not statistically significant.

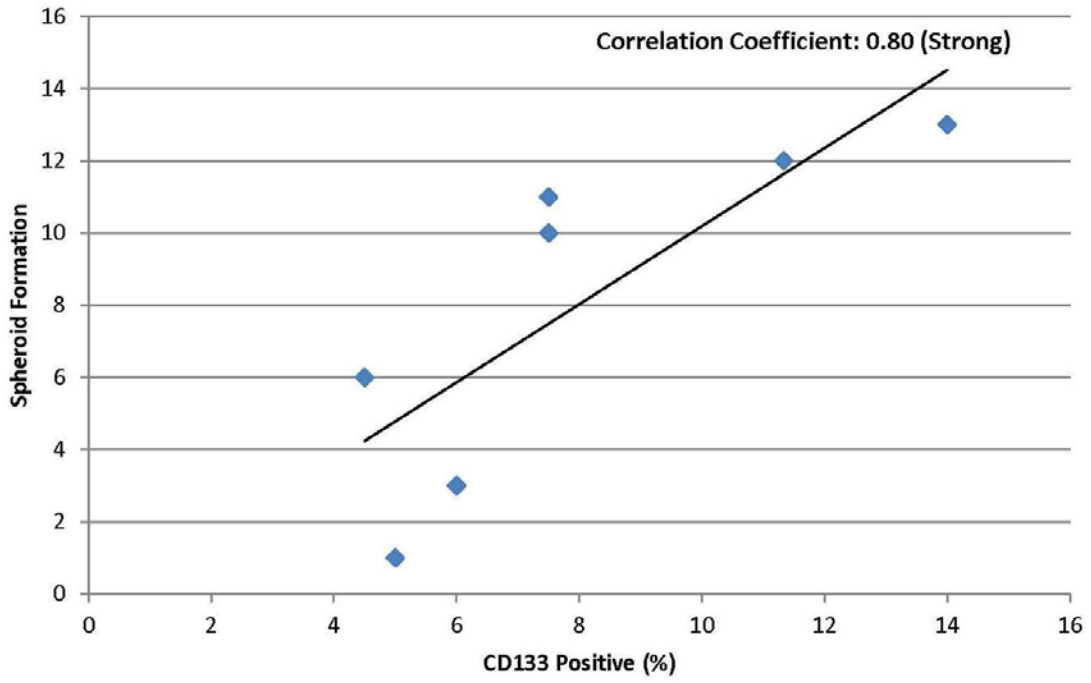

Figure 31. Correlation analysis between CD133 positive (+++) cells and spheroid formation showing a strong correlation

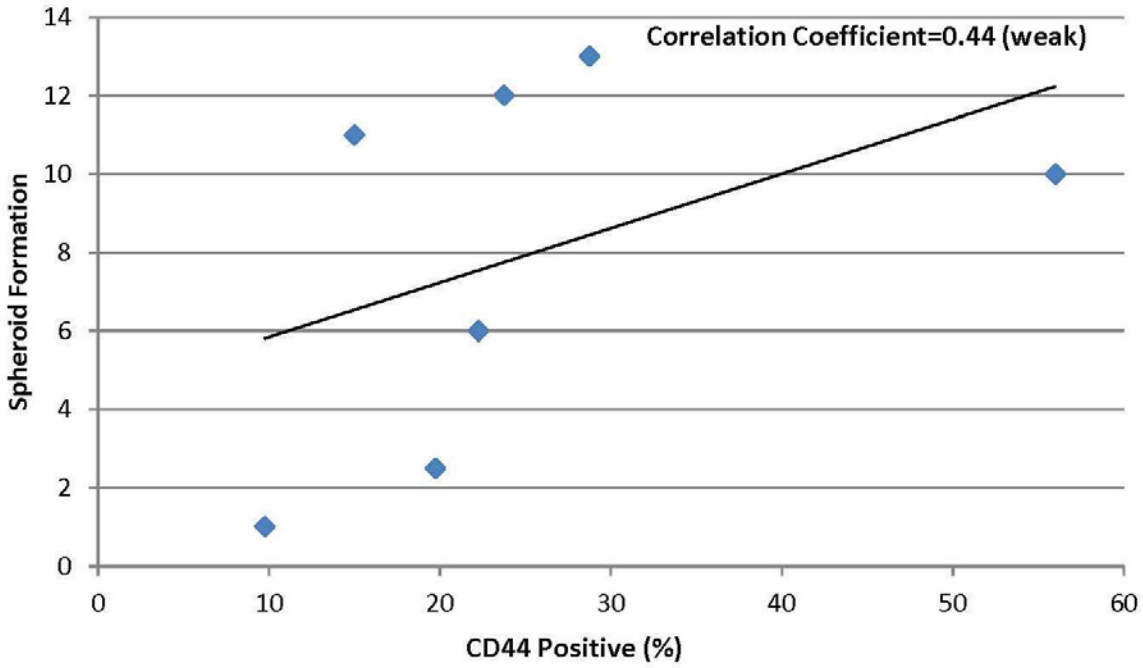

Figure 32. Correlation analysis between CD44 positive (+++) cells and spheroid formation showing a weak correlation

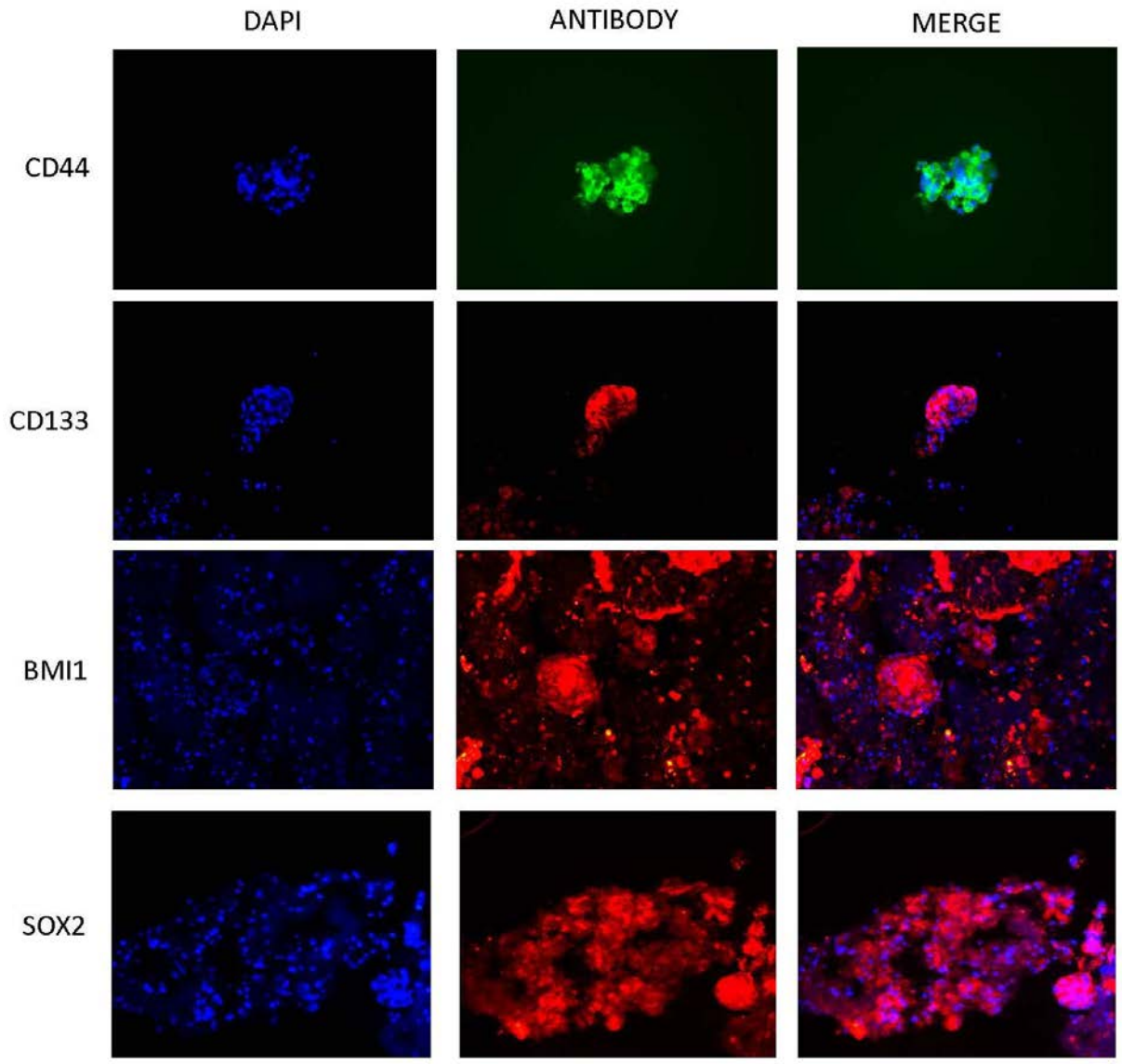

Figure 33. IF staining of spheroids enriched from OSCC cell line UPCI:SCC029B showing positive cells in enriched spheroids and grape-like colonies

IF suspension staining of the spheroids using stemness markers (CD44, CD133, SOX2 and BMI1) showed variable increases in positive (+++) cells expressing the marker especially in the spherical or grape-like structures; dispersed cell clusters were largely negative for the markers.

A

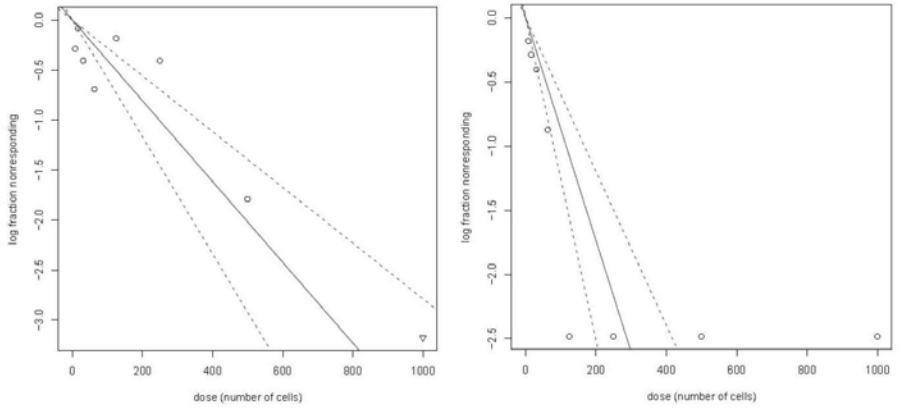

B

1000	1000	1000	1000	1000	1000	1000	1000	1000	1000	1000	1000
500	500	500	500	500	500	500	500	500	500	500	500
250	250	250	250	250	250	250	250	250	250	250	250
125	125	125	125	125	125	125	125	125	125	125	125
63	63	63	63	63	63	63	63	63	63	63	63
31	31	31	31	31	31	31	31	31	31	31	31
16	16	16	16	16	16	16	16	16	16	16	16
8	8	8	8	8	8	8	8	8	8	8	8

C

Stem Cell Frequency	
OSCC cell lines	CSLC estimation
UPCI:SCC029B	**1/270** UL:1/186, LL:1/391
UPCI:SCC040	**1/225** UL:1/155, LL:1/327
UPCI:SCC066	**1/231** UL:1/159, LL: 1/334
UPCI:SCC116	**1/259** UL:1/179, LL:1/377
UPCI:SCC131	**1/252** UL:1/173, LL:1/369

Figure 34. Stem cell frequency assessment by extreme limiting dilution analysis

A. Goodness of fit tests. Rejection of the tests may be due either to batch effects (heterogeneity in the stem cell frequencies or assay success rate) or to a failure of the stem cell hypothesis. Single hit likelihood ratio was statistically significant, $p<0.05$ in all UPCI:SCC cell lines; likelihood ratio based on goodness of fit plot in UPCI:SCC040 and UPCI:SCC131 is represented.

B. Limiting Dilution plate setup: 2000 cells/well were serially diluted to 8 cells/well.

C. Stem Cell Frequency was estimated by extreme limiting dilution assessment utilizing SC analysis software (Hu and Smyth 2009) in cell lines with distal 11q loss (UPCI:SCC029B, 040 and 131) and without distal 11q loss (UPCI:SCC066 and 116). The values represent the estimation of CSLC frequency with upper limit (UL) and lower limit (LL) values setting a range. No statistically significant difference was observed between the two groups.

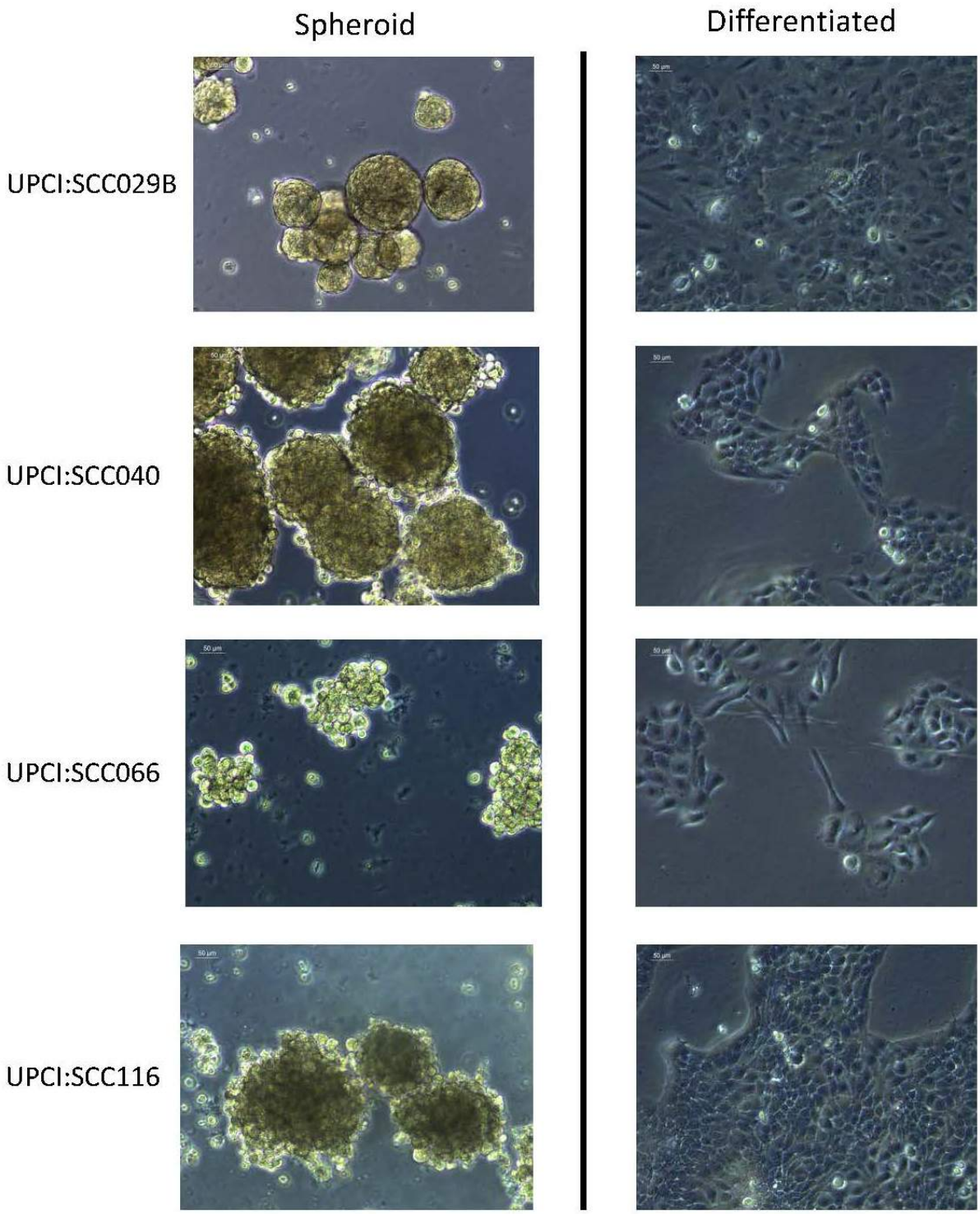

Figure 35. Differentiation assay of OSCC CSLC

CSLC enriched as spheroid (non-adherent) can differentiate into heterogeneous colonies which are comprised of cells that vary in shape and size when cultured in serum-rich media.

3.6 CSLC RADIORESISTANCE PATTERNS IN OSCC

3.6.1 Role of distal 11q loss in CSLC radioresistance

The response of OSCC CSLC cells to IR was assessed by spheroid survival assay, cell viability assay, ELDA and growth assay. The response of parental OSCC was previously studied previously in our lab and was confirmed by clonogenic survival assays (Parikh, et al. 2007). The cell lines were divided into two groups: 'Distal 11q loss' and 'No distal 11q loss.' Cells were treated with IR doses of 2.5 Gy and 5 Gy, based on previous studies in our lab (Parikh, et al. 2007; Sankunny, et al. 2014). Results were reported as 'Surviving Fraction' for each IR dose after normalization against untreated cells (UT). The clonogenic survival assays of the parental cell lines showed similar trends to that previously reported by our lab, with the 'Distal 11q loss' group (UPCI:SCC029B and 040) showing radioresistance compared to the 'No distal 11q loss' group (UPCI:SCC066 and 116) (Figures 38, 39) (Parikh, et al. 2007; Sankunny, et al. 2014). Interestingly, spheroid survival assays of the two groups, 'Distal 11q loss' and 'No distal 11q loss' also showed a similar overall trend (Figures 35, 36). However, we observed marked radioresistance and a SF above 50% in spheroids regardless of IR dose or 11q copy number status. The overall trends in the spheroid survival assay were confirmed by cell viability assays; CSLC with distal 11q loss showed greater radioresistance compared to cells without distal 11q loss (Figure 40). We assessed the SFE by ELDA in response to IR; neither group showed a statistically significant reduction in CSLC (Table 9). Furthermore, we assessed spheroid growth on agarose-coated plates utilizing a low cell seeding density approach (Figures 41-44). No statistically significant reduction in spheroid size was observed in response to IR in either group (distal 11q loss/no distal 11q loss). Overall, our results confirm that CSLC are radioresistant

through all the approaches (Figures 36-44). Distal 11q loss was associated with radioresistance in CSLC as shown by both the spheroid survival assay and cell viability assay (Figure 36-40). No statistical significance was observed in the SFE as examined by ELDA and spheroid growth assay (Table 9; Figure 41-44). Overall, our results may suggest a role for distal 11q loss in OSCC CSLC. Further investigation of this possibility is warranted in a larger sample of cell lines.

Table 9. Stem cell frequency assessment by ELDA in OSCC cell lines in response to IR*

Stem Cell Frequency			
	0 Gy	2.5 Gy	5 Gy
UPCI:SCC040	**1/225** UL:1/155, LL:1/327	**1/179** UL:1/154, LL:1/215	**1/144** UL:1/131, LL:1/265
UPCI:SCC131	**1/252** UL:1/173, LL:1/369	**1/189** UL:1/48, LL:1/231	**1/196** UL:1/136, LL:1/284
UPCI:SCC066	**1/231** UL:1/159, LL: 1/334	**1/347** UL:1/239, LL:1/503	**1/469** UL:1/320, LL:1/686
UPCI:SCC116	**1/259** UL:1/179, LL:1/377	**1/923** UL:1/581, LL:1/1466	**1/908** UL:1/574, LL:1/1439

* Stem cell frequency was estimated by extreme limiting dilution assessment utilizing SC analysis software (Hu and Smyth 2009).
*The values represent the estimation of SC frequency with upper limit (UL) and lower limit (LL) values setting a range.
* UPCI:SCC040, 131 and 066 showed no significant statistical reduction in CSLC frequency in in response to IR; UPCI:SCC116 showed a statistically significant reduction in CSLC frequency that is probably not biologically significant.

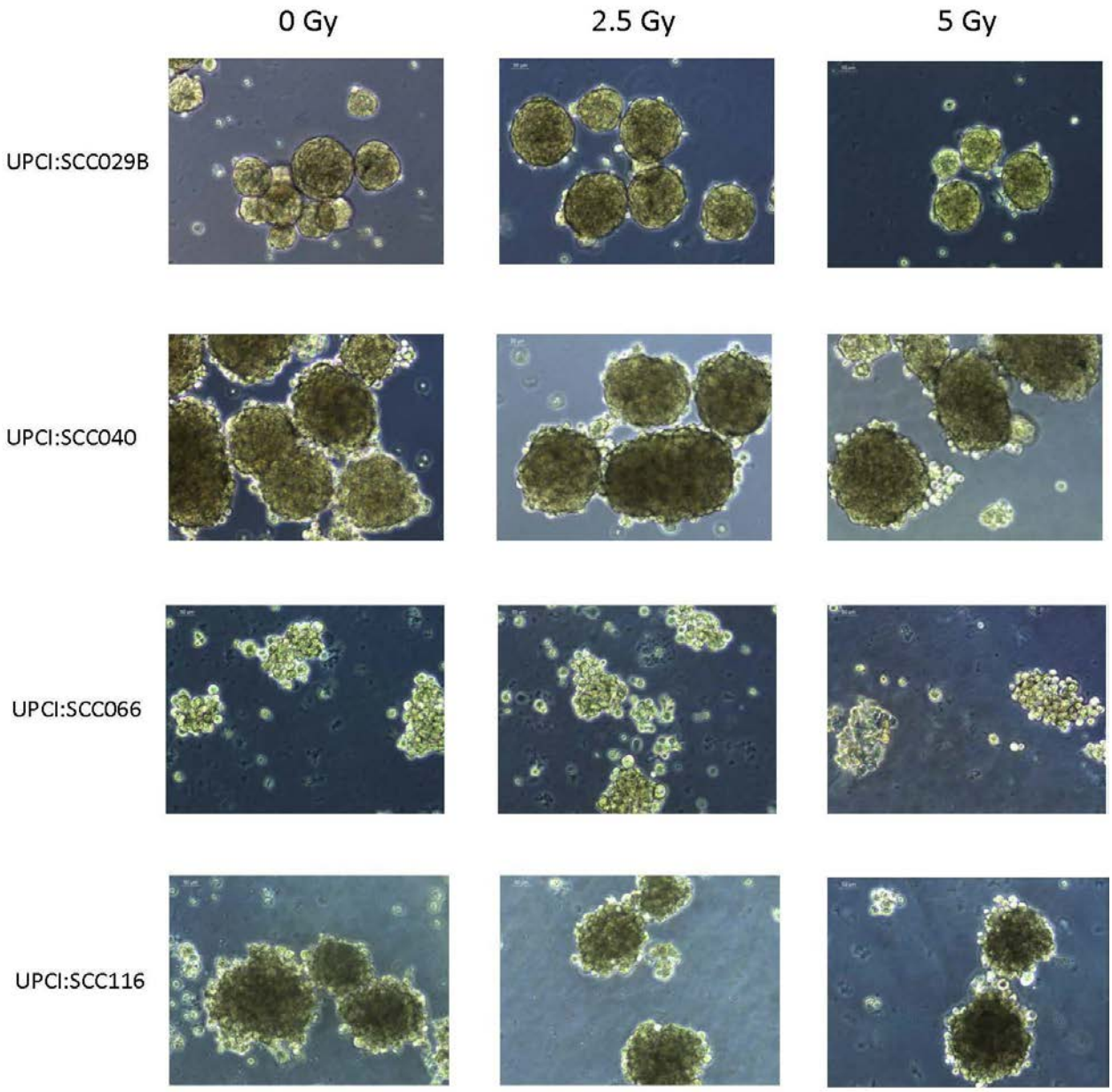

Figure 36. Spheroid survival assay in UPCI:SCC cell lines after treatment with IR

The surviving fraction of spheroids at specific IR doses is higher in the "Distal 11q loss" group (UPCI:SCC029B and 040) when compared to the "No distal 11q loss" group (UPCI:SCC066 and 116). Statistical assessment is shown in Figure 37.

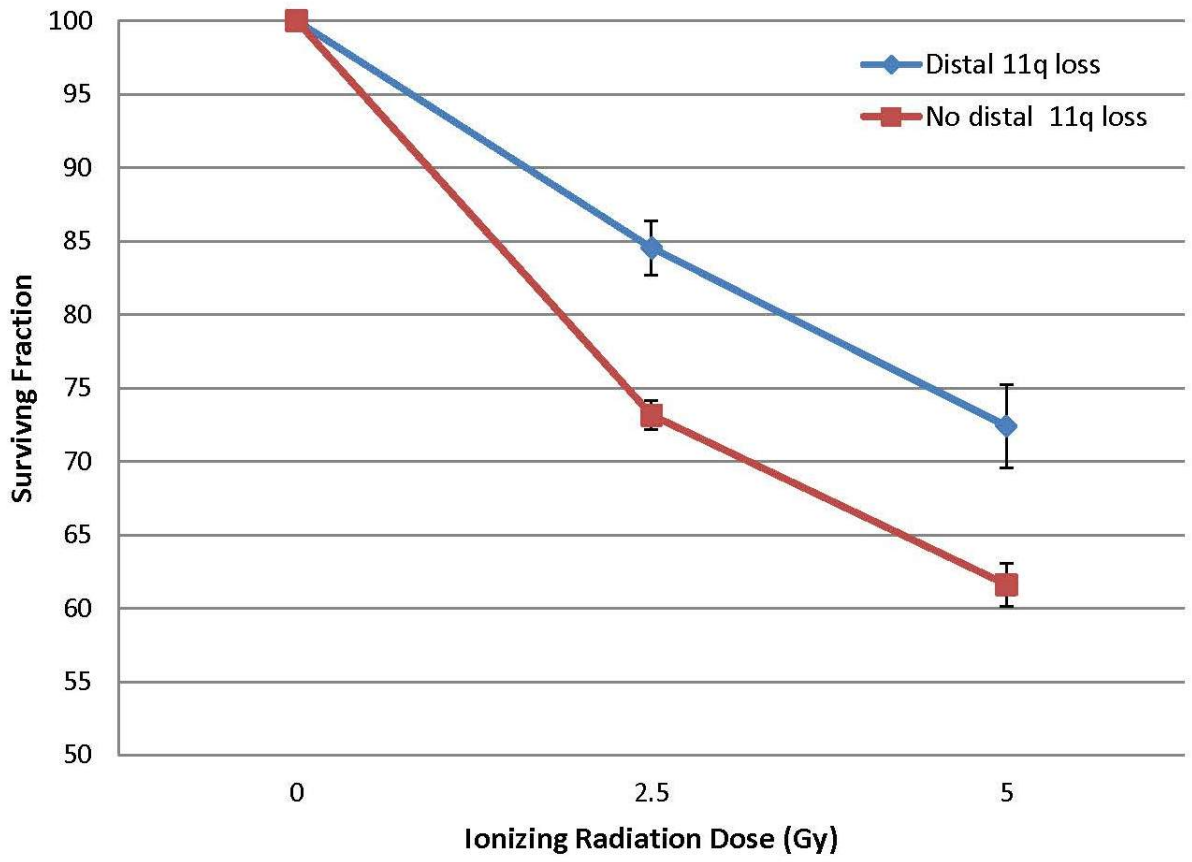

Figure 37. Spheroid survival Assay in UPCI:SCC cell lines

The surviving fraction of spheroids at specific IR doses is plotted with error bars (+/-SEM). Spheroids in the "distal 11q loss" group (UPCI:SCC029B and 040) showed increased survival compared to the "no distal 11q loss" group (UPCI:SCC066 and 116).

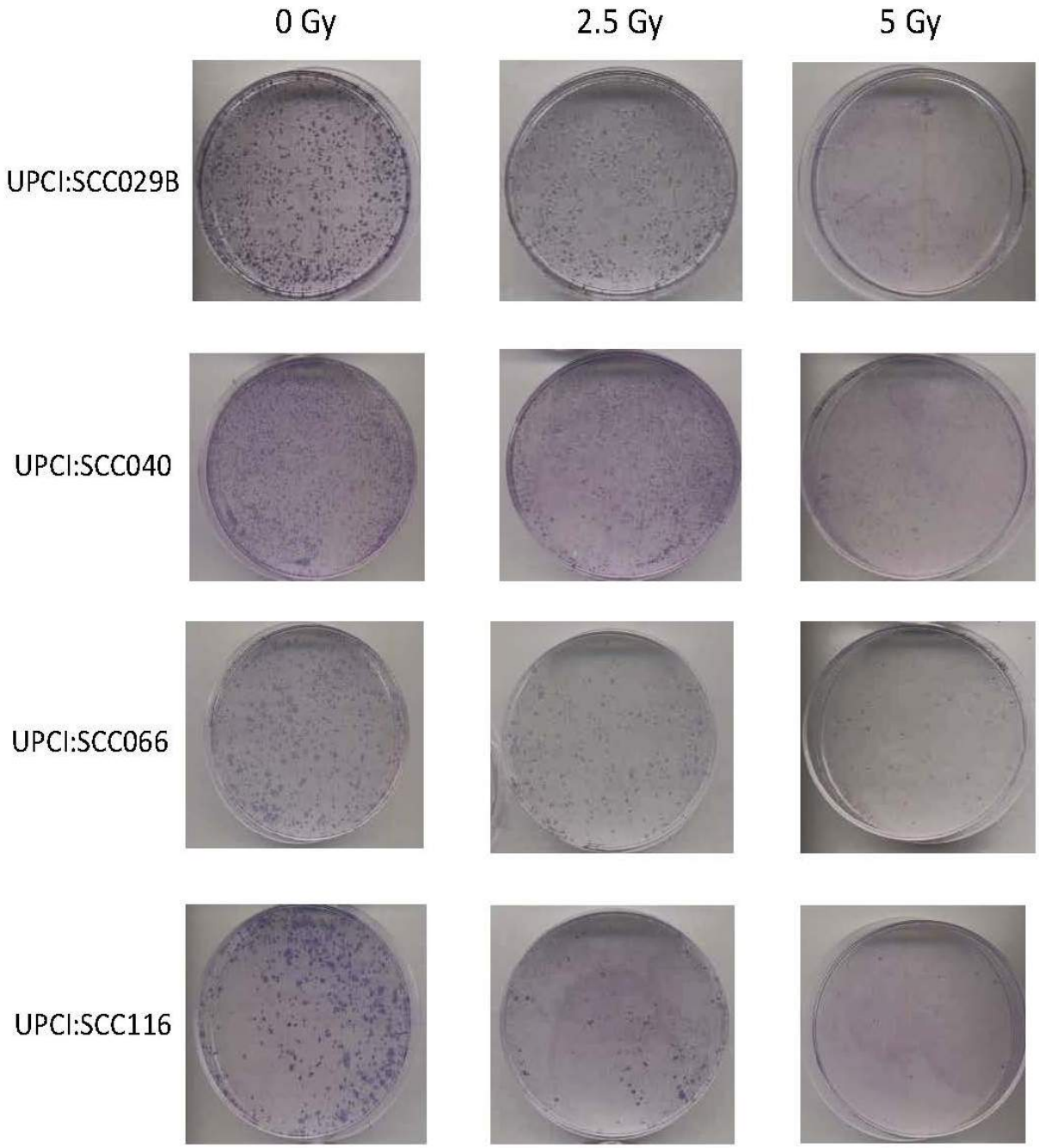

Figure 38. Clonogenic survival of UPCI:SCC cell lines after treatment with IR

The surviving fraction of cells at specific IR doses is higher in the "distal 11q loss" group (UPCI:SCC029B and 040) when compared to the "no distal 11q loss" group (UPCI:SCC066 and 116). Statistical assessment is shown in Figure 39.

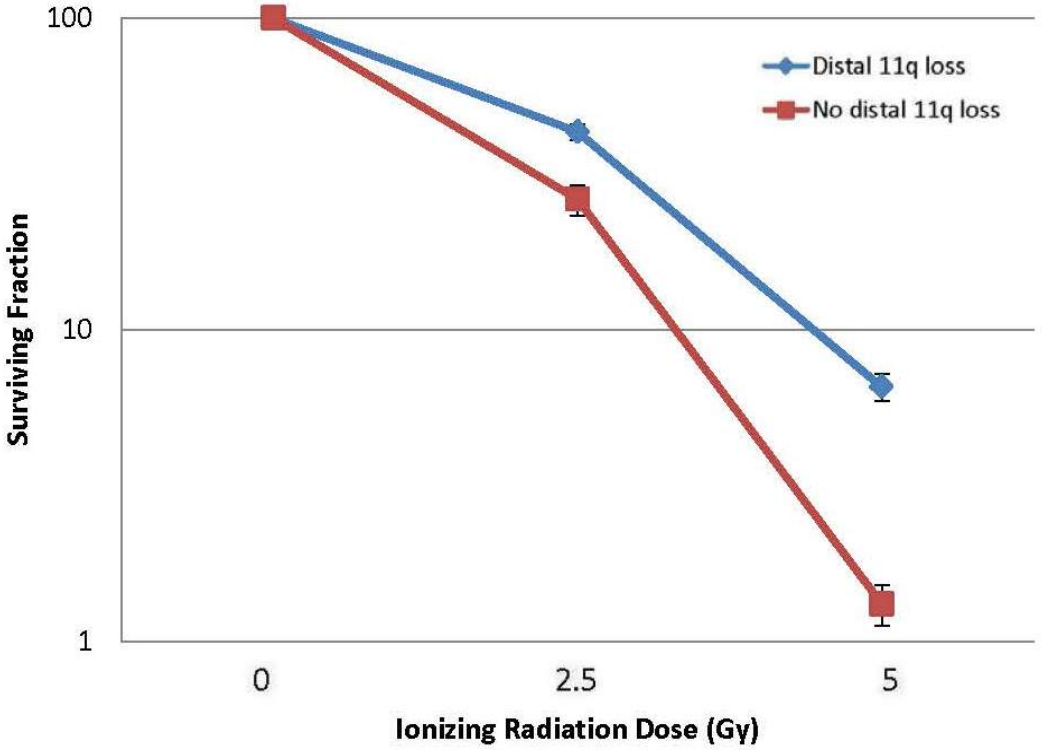

Figure 39. Clonogenic survival assay in parental OSCC cell lines

The surviving fraction of cells at specific IR doses is plotted with error bars (+/-SEM) on a logarithmic scale. Cancer cells in the "Distal 11q loss" group (UPCI:SCC029B and 040) showed increased survival when compared to the "No distal 11q loss" group (UPCI:SCC066 and 116).

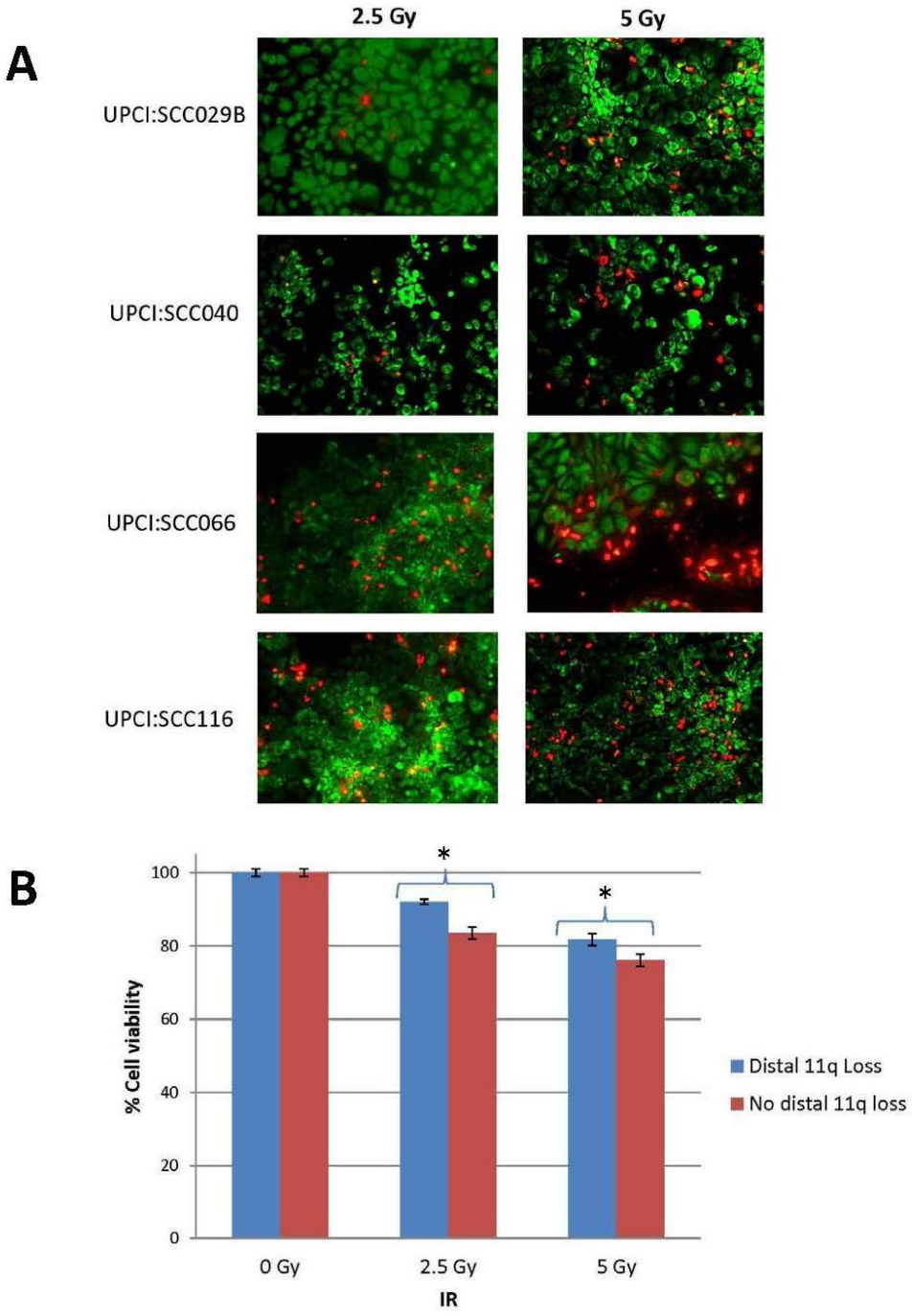

Figure 40. Assessment of CSLC survival in cells with and without distal 11q loss grown on matrigel-coated plates

A. Cell viability assay; red refers to dead cells and green refers to live cells.
B. CSLCs in the "distal 11q loss" group (UPCI:SCC029B and 040) showed increased survival compared to the "no distal 11q loss" group (UPCI:SCC066 and 116)(* $p<0.05$).

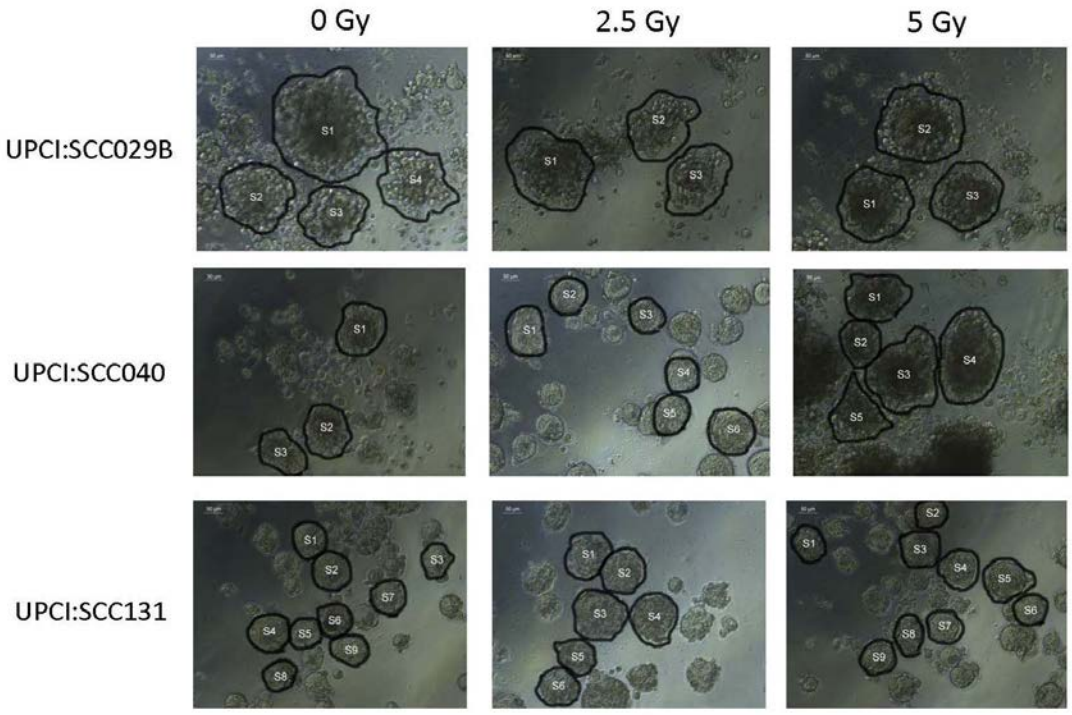

Figure 41. Spheroid growth assay in OSCC cell lines with distal 11q loss
Spheroid growth assessment was done by culturing OSCC cells in agarose-coated 96-well plates, utilizing a low cell seeding density approach. Spheroids >65µm were marked, counted and analyzed for size growth using image analysis software (Image J). Statistical assessment is shown in Figures 43 and 44.

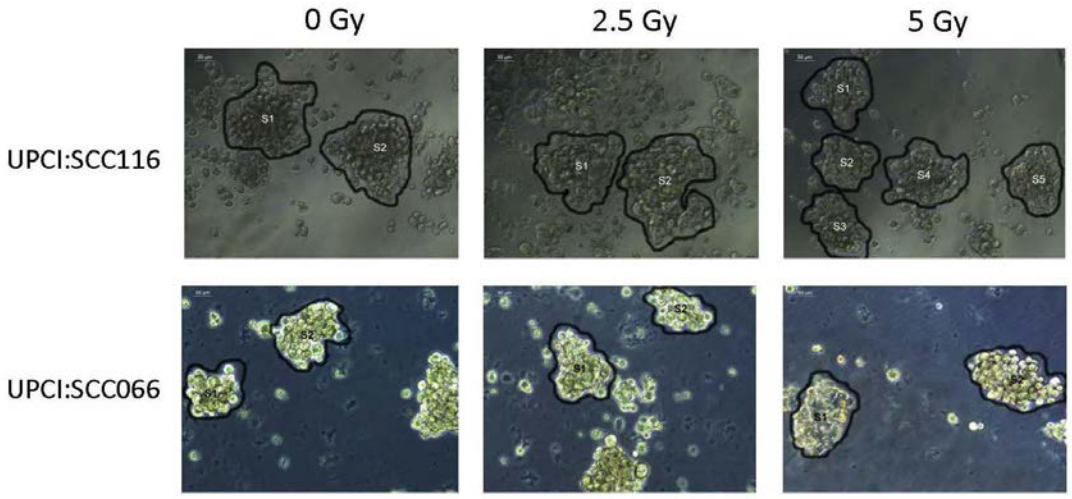

Figure 42. Spheroid growth assay in OSCC cell lines without distal 11q loss
Spheroid growth assessment was done by culturing OSCC cells in agarose-coated 96-well plates, utilizing a low cell seeding density approach. Spheroids >65µm were marked, counted and analyzed for size growth using image analysis software (Image J). Statistical assessment is shown in Figures 43 and 44.

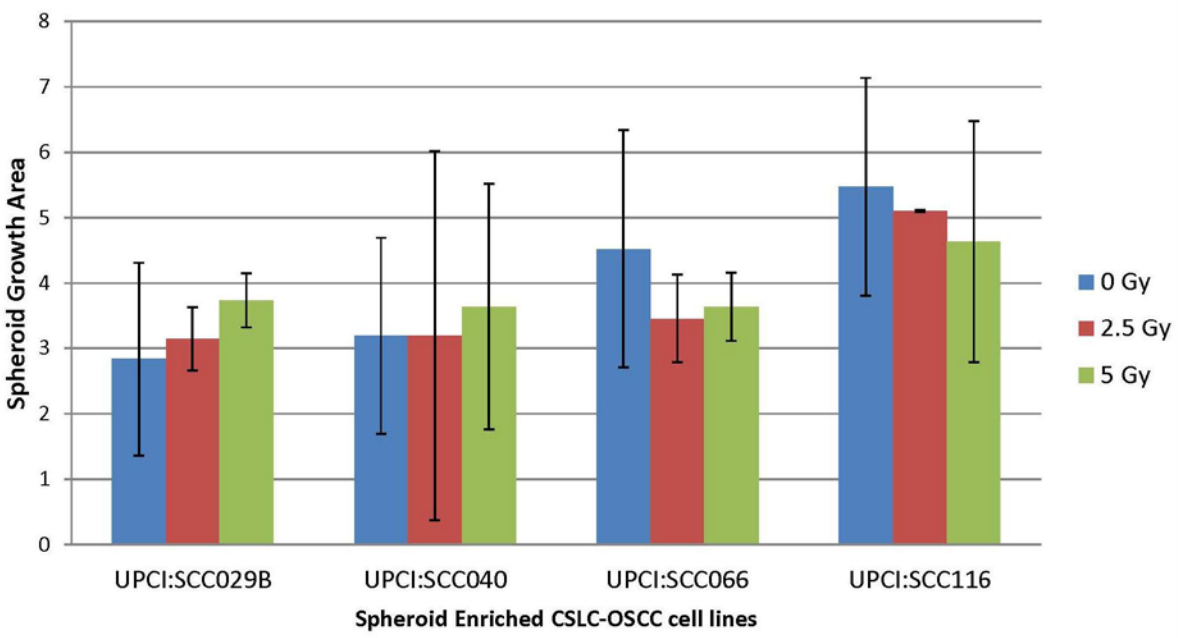

Figure 43. Assessment of spheroid growth assay in OSCC cell lines

Spheroid size (growth) assessment in cell lines with 'Distal 11q loss' (UPCI:SCC029B and 040) when compared to cell lines with "No distal 11q loss" (UPCI:SCC066 and 116).

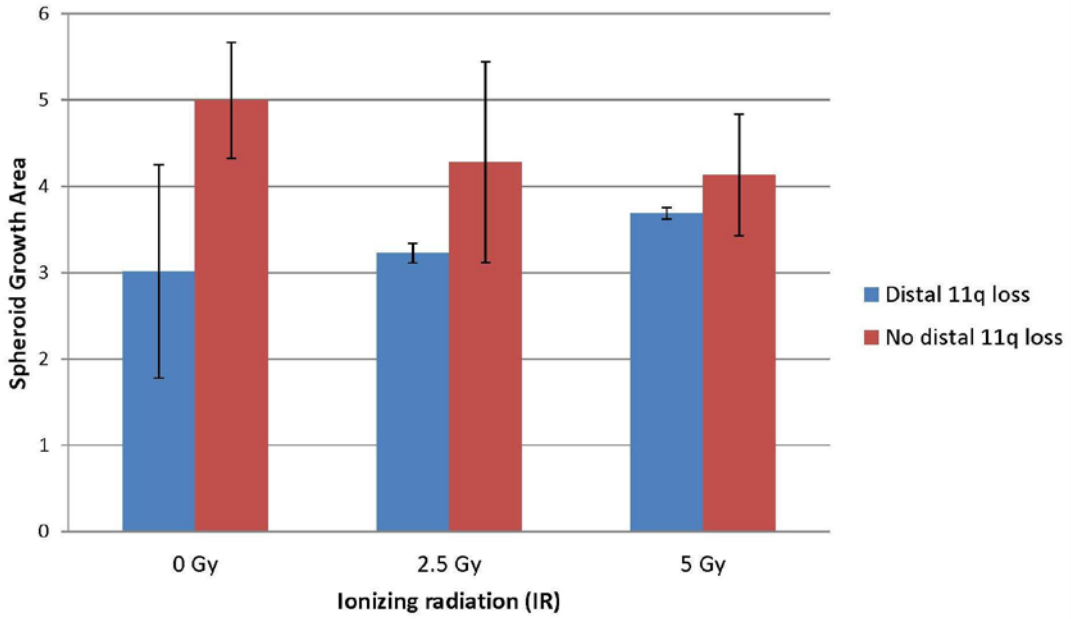

Figure 44. Assessment of spheroid growth in OSCC cell lines with distal 11q loss and without distal 11q loss

Spheroid size (growth) assessment in cell lines with 'Distal 11q loss' (UPCI:SCC029B and 040) when compared to cell lines from the "No distal 11q loss" group (UPCI:SCC066 and 116). No statistically significant difference was observed between the two groups.

3.6.2 Role of CSLC in radioresistance

In an effort to replicate the clinical therapeutic scenario (Lagadec, et al. 2010), in which patients receive multiple doses of IR (2.5 Gy) daily over a period of weeks, we irradiated CSLC with 2.5 Gy every other day for 1 or 2 weeks respectively. The surviving fraction of spheroids at different total IR doses showed no statistical significance at 2.5 Gy*1, 2.5 Gy*3 and 2.5 Gy*6, confirming the possible contributory role of CSLC to radioresistance (Figure 45).

Next, we assessed the spheroid migration zone, a standardized approach used to measure the short-term therapeutic response of CSLC; the approach also mimics the initiation of metastases or recurrence that occurs *in vivo* (Vinci, et al. 2013). The enriched spheroids from the 'No distal 11q loss' cell lines (UPCI:SCC066 and 116) did not migrate on matrigel or poly-L-lysine coated plates. On the other hand, the 'Distal 11q loss' cells (UPCI:SCC040 and 131) formed a migration zone on matrigel-coated plates. The assay showed mild reduction in the spheroid migration zone in response to IR in UPCI:SCC131 and no significant reduction in spheroid migration area in UPCI:SCC040, confirming the role of CSLC in radioresistance (Figure 46). Overall, the trends that we observed in the migration assays (Figure 46) were similar to the trends that we observed in the long-term therapeutic response experiments (spheroid survival assay, cell viability assay, ELDA, spheroid growth assay) (Figures 36, 37, 40-44; Table 9).

In order to assess the response of the DDR machinery in CSLC post-IR, CSLC were cultured on matrigel™-coated plates in enriched SC media. Various DDR components (γH2AX, pCHEK1 and KU70) showed a statistically significant increase in foci after IR (Figure 47), confirming the role of DDR in CSLC response to IR 2.5 Gy. Overall, our results confirm that CSLC are an important factor in radioresistance of OSCC.

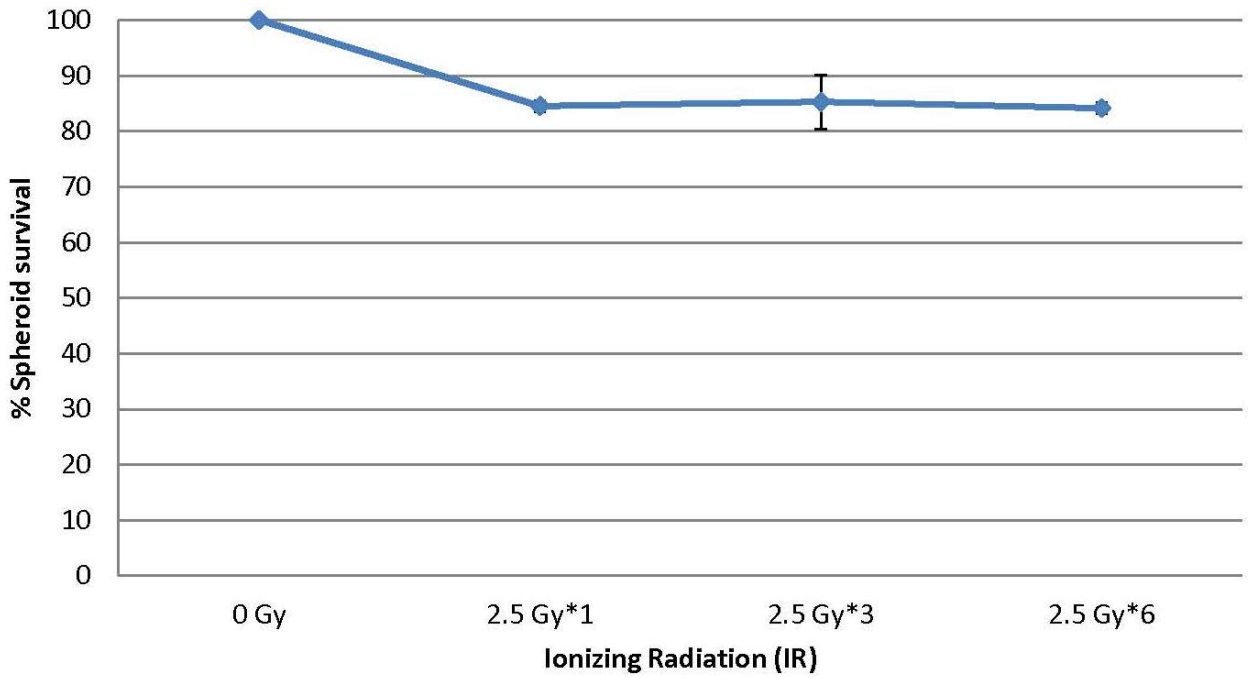

Figure 45. Spheroid survival assay in OSCC cell lines after treatment with IR regimens

The surviving fraction of spheroids (UPCI:SCC0040 and 131) at different total doses of IR shows no statistical significance across regimens.

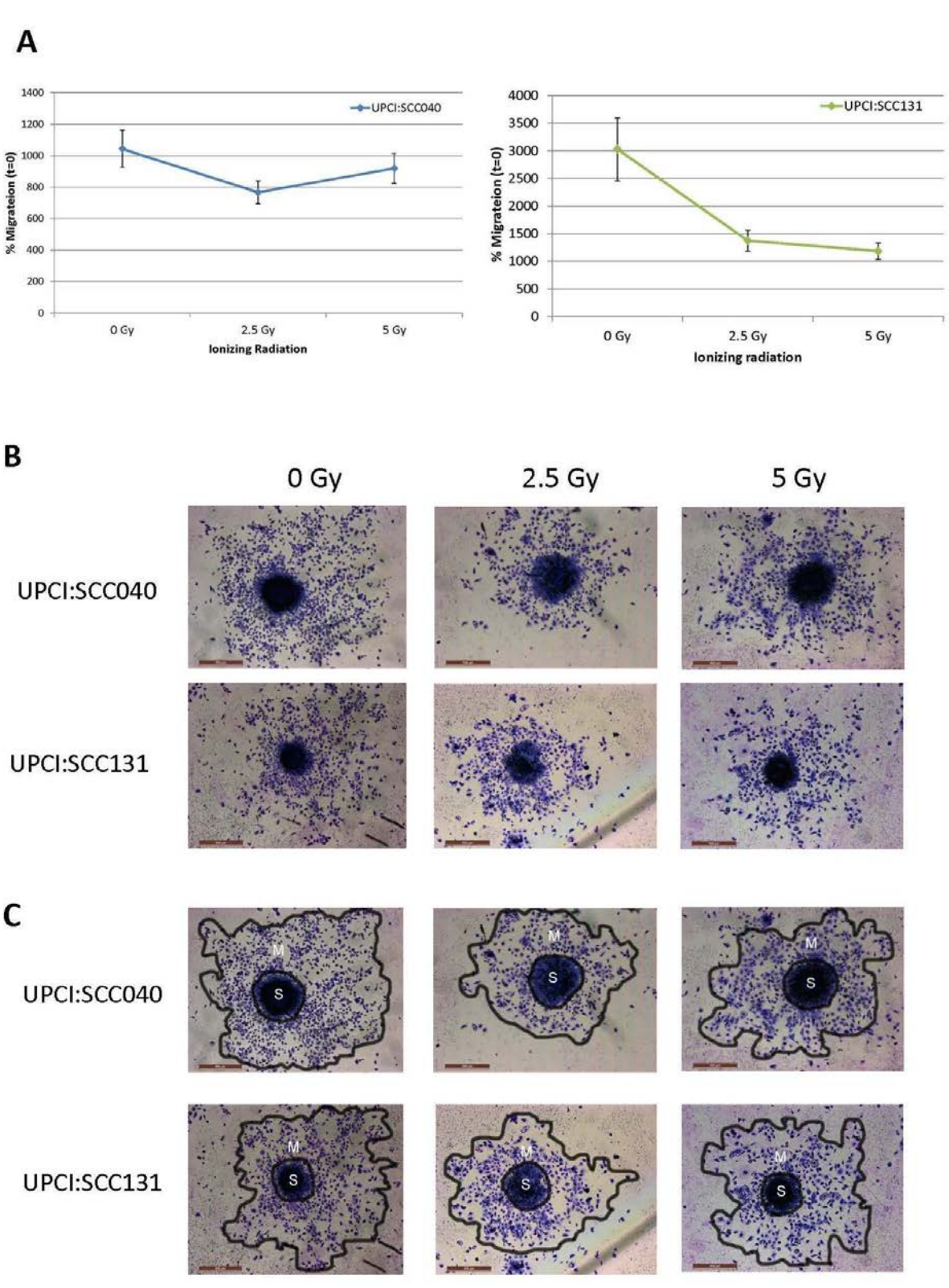

Figure 46. Quantification of spheroid-based migration in response to IR

A. Line graphs showing quantification of UPCI:SCC040 and 131 cell migration on Matrigel™-coated plates at 96 hr in response to IR (mean ± SEM of replicate spheroids). Migration was assessed at 96 hr relative to original spheroid size at (t=0) for each condition. The area of the spheroids (S) at t = 0 and the area covered by the cells that have migrated from the spheroids (M) was determined after 4 days. Data were normalized to the original spheroid recorded using the following formula: % migration zone=migrated area (M)(t= 96 hr) /original spheroid (S) (t = 0) × 100.
B. Images showing spheroid-based migration in response to IR (stained with Giemsa stain).
C. Analyzed images showing spheroid-based migration marked as M (Migration Zone) and original Spheroid at (t=0) S (Spheroid Zone).

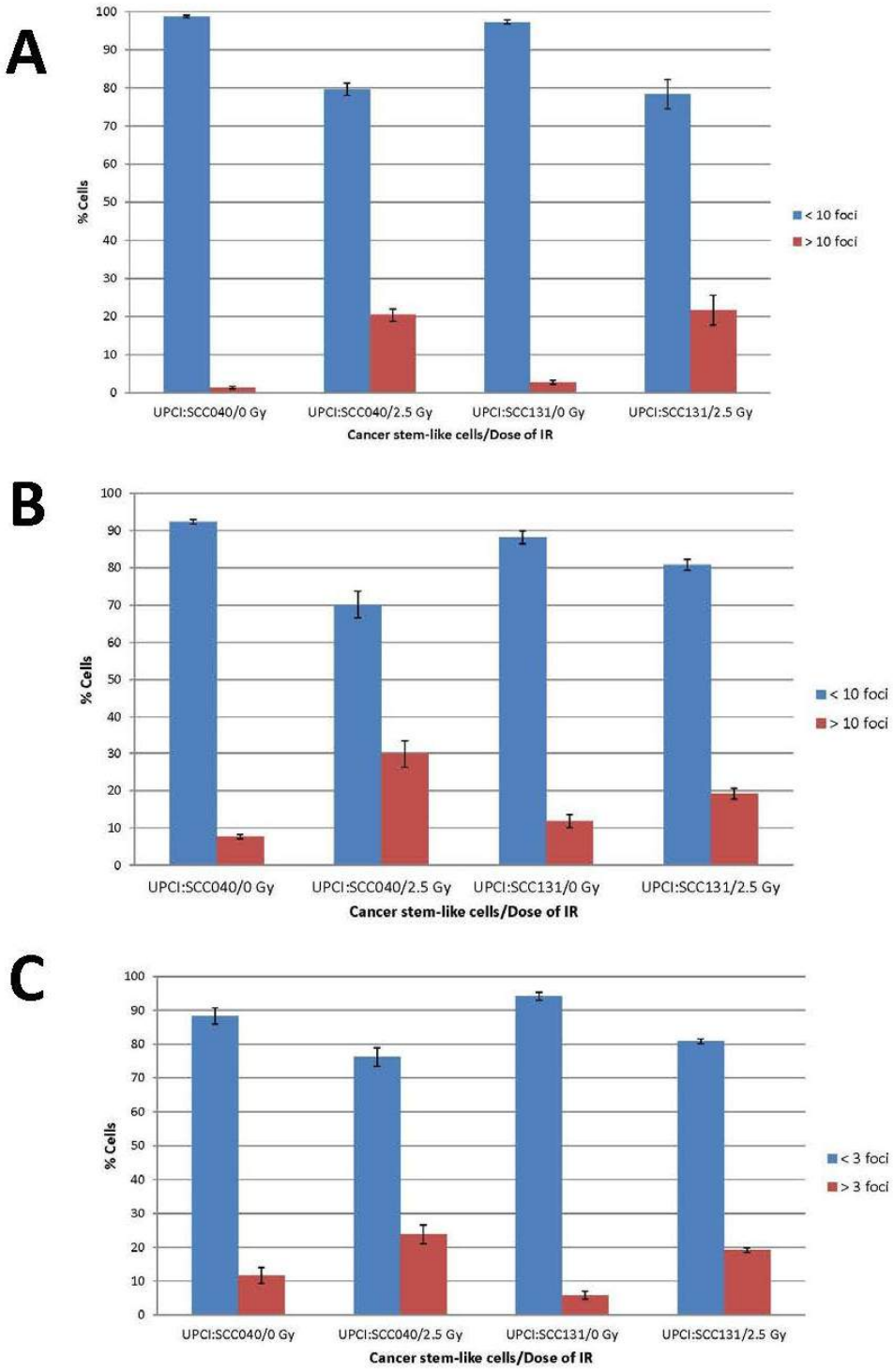

Figure 47. DNA damage response in cancer stem-like cells enriched from UPCI:SCC cell lines in response to IR

A. γH2AX foci in cancer stem-like cells, untreated and 1 hr post-IR (mean ± SEM).
B. KU70 foci in cancer stem-like cells, untreated and 1 hr post-IR (mean ± SEM).
C. pCHEK1 foci in cancer stem-like cells, untreated and 1 hr post-IR (mean ± SEM).

3.7 COMBINED IR AND CHEK1 INHIBITION OF CSLC IN OSCC

Our group and others have shown previously that a CHEK1 SMI can radiosensitize cancer cells to IR (Blasina, et al. 2008; Sankunny, et al. 2014). We tested the response of CSLC to combined therapy with IR and CHEK1, by the following measures: spheroid survival assay, cell viability assay, ELDA and spheroid migration assay. CSLC were treated with CHEK1 for 48 hr (8 hr before-radiation treatment) based on our previous findings (Sankunny, et al. 2014). The combination of IR and CHEK1 SMI reduced the survival of CSLC compared to a single IR treatment (Figures 48-50). The spheroid survival assay showed no statistical significance between CSLC with and without distal 11q loss across all combinations assessed (2.5 Gy/100 nM, 2.5 Gy/1 µM and 2.5 Gy/10 µM) (Figure 48). Only 2.5 Gy/10 µM was potent in eradicating CSLC in either group. On the other hand, ELDA showed that the combination 2.5 Gy/1 µM was statistically significant when compared to 2.5 Gy/0 nM; however, only the combination 2.5 Gy/10 µM inhibited stem cell frequency effectively to less than 1/1000 in both groups (Table 10). Again, our results in Table 10 showed no statistically significant difference in SC frequency in response to the therapeutic combination based on distal 11q loss (Distal 11q loss group: UPCI:SCC040 and 131; No distal 11q loss group:UPCI:SCC066 and 116). Our results of a cell viability assay demonstrated that only the combination of 2.5 Gy/10 µM could possibly inhibit CSLC to less than 20% (Figure 49). Our results also showed no statistically significant difference between the two groups based on distal 11q loss (Figure 49). The spheroid migration assay was done only on CSLC derived from distal 11q loss spheroids (UPCI:SCC040 and 131) because spheroids derived from CSLC without distal 11q loss (UPCI:SCC066 and 116) did not migrate on Matrigel™-coated plates. The results confirmed that only the combination of 2.5

Gy/1 µM could partially inhibit spheroid migration. The 2.5 Gy/10 µM combination effectively inhibited spheroid migration completely in both cell lines.

Overall, the spheroid survival assay, cell viability assay and spheroid migration assay showed that a high CHEK1 inhibitor dose, as high as 100-fold the dose effective on parental cell lines was required to effectively inhibit CSLC (Figures 47, 48; Table 10). Effective CHEK1 inhibitor doses of ≈300-500 nM/dl were effective in inhibiting cancer cells *in vitro* (Blasina, et al. 2008; Sankunny, et al. 2014), while only doses ≈1-10 µM/dl were effective in CSLC (Figures 48-50; Table 10). The response to the IR/CHEK1 combination was not 'Distal 11q loss' driven, suggesting that CSLC possess a complex DDR therapeutic resistance machinery that differs from that in non-CSLC.

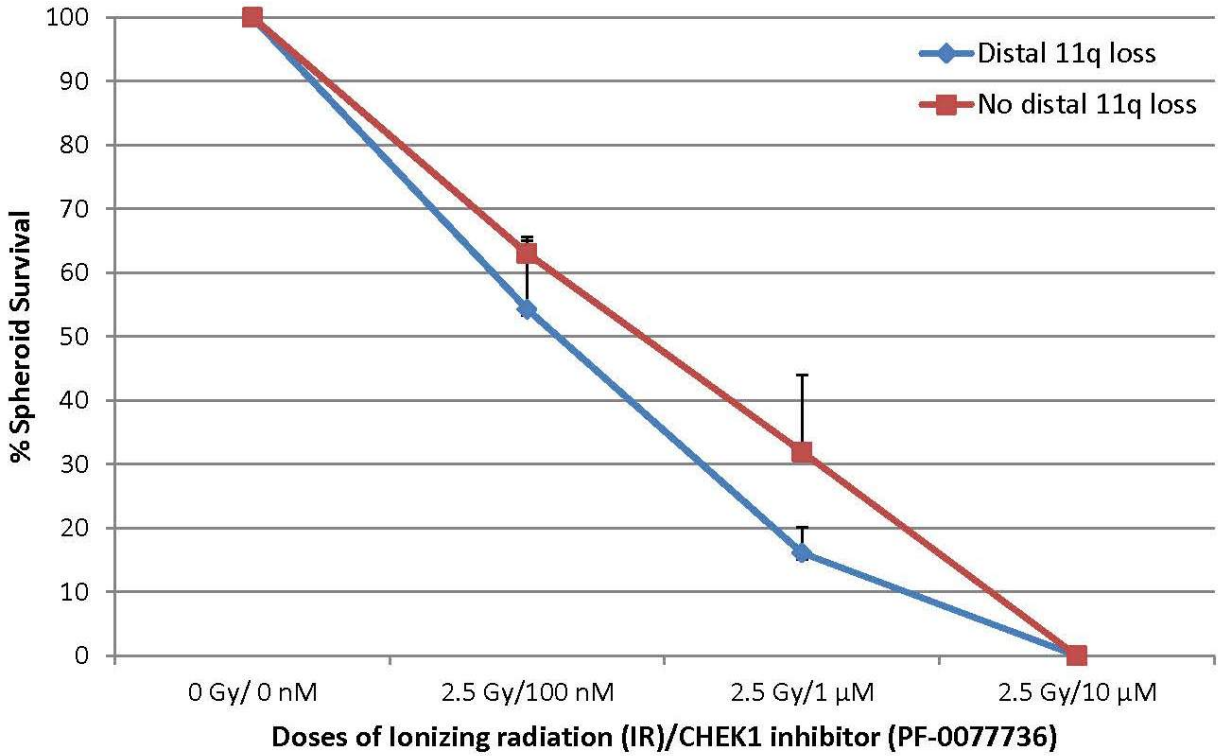

Figure 48. Spheroid survival in CSLC with and without distal 11q loss in response to combined IR and CHEK1 SMI (+/- SEM)
The results show no statistical significance between the two groups in response to different IR/CHEK1 combinations. Distal 11q loss (UPCI:SCC029B and UPCI:SCC040), No distal 11q loss (UPCI:SCC066 and UPCI:SCC116).

Table 10. Stem cell frequency in OSCC cell lines, assessed by ELDA in response to combined IR and SMI CHEK1*

Stem Cell Frequency				
	0 Gy/0 nM CHEK1 inhibitor	2.5 Gy/100 nM CHEK1 inhibitor	2.5 Gy/1 μM CHEK1 inhibitor	2.5 Gy/10 μM CHEK1 inhibitor
UPCI:SCC040	**1/225** UL:1/155, LL:1/327	**1/843** UL:1/538, LL:1/1321	**1/1239** UL:1/743, LL:1/2065	**1/1658** UL:1/936, LL:1/2934
UPCI:SCC131	**1/252** UL:1/173, LL:1/369	**1/845** UL:1/539, LL:1/1325	**1/801** UL:1/514, LL:1/1247	**1/1821** UL:1/1006, LL:1/3296
UPCI:SCC066	**1/231** UL:1/159, LL: 1/334	**1/393** UL:1/269, LL: 1/576	**1/715** UL:1/466, LL: 1/1098	**1/11579** UL:1/2903, LL: 1/46191
UPCI:SCC116	**1/259** UL:1/179, LL:1/377	**1/488** UL:1/329, LL:1/724	**1/683** UL:1/447, LL:1/1044	**1/2054** UL:1/1101, LL:1/3830

* Stem cell frequency was estimated by extreme limiting dilution assessment utilizing SC analysis software (Hu and Smyth 2009).
*The values represent the estimation of SC frequency with upper limit (UL) and lower limit (LL) values setting a range limit.
*Only the combination 2.5 Gy/10 μM inhibited stem cell frequency effectively to less than 1/1000 in both groups.

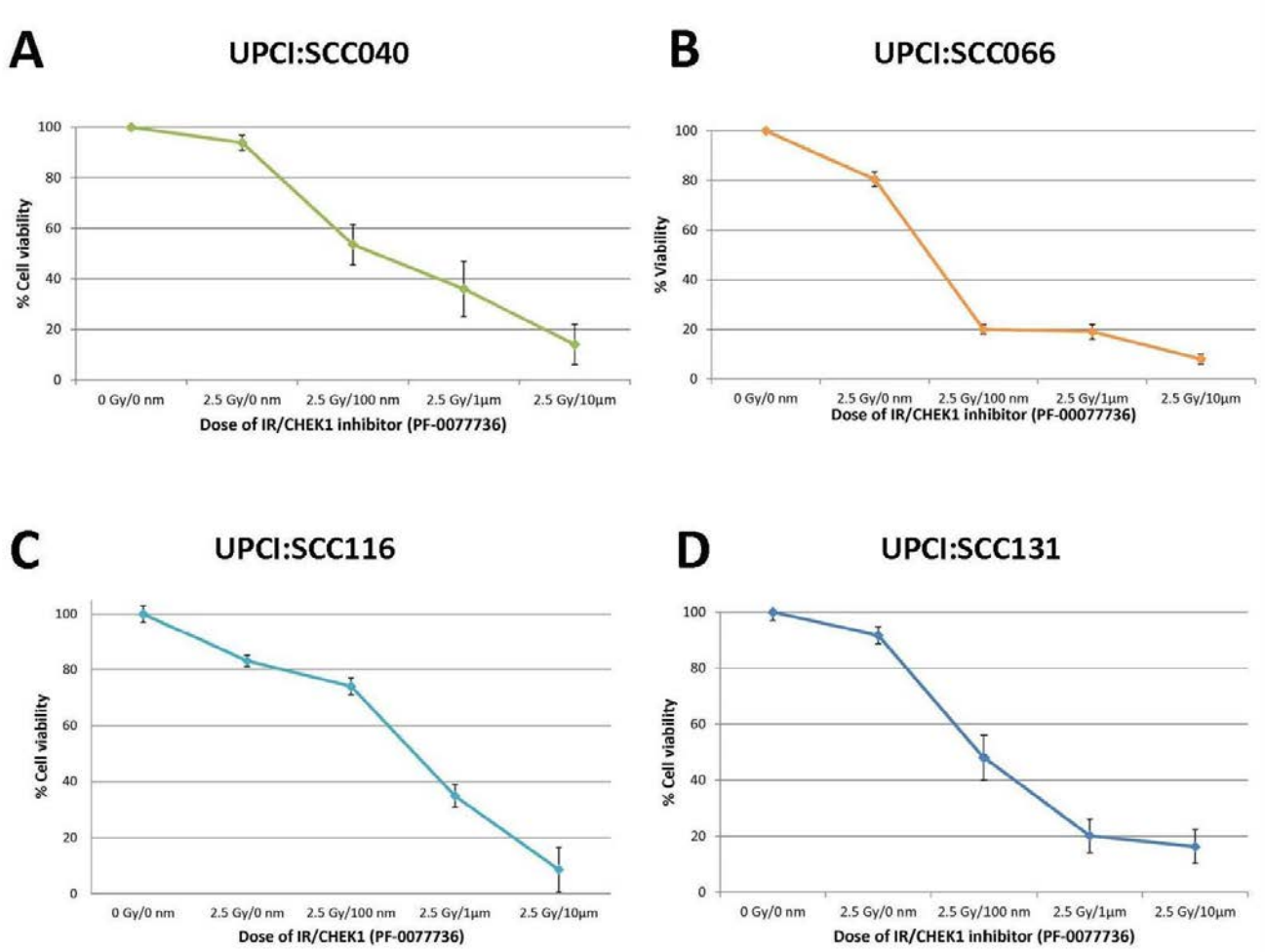

Figure 49. Cell viability in response to combined IR and CHEK1 SMI inhibitor (PF-0077736), comparing various doses of SMI

Line graphs showing response of **A.** UPCI:SCC040, **B.** UPCI:SCC066, **C.** UPCI:SCC116 and **D.** UPCI:SCC131 CSLC to IR/CHEK1 inhibitor combination (0 Gy/0 nM, 2.5 Gy/100nM, 2.5 Gy/1 µM and 2.5 Gy/10µM). Distal 11q loss cell lines (UPCI:SCC040 and 131) and no distal 11q loss cell lines (UPCI:SCC066 and 116). No statistical significance was observed between the two groups.

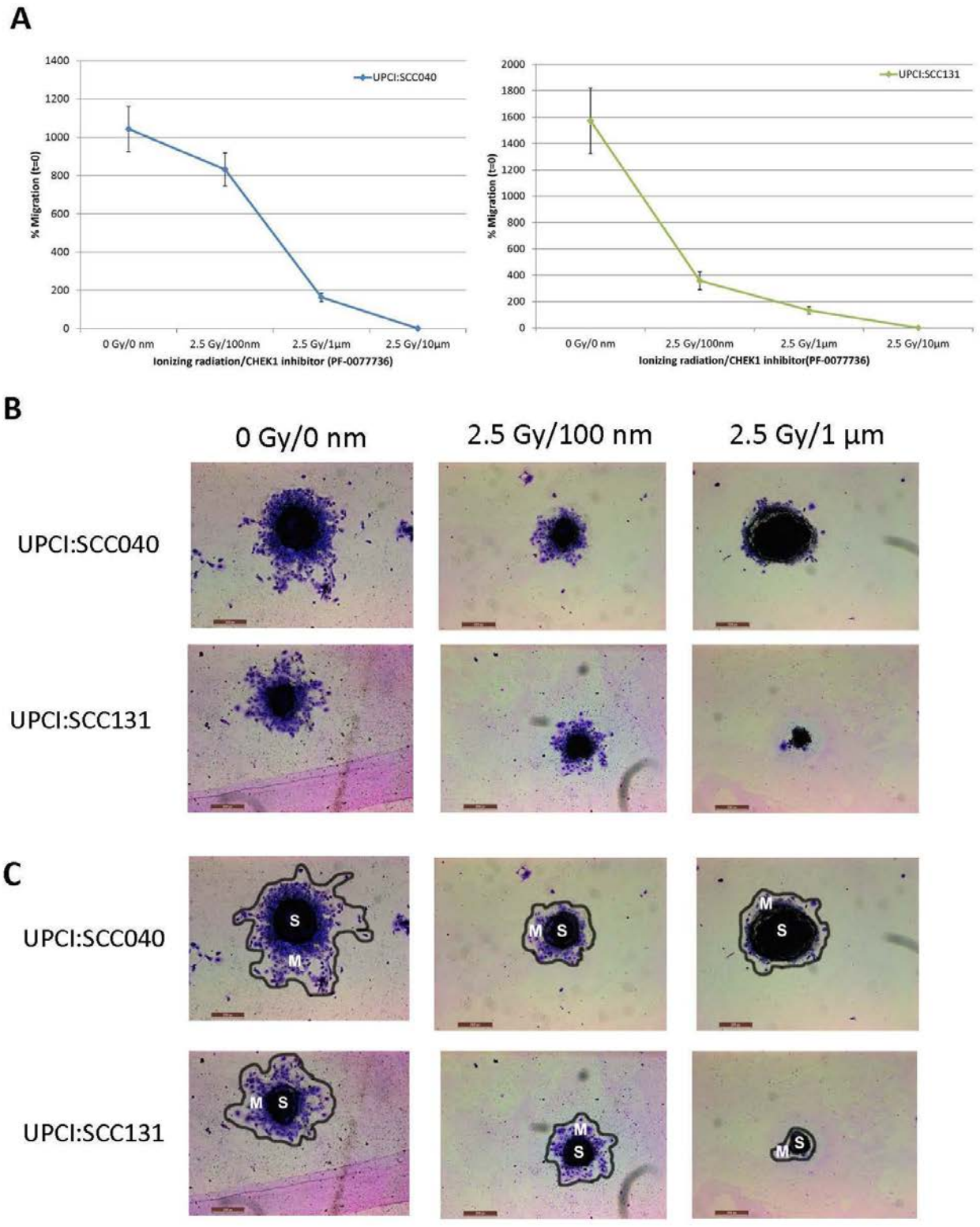

Figure 50. Quantification of spheroid migration in response to combined IR2.5 and CHEK1 small molecule inhibitor

A. Line graphs showing quantification of UPCI:SCC040 and 131 cell migration on Matrigel™-coated plates at 96 hr in response to combined IR and CHEK1 small molecule inhibitor (mean ± SEM of replicate spheroids). Migration was assessed at 96 hr relative to original spheroid size at (t=0) for each condition. The area of the spheroids (S) at t = 0 and the area covered by the cells that have migrated from the spheroids (M) was determined after 4 days. Data were normalized to the original spheroid recorded using the following formula: % migration zone=migrated area (M)(t= 96 hr) /original spheroid (S) (t = 0) × 100.
B Images showing spheroid-based migration in response to combined IR and CHEK1 small molecule inhibitor (2.5 Gy/100 nM and 2.5 Gy/1 μM) (stained with Giemsa stain).
C. Analyzed images showing spheroid-based migration marked as M (Migration Zone) and original Spheroid at (t=0) S (Spheroid Zone).

4.0 DISCUSSION

4.1 CSLC MARKERS IN OSCC CELL LINES

One of the characteristics of CSLC is the presence of unique cell surface markers. Breast cancer was the first solid tumor in which CSLC were isolated, as a result of the expression of a high level of CD44 and a low level of CD24 cell surface markers (Al-Hajj, et al. 2003). Identifying CSLC using cell surface markers aids in quantifying these cells in tumors. We used low cell line passages that resemble to a large extent the primary tumors (Wilson, et al. 2012). We investigated by IF the frequency of four markers CD44, CD133, SOX2 and BMI1 a panel of 18 UPCI:SCC cell lines (Table 6). Based on analysis of our results, we observed that OSCC can be classified based on intensity of staining into three major categories (+/++/+++); CD133 and CD133/1 were the only markers expressed as (+/-). OSCC cells with positive (+++) were categorized as CSLC based on the correlative evidence we observed on double IF staining as well as previous research (Harper, et al. 2007; Li, et al. 2014; Locke, et al. 2005).

Our IF and flow cytometry results showed that CD44 is not be a suitable marker for identifying CSLC in OSCC. The average frequency of CD44-positive (+++) cells in 18 OSCC cell lines was 23% (Table 5), which is higher than expected compared to the findings of other research groups testing CSLC markers (Clay, et al. 2010; Zhang, et al. 2010). Further, the flow cytometry results confirmed that CD44 is constitutively expressed in three of four cell lines that

we assessed, making flow sorting for CSLC using this marker less useful. On IF, only rare cells did not express CD44, so we did not include a non-expressing category. Our average CD44-positive frequency seems to concur with results obtained by Joshua et al., who found an average of 25% CD44-positive cell in a panel of 31 HNSCC primary tumors (Joshua, et al. 2012). Double IF staining with other stemness markers, including SOX2, BMI1 and NESTIN confirmed that the majority of CD44-positive cells did not double-stain with other stemness markers, adding further evidence to our conclusion that CD44 is not a sensitive CSLC marker (Figures 14, 15). Furthermore, IF staining of the control cell line, OKF6, showed the CD44-positive cells at ≈ 5%, confirming that CD44 is not cancer-specific (Figures 12, 13). Research has shown that CD44 and variant CD44 isoforms are expressed in both normal and cancerous oral tissue (Mack and Gires 2008). The expression of CD44 in normal oral cells as well as CSLC therefore necessitates the addition of another specific CSLC marker. Overall, our results concur with other papers that concluded that CD44 might not be a suitable marker for CSLC in OSCC or HNSCC (Chen, et al. 2012; Shrivastava, et al. 2015).

CD133 and CD133/1, on the other hand, are more promising cell surface markers of CSLC in OSCC cell lines. The mean frequency of CD133-positive cells was ≈ 6%, which is concordant with being a small subpopulation in the tumor according to the hierarchic CSLC model. CD133 was highly correlated with other stemness markers on double IF and correlated highly with spheroid-forming capacity when assayed in a series of cell lines (Figures 14, 15). Overall, our results concur with other papers that concluded that CD133 and CD133/1 is a suitable markers for CSLC in OSCC (Chen, et al. 2012; Shrivastava, et al. 2015). CD133 (Abcam) was consistent, clear and robust across cultures, unlike CD133/1 (Miltenyi). Problems of CD133/1 as a possible cell surface marker in OSCC include faint/dim staining and

inconsistency across cultures (Figure 8). Furthermore, we concur that the dimness of CD133/1 makes the flow cytometric analysis of the population difficult (Harper, et al. 2007). Inconsistency of CD133/1 IF staining across cultures has been reported previously in colorectal CSLC (Dalerba, et al. 2007; Odoux, et al. 2008). Possible explanations for the CD133/1 inconsistency include the inter-observer bias because of the difficulty of assessing dim/faint sub-populations in IF/flow cytometry and manufacturing properties related to the CD133/1 antibody itself. The antibody as produced by the company has a very limited stability (6 months) and is prepared in an extremely diluted form that requires an extremely unusual low dilution of ≈1/10. These observations were discussed with the manufacturing company (Miltenyi, Inc.) and we were one of the labs that tested their new, improved CD133/1 conjugated with viobright-FITC. Unfortunately, the new product was as dim/faint as the earlier product. Overall, technical difficulties related to CD133/1 staining in OSCC are clear and have been observed previously by others (Locke, et al. 2005).

CSLC markers in primary tumors and cell lines may not truly reflect all of the biological features of CSLC, primarily due to loss of the niche interaction that plays an important role in regulating many properties of CSLC, including cell division pattern and rate. In addition, culture adaptation and genetic alterations taking place during long-term culture under hypoxic culture conditions may lead to overestimation of the frequency of CSLC markers in cell lines (Wang, et al. 2013). In spite of this, some research groups observed consistent CSLC markers between early and late passages (Bunger, et al. 2012; Harper, et al. 2007; Locke, et al. 2005). Further research on CSLC identification markers seems crucial to enable researchers to further study this subpopulation.

Our results show that the ability to form large spheroids (>100 μm) does not correlate with the percentage of CSLC detected either by single or double marker staining. This concurs with CSLC analysis of primary breast tumors (Grimshaw, et al. 2008). CD133-positive cells highly correlated with spheroid-forming capacity in a group of OSCC cell lines that we assessed (Figure 31); however, increasing the sample size to verify our results is warranted. In conclusion, currently there is no consensus regarding the most suitable cell surface markers for the identification of CSLCs in OSCC. Our results show that double immunostaining is the most effective approach in analyzing the CSLC population in OSCC cell lines and possibly, primary tumors.

4.2 PROGNOSTIC SIGNIFICANCE OF CSLC IN OSCC CELL LINES

The identification of biomarkers in OSCC that predict the potential of recurrence or progression in patients will aid in selecting patients who could benefit the most from adjuvant treatments. We did not find prognostic significance between CSLC markers and various parameter of disease (Table 6). We expected the results to some extent because OSCC is a complex heterogeneous cancer driven by multiple genetic and environmental factors. In addition, the functional assessment of CSLC potential using extreme limiting dilution showed similar tumor initiating potential (<0.1%), suggesting that CSLC frequency is not the main force driving disease progression (Figure 34). Furthermore, double IF staining with CSLC markers showed that our cell lines had similar frequencies of CSLC-positive cells (1-3%) when double stained with CSLC markers (Figures 14, 15). These results suggest that not all cells with CSLC markers possess tumor initiating potential. Furthermore, non-CSLC cells, such as CD44-negative cells,

have been shown to be tumorigenic in HNSCC and other cancers, suggesting that single CSLC markers are insufficiently sensitive enough to assess CSLC in tumors (Oh, et al. 2013; Wang, et al. 2008). Our results strongly suggest that the CSLC subpopulation is dynamic and can be influenced by stochastic factors, such as IR and tumor re-initiation modeled by culture cloning as suggested by Lagasse (Lagadec, et al. 2010; Lagasse 2008; Odoux, et al. 2008).

A longitudinal clinical study in a large population to assess the prognostic value of CSLC in OSCC is necessary to validate our results. However, the inconsistencies in the prognostic value of CSLC markers in OSCC are clear when reviewing the literature (Table 2), and extend across other tumors, such as hepatocellular carcinoma (Salnikov, et al. 2009). The lack of tumor specificity of CSLC markers, such as CD44 further adds complexity to the assessment of CSLC frequency in tumors. Overall, based on our current results and a review of the current literature we believe that the tumorigenicity of CSLC will likely be closely linked to multiple factors that include HPV status (Zheng and Franzmann 2013), the mutational status of driver genes, as well as the copy number status within the tumor (Gollin 2014).

4.3 DIVISION PATTERNS OF CSLC IN OSCC CELL LINES

Division utilizing both symmetrical and asymmetrical cell division is an important characteristic of SC. The facultative use of symmetric or asymmetric divisions by SCs is a key adaptation crucial for both development and regeneration (Morrison and Kimble 2006). Asymmetric cell division is important in growth and development of many invertebrates such as *Drosophila melanogaster* and *Caenorhabditis elegans* (Knoblich 2010). Cell division fate is regulated by intrinsic and extrinsic mechanisms. Intrinsic mechanism are regulated by the partitioning of cell

components that determine cell fate such as cell polarity and segregation determinants; while extrinsic mechanisms are regulated by signaling from the external environment (Morrison and Kimble 2006). In *Drosophila melanogaster*, asymmetric cell division is mediated by the protein Numb that inhibits Notch–Delta signaling; this is followed by asymmetric localization of adaptor proteins, such as Brat (Knoblich 2010). Asymmetrical division is tightly regulated during interphase through telophase (Knoblich 2010; Morrison and Kimble 2006). Par proteins mediate spindle orientation; in asymmetric cell division, cell fate determinants are inherited by only one of the two daughter cells (Betschinger and Knoblich 2004; Knoblich 2001; Knoblich 2010; Wang, et al. 2007). Functional differences in cellular properties as well as differences in cell size have been noted in invertebrates immediately post-mitosis (Knoblich 2010). In mammalian cells, the critical role of NUMB was confirmed in both mouse and human cells and has been critical to our understanding of the process of asymmetrical division. NUMB was found to localize to one edge of a daughter cell, forming a crescent-shaped pattern that segregates into only one of the two daughter cells. NUMB mediates NOTCH signaling, that in turn regulates PROX1, a transcription factor and BRAT, a regulator of post-transcriptional events (Knoblich 2010).

In some adult SCs, such as hematopoietic SC, asymmetrical division is the main form of division employed to maintain tissue homeostasis. However, in the case of injury or disease, switching to symmetrical division is possible (Morrison and Kimble 2006). Similarly, SCs in mammalian epithelial tissues require asymmetrical division and axis polarity to generate specialized differentiated cell progeny, while ensuring SC equilibrium (Clevers 2005). The interconnection between SCs, asymmetric cell division and carcinogenesis has been an active area of research for more than a decade. The hallmark study by Caussinus and Gonzalez in *Drosophila*, showed that tumor formation is associated with the switch of SC division machinery

from asymmetrical to symmetrical (Caussinus and Gonzalez 2005). Functional studies by Caussinus and Gonzalez showed that defective asymmetrical division of neuroblast SC was associated with marked cellular hyperplasia as well as generation of satellite tumors distant from the site of injection; further, sequential transplantation was also associated with tumor initiation and the emergence of genomic instability in cells (Caussinus and Gonzalez 2005). In mammalian SC, asymmetric cell divisions are correlated with tumor suppression (Humbert, et al. 2003). Functional studies in breast cancer cells demonstrated that loss of NUMB may be associated with the hyperactivation of NOTCH pathway signaling that leads to an increase in symmetrical division (Pece, et al. 2004). Symmetrical cell division also seems to promote genetic instability, an important characteristic of solid tumors (Gollin 2005; Hanahan and Weinberg 2000; Hanahan and Weinberg 2011; Morrison and Kimble 2006; Reshmi, et al. 2004). Research has shown that asymmetrical cell division is a more tightly regulated process because of the need to change the fate of one of the daughter cells; therefore symmetric divisions might not only increase CSLC numbers, but also increase the probability of genetic instability and other secondary mutations by disrupting the controls on centrosomes and mitotic spindles (Caussinus and Gonzalez 2005; Morrison and Kimble 2006).

Understanding the regulation of asymmetric cell division in CSLCs will provide insight into tumor initiation, growth, and maintenance (Pine, et al. 2010). One of the key questions in CSLC biology concerns the mechanisms that regulate division patterns of CSLC, and thereby tightly regulate the self-renewal/differentiation balance within the tumor. Different epigenetic profiles have been suggested as one of the mechanisms that might regulate cell fate (Lansdorp 2007). Improvements in immunostaining, cell culturing and imaging technology, such as time lapse imaging have given researchers new tools to study cell division in CSLC. In the field of

CSLC, there remains a need to assess which molecules can segregate asymmetrically in order to identify this type of division.

Recently, Tomasetti and Vogelstein proposed a theory based on the cancer stem cell (CSC) stochastic model (Tomasetti and Vogelstein 2015). They proposed that differences in organ-specific cancer risk is largely due to mutation in non-CSC. Based on Tomasetti and Vogelstein's mathematical modelling, the stochastic origin of CSC might be a bigger contributor to cancer than hereditary and environmental factors. They based their assumption on the fact that most human cells have similar mutation rates, but different proliferative rates; a functional property regulated by SCs within each organ. Correlation analysis of SC division and cancer life time risk across 31 different tumors was highly significant (0.804; $p<0.05$) (Tomasetti and Vogelstein 2015).

Research has shown that CSLC are present in cell lines and that they can be isolated and propagated for a number of passages on laminin or other ECM proteins, such as Matrigel™ (Sun, et al. 2008). The frequency of asymmetric division of BrdU-labeled template DNA in NSCLC was ≈ 5% (Pine, et al. 2010), similar to the asymmetrical division ratio in murine muscle satellite cells *in vitro* (Shinin, et al. 2006). Pine et al. showed that environmental factors, such as increased cell density, hypoxia and serum deprivation decreases asymmetrical division in CSLC (Pine, et al. 2010). Lathia et al. demonstrated using CD133 and time-lapse imaging that CSLC in glioma divided both symmetrically and asymmetrically (70%:30%). They observed that only CD133, and no other CSLC markers are distributed both symmetrically and asymmetrically. Further, they observed that symmetrical division increases with the introduction of enriched CSLC culture medium (Lathia, et al. 2011). Liu et al. showed that asymmetrical division in breast CSLC correlates with increased invasion and migration (Liu, et al. 2013). This is possibly

because non-CSLCs possess a higher proliferative capacity. Further, they showed that division patterns of CSLC might be affected by the CSLC niche, such as the presence of mesenchymal cells (Liu, et al. 2013). Izumi and Kaneko found that cell division might be regulated by driver oncogenes, such as *MYCN* in neuroblostoma cell lines; *MYCN* overexpression being associated with symmetrical division (Izumi and Kaneko 2012). The pioneering work of Izumi and Kaneko might be of significant value if similar results are observed in other cancers. Overall, it is clear that CSLC division is an interesting new area of research with topics such as the implications of the type of division on mutation accumulation still remains unclear (Shahriyari and Komarova 2013).

Our group has shown previously that cancer cells in OSCC cell lines show abnormal cell division patterns, dysfunctional cytokinesis, and segregation defects (Sankunny, et al. 2014; Saunders, et al. 2000). We studied the division patterns in two of our cell lines (UPCI:SCC040 and 131) using CSLC markers (CD44, CD133, SOX2 and BMI1). SOX2 was the only marker that showed statistically significant symmetrical and asymmetrical division patterns; analysis of other CSLC markers only showed symmetrical division. Sex-determining region Y [SRY]-box (SOX2) is a SC transcription factor that was originally demonstrated in embryonic SC (ESC) and was found to mediate self-renewal and pluripotency of SC (Okumura-Nakanishi, et al. 2005; Sarkar and Hochedlinger 2013). In addition, SOX2 is one of the key transcription factors capable of reprogramming differentiated somatic cells into induced pluripotent stem (iPS) cells (Takahashi, et al. 2007; Yu, et al. 2007). Later, another research group identified SOX2 in adult tissue SC, including squamous epithelium of the tongue (Okubo, et al. 2009). Recently, SOX2 has also been found to be a functional marker of CSLC in various tumors, including HNSCC (Lee, et al. 2014). Silencing of SOX2 *in vitro* has been shown to decrease CSLC self-renewal,

chemoresistance, invasion capacity, and *in vivo* tumorigenicity (Lee, et al. 2014). SOX2 overexpression in HNSCC was found to lead to cyclin B1 and SNAI1 overexpression, as probable mechanisms that might give these cells a survival advantage (Lee, et al. 2014). A possible role for SOX2 as an independent CSLC marker in HNSCC has also been suggested by multiple studies (Table 2). Overall, the role of SOX2 in CSLC has been confirmed in multiple studies of different tumors.

Our OSCC division results are similar to that observed in other tumors such as neuroblastoma and glioblastomas (Beckmann, et al. 2007; Izumi and Kaneko 2012; Lathia, et al. 2011) and other SC such as hematopoietic SCs (Beckmann, et al. 2007). Our results establish the UPCI:SCC cell lines as useful experimental preclinical models for further assessment of the biology of CSLC cell division and for testing possible therapeutic strategies that target the stemness pathway.

Analysis of our results showed that the division pattern did not change based on IR treatment strategies, suggesting that cell division patterns of CSLC might be difficult to manipulate utilizing standard therapeutic approaches. The high prevalence of symmetrical division, even after IR treatment, might be explained by the enhanced radioresistance of CSLC compared to differentiated progeny, a robust mechanism which can thereby maintain tissue homeostasis even in unfavorable conditions (Shahriyari and Komarova 2013). Further, CSLC had fewer segregation defects when compared to non-CSLC. The decreased segregation defects in addition to the predominance of symmetrical division protect CSLCs from IR-induced DNA damage**.** Understanding CSLC biology and division is essential before effective targeting of this subpopulation can be implemented. Unanswered questions in CSLC biology include how the type/rate of cell division contributes to SC regulation, how SC switch between the two modes of

division, and how cancer changes SC division (Shahriyari and Komarova 2013). Previous studies showed that human OSCC contain CSLC with a distinct phenotype, including features of self-renewal, induction of multi-lineage cell differentiation, and high drug efflux capacity (Harper, et al. 2007; Lim, et al. 2011; Liu, et al. 2012). Our present findings add the asymmetrical division phenotype to the features of OSCC CSLC. We showed in our current work that it is possible to analyze asymmetric cell division in cultured OSCC cells. Division patterns in OSCC that we observed are mainly related to the intrinsic cellular machinery and not dependent on cell-to-cell contact or a stem cell niche. Changes in cell microenvironment, such as CSLC enriched medium leads to an increase in symmetrical division. On the other hand, IR therapy did not change the CSLC division patterns. The possibility of therapeutic interventions affecting cell fate could alter the therapeutic effectiveness. For instance, if a targeted drug could shift the symmetrical:asymmetrical ratio towards asymmetrical division, classical therapeutic interventions could be more efficient. Possible limitations of our current work include the inability to assess the effects of the SC niche and the inability to test whether post-mitotic alteration of the daughter cells occurs (Beckmann, et al. 2007). For example, it is possible that a CSLC could differentiate post-mitosis; such a possibility could be only studied by lineage tracing experiments. Interestingly, research has shown that the NOTCH signaling pathway can post-mitotically alter the developmental fate of cells (Betschinger and Knoblich 2004; Martinez Arias, et al. 2002). Overall, we believe that the manipulation of CSLC division from symmetrical to asymmetrical through therapeutics might be one approach to eradicating tumors.

4.4 DISTAL 11Q LOSS AND CHROMOSOMAL INSTABILITY IN OSCC CSLC

Our group has demonstrated previously that distal 11q loss as marked by loss of the *ATM* gene plays a role in predicting radioresistance and a favorable response to combined therapy using IR and an ATR/CHEK1 pathway inhibitor. CSLC are a subset of cells that influence therapeutic resistance in cancers. Identifying CSLC-related DNA repair vulnerabilities might facilitate more effective therapeutic targeting of these cells. Understanding the role of *ATM* loss in CSLC will aid in highlighting the functional context of copy number alterations in CSLC. Like all cancer cells, CSLC are genetically heterogeneous and may acquire genetic changes that favor resistance to various therapeutic approaches (Bakhoum, et al. 2015; Gollin 2014; Lagasse 2008; Odoux, et al. 2008).

Our results suggest that CSLC show genetic alterations identical to the genetic variations observed in non-CSLC (Figure 26; Table 7), suggesting a common ancestral origin and the possibility of a hierarchic model. The copy number variation observed within CSLC clones suggests that CSLC show different therapeutic resistance properties, a qualitative trait; and that the frequency of CSLCs, a quantitative trait in the tumor might not be the driving force behind CSLC therapeutic resistance (Figures 27, 28). Our current results suggest that CSLC frequency is not a consistent prognostic marker across OSCC (Table 2). Recently, in non-CSLC, chromosomal instability was shown to be an important factor driving radioresistance (Bakhoum, et al. 2015). Further assessment of the possible role of CIN in CSLC is warranted.

Our results confirm the model presented by Lagasse suggesting that CSLC show dynamic rather than fixed therapeutic resistance (Lagasse 2008). The enhanced therapeutic resistance that occurs as a result of the complex interaction of stemness factors, driver mutations and copy number alterations may contribute to the unique evolutionary survival capacity of these cells

(Garcia, et al. 2000; Lagasse 2008). Understanding the mechanisms of CIN in oral CSLC will aid in devising approaches to understand which patients are more prone to therapeutic resistance (Bakhoum, et al. 2015). The genetic heterogeneity of CSLC will probably necessitate using multiple therapeutic approaches as well as re-assessing the genetic alterations in metastatic/recurrent tumors (Lagasse 2008). Although, CSLC and non-CSLC share important genetic alterations, curative rates in cancers are still not high and are sometimes inconsistent. For instance, in CML patients, where there are high remission rates due to targeted drugs against the *BCR/ABL1* translocation, curative rates are intermediate and recurrence occurs due to development of bypass mutations in CSLC (Graham, et al. 2002; Lagasse 2008).

4.5 SPHEROID ENRICHMENT IN OSCC

Based on the current literature and the lack of a clear cut marker for CSLC, spheroid enrichment emerges as the most suitable approach to study CSLC (Pastrana, et al. 2011; Shrivastava, et al. 2015). Growing CSLC in suspension or adherently attached on Matrigel™-coated plates were both utilized in our study. This enabled the versatility of studying and assessing more properties of CSLC. Morphologically, the spheroids were either spheroid (sphere-like) in shape or grape-like in shape; both morphological types have been described previously in the literature (Hueng, et al. 2011; Lim, et al. 2011). In gliomas, spheroid/grape-like morphologies were associated with different genetic signatures and functional capacities; the typical spheroid morphology being associated with ESC origin and the grape-like morphology being associated predominantly with mesenchymal SC (MSC) origin. Such a possibility might exist across other tumors as well, and needs further investigation in our cell lines (Mao, et al. 2013). Adherent, enriched CSLC

characteristically grew as small tightly packed cells in rounded colonies similar to the holoclone morphology described by Locke et al. (Locke, et al. 2005). Locke et al. previously described that colonies in OSCC cell lines can be classified into: 'holoclones', 'paraclones' or 'meroclones;' holoclones are compact round colonies, paraclones are loose, irregular colonies, and meroclones have intermediate features. Holoclones are characteristically associated with CSLC (Locke, et al. 2005). The *in vitro* colony classification and the higher frequency of CSLC were also identified in other tumors as well, such as lung SCC (Wang, et al. 2013) and pancreatic cancer (Tan, et al. 2011).

Spheroid enrichment as an approach for studying CSLC has advantages and disadvantages. Advantages include that the approach is more affordable and more versatile when compared to FACS. Second, the approach has been standardized (Pastrana, et al. 2011; Vinci, et al. 2013). Disadvantages include that spheroids do not enrich exclusively for CSLC; second, not all spheroids arise from SCs, but sometimes from transient progenitor cells as well; third, spheroids might not arise from quiescent SCs; fourth, spheroids might aggregate, leading to difficulties in assessing clonality (Friedrich, et al. 2009; Pastrana, et al. 2011; Perego, et al. 2011). Improvements and modifications to the spheroid enrichment procedure have potentially eliminated some of the disadvantages. For instance, assessing clonality is critical in assessing self-renewal and/or therapeutic response; this issue has been overcome by ensuring a proper clonal density of 0.2 to 20 cells per µL which can be achieved by using limiting dilution. Research has shown that spheroid diameter ranges from 40–150 µm and that bigger spheroids tend to originate from SC and smaller spheroids from progenitor cells (Pastrana, et al. 2011). In addition, the use of adherent systems with CSLC-enriched medium, a modification to the non-adherent system, is rapidly gaining ground as it ensures full exposure of adherent CSLCs to the

enriched medium thereby inhibiting CSLC differentiation and increasing CSLC propagation (Woolard and Fine 2009). As our understanding of CSLC biology and the CSLC niche progresses, bioengineering approaches will enable researchers to create an *in vitro* substrate similar to the *in vivo* extracellular matrix. Such models will yield information with high translational value (Vunjak-Novakovic and Scadden 2011).

4.6 CSLC RADIORESISTANCE PATTERNS IN OSCC

CSLCs have been found to contribute to therapeutic resistance, recurrence and metastasis. If the proportion of CSLCs in tumors could be targeted and reduced, then the mortality rates of patients may improve. Our results using a variety of approaches showed that enriched CSLCs are resistant to IR through different approaches (Figure 36-46). To simulate the clinical setting, we administered IR regimens (2.5 Gy IR EOD*3) and (2.5 Gy IR EOD*6), to CSLC-enriched cultures and assessed the colony forming capacity of both regimens. Spheroid-enriched CSLC showed persistent radioresistance across both regimens (Figure 45).

To study the role of distal 11q loss in CSLC radioresistance we used a number of experimental approaches. Both spheroid survival and cell viability assays showed similar radioresistance trends based on distal 11q (Figure 36-40). However, the analysis of spheroid size and ELDA in response to IR did not differ as a function of distal 11q loss (Figure 41-44; Table 9), suggesting a possible complex role of distal 11q loss in OSCC. Overall, our CSLC therapeutic radioresistance trends seem to coincide with the patterns observed by Chen et al. in OSCC (Chen, et al. 2012). Chen et al. showed that different IR regimens (up to 10 Gy) did not lead to a statistically significant reduction in CSLC survival; while on the other hand, parental

cancer cells showed an IR dose-dependent reduction in survival (Chen, et al. 2012) Unlike the results shown by Lagadec et al. and Ghisolfi et al. (Ghisolfi, et al. 2012; Lagadec, et al. 2010), the IR regimens did not enrich the cell lines for CSLC. Our results suggest that IR may not be a suitable CSLC enrichment tool across different tumors. This could possibly be due to the heterogeneity of solid tumors and the different genetic signatures of each tumor type.

One of the limitations of the spheroid survival assay is that spheroids are motile and they might merge, leading to inaccuracies in the estimation of the number of colonies (Singec, et al. 2006). To overcome this limitation we repeated the experiments three times. Furthermore, appropriately low clonal density was used in these experiments (Pastrana, et al. 2011). In addition, other approaches, such as viability assays, proliferation assays, ELDA and migration assays were done to confirm our findings. Unlike the early days of CSLC culture (Singec, et al. 2006), many labs are currently using standardized spheroid culturing approaches, decreasing experimental variability based on the approach. In addition, the spheroid growth and extreme limiting dilution assays using lower cell density in 96-well plates allowed us to assess the therapeutic effect more thoroughly (Singec, et al. 2006). A real problem that we faced in the project was isolating CSLC from spheroids for further assessment of CSLC properties of proliferation, differentiation, viability and segregation defects. We tried a number of approaches to dissociate spheroids into single cell suspensions, but the net yield was usually low (Woolard and Fine 2009). We decided to isolate the CSLC based on their Matrigel™ migration, in addition to a secondary enrichment process on another Matrigel™ substrate. This dual enrichment approach yielded a sufficient number of CSLC for further experimentation. The approach also incorporated the important advantages of CSLC enrichment observed in adherent monolayers; most importantly, the long-term serial passaging potential, the ease of further experimentation

and the possibility of establishing stable CSLC cell lines (Sun, et al. 2008; Woolard and Fine 2009). Two important limitations of the approach include the problem that not all enriched spheroids migrate on Matrigel™ plates and the time factor, as this approach takes double the time of any other one step adherent or non-adherent culturing method.

The radioresistance of CSLC might be explained by the different gene expression pattern of CSLC when compared to parental cell lines as shown previously by Wilson et al. (Wilson, et al. 2013). The results of our assessment of gamma-H2AX foci post-IR in CSLC compared to parental tumors (Parikh, et al. 2007) showed that CSLC expressed more foci, which indicates that these cells might be detecting DNA damage more efficiently than non-CSLC (Figure 47). Assessing KU70 and pCHEK1 foci post-IR also showed statistically significant changes in CSLC, confirming the role of the DDR in CSLC as well as non-CSLC (Sankunny, et al. 2014).

Traditional culture approaches for the evaluation of tumor cell initiation, migration and invasion *in vitro* generally employ two-dimensional (2D) cultures that do not represent the dynamics of how tumor colonies grow and invade the extracellular matrix proteins. Three-dimensional colony formation can more accurately reflect the complexity of cell-cell interaction and cell-environment interaction to a large extent (Vinci, et al. 2013). The spheroid migration model (Figure 51) depicts the critical mobilization of the tumor into the surrounding matrix, a process called ‘infiltration’ and the establishment of new colonies in secondary organs, a process critical in carcinogenesis and referred to as ‘metastasis.’ This critical process is usually associated with the poor prognosis that is reflected in the advanced tumor staging of these patients. Our results show that migratory CSLC were radioresistant, and that the overall trend in response to IR is similar to spheroid survival, spheroid growth and cell viability assays (Figures 36-46).

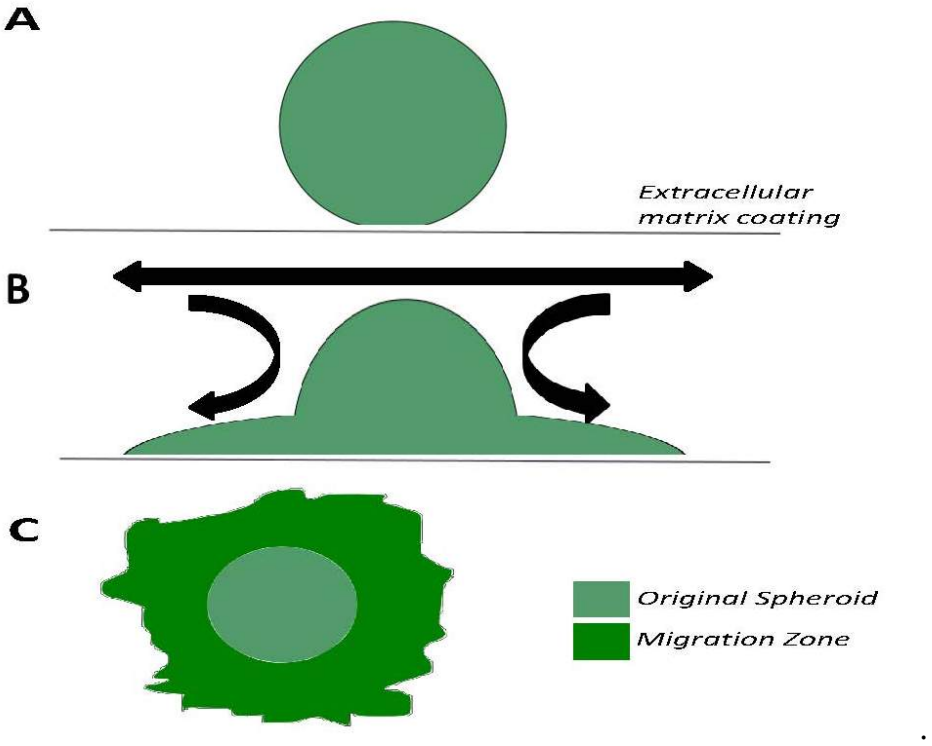

Figure 51. Spheroid migration zone assay for short-term therapeutic assessment

A. The spheroid enriched for CSLC attaches to the extracellular matrix coating, such as Matrigel™.
B. The attached CSLC in the spheroid then migrates on the extracellular matrix.
C. The migration area can be assessed and normalized to the original spheroid area.

4.7 COMBINED IR AND ATR/CHEK1 PATHWAY INHIBITION OF CSLC IN OSCC

Conventional IR and chemotherapy treatment seem incapable of preventing tumor recurrence and/or metastases in OSCC, possibly due to therapeutic resistance of CSLC. The radioresistance of CSLC that we and others have observed makes exploration of novel strategies to inhibit CSLCs a necessity (Bao, et al. 2006). The work of Bao et al. in glioma CSLC showed that DDR inhibitors might hold the promise of targeting CD133-positive CSLC when compared to CD133-

negative CSLC (Bao, et al. 2006). The effectiveness of new DDR-targeted agents, which have been effective experimentally in various cancers need to be studied thoroughly in CSLC as potential targeted therapies.

The spheroid (3D) survival assay that we used in our study has a number of advantages that makes the assay system more robust and reliable than conventional monolayer (2D) culture. These advantages include: the limitation in drug penetration, contact-dependent multidrug resistance, and hypoxia (Friedrich, et al. 2009). Our results show that the combination of IR/CHEK1 may not always inhibit CSLC. An effective CHEK1 dose of 540 nM in parental cell lines did not affect the colony forming capacity or survival of CSLC; a dose-response curve showed that only a 100-fold higher dose of the drug could inhibit CSLC. Our results concur with those of Francipane and Lagasse, who found that of six different mTOR targeting compounds, only one compound at a high concentration produced a statistically significant reduction in survival (Francipane and Lagasse 2013). In ESC, at least a 10-fold higher dose of ATM inhibitor was necessary to inhibit ATM function when compared to somatic cells (Momcilovic, et al. 2010). These results suggest that the ESC genetic signature might be playing a role in CSLC as shown previously by others (Mao, et al. 2013). Further, assessment of the genetic signature of the CSLC enriched-spheroids and parental OSCC is warranted to investigate possible therapeutic targets specific to OSCC.

The high CHEK1 inhibitor dose might suggest that CSLC have higher drug efflux capacity as previously shown by others (Liu, et al. 2012; Monzani, et al. 2007). We observed no response based on ‘Distal 11q loss’ in CSLC as previously shown in non-CSLC, this observation suggests that CSLC does not respond in the same ways as cancer cells and that the stemness property overrides many important factors that drive radiosensitivity in cancer cells.

Overall, our results suggest that distal 11q loss (*ATM* loss) might be a useful marker in conjunction with other markers in assessing radioresistance of CSLC. Unlike parental cell lines, CSLC seem to be more robust and were radioresistant despite a two week regimen; suggesting a more complex DDR in CSLC when compared to non-CSLC. Our study had some limitations. Our data only provided *in vitro* evidence of the radiosensitizing effect of CHEK1 knockdown on the enriched OSCC CSLC, lacking *in vivo* evidence; future *in vivo* studies are important to confirm our findings. However, the present study suggests for the first time, that CHEK1 knockdown radiosensitizes and limits the local invasion of OSCC CSLCs. Future directions of our work include further assessing possible cell surface CSLC markers, *in vivo* studies, combination DDR inhibitors and functional studies to understand the DDR in CSLC. Combining other DDR inhibitors, such as PARP or WEE1 inhibitors to a CHEK1 inhibitor may be important to achieve tolerable therapeutic concentrations of these drugs. Such a step would be critical before progression to clinical trials can be achieved.

4.8 CONCLUSION

Recent developments in CSLC research have added further evidence to support the role of CSLC in therapeutic resistance. The characterization of CSLC in OSCC will greatly advance our understanding of these tumors. In the current study, we demonstrate that compared to parental cancer cells, spheroid-enriched CSLCs possess features of stemness and display enhanced radioresistance, asymmetrical cell division, clonogenicity, tumorigenicity, and a more robust DDR-sensing machinery. Definitive CSLC markers for OSCC have yet to be characterized, although several studies have proposed different markers. Our results suggest that the use of dual

markers identification is important for better identification of CSLC in OSCC. CD133/SOX2 dual staining was the most promising combination in our study. SOX2 plays an important role in regulating stemness in both CSLC and normal SC (Tian, et al. 2012). Our finding that this marker can be used to assess the division patterns of CSLC, adds evidence that SOX2 is useful in the identification of CSLC. In addition, the expression of SOX2 may be a potential prognostic biomarker in OSCC (Li, et al. 2014). Limitations of the current study include the reliance on the *in vitro* model which needs to be confirmed using an *in vivo* model, and the exclusion of ALDHA1 from our CSLC marker panel analysis. We assessed the possible prognostic significance of CSLC markers (CD44, CD133/1, SOX2 and BMI1) in a panel of OSCC cell lines that were previously studied in our lab (White, et al. 2007). We did not observe prognostic significance based on these markers; this might be due the small sample size, the use of low passage cell lines rather than primary tumors, possibly confirming the observations that CSLC markers may not be suitable independent prognostic markers, as observed by others (Table 7).

One of the main objectives of our study was to assess the radioresistance patterns of spheroid-enriched CSLC in comparison to parental cancer cells (Parikh, et al. 2007; Sankunny, et al. 2014). There was a statistically significant difference between the parental cells and CSLC based on colony forming capacity tests. We observed statistically significant differences in radioresistance by spheroid survival and cell viability based on distal 11q loss. On the other hand we observed no statistically significant differences in radioresistance based on distal 11q loss using ELDA and spheroid growth assays. The response of CSLC to combined IR and CHEK1 inhibitor was totally different when compared to parental cancer cells. A 100-fold higher CHEK1 inhibitor dose was required to inhibit CSLC colony forming capacity, cell survival, and colony growth. As discussed earlier, we believe that the stemness of CSLC supersedes possible cancer

cell biomarkers. This observation needs to be confirmed in a larger study, assessing other OSCC biomarkers in CSLC and assessing the genetic signature of OSCC CSLC in comparison to parental cancer cells. Future directions of our work include assessing the value of flow cytometry sorted CSLC to confirm the radioresistance of these cells and to assess their response to IR and CHEK1 combination; *in vivo* studies to confirm the response of CSLC to IR and CHEK1 combination; functional studies to understand the DDR in CSLC compared to parental cancer cells. Combining other DDR inhibitors, such as PARP inhibitors with CHEK1 inhibitors could possibly be synergistic and effective in achieving tolerable therapeutic drug concentrations of these drugs. Such a step would be necessary before progress into clinical trials can be achieved.

APPENDIX A: CHEKI SMALL MOLECULE INHIBITOR

PF-0077736, a potent, specific CHEK1 small molecule inhibitor (SMI) was a purchased from Selleck Chemicals, Houston, TX, USA.

APPENDIX B: LIST OF ANTIBODIES USED FOR IF

Antibody	Type	Company	Catalog No.	Dilution
CD44	Mouse Monoclonal	BD	550392	1:100
CD133	Rabbit	Abcam	Ab19898	1:200
CD133/1(AC133)	Mouse IgG1 Monoclonal	Miltenyi Biotec	130-090-422	1:10
CD133/1 (AC133)-VioBright FITC	Mouse IgG1 Monoclonal	Miltenyi Biotec	130-105-226	1:10
CD133/1 (AC133)-PE	Mouse IgG1 Monoclonal	Miltenyi Biotec	130-098-826	1:10
BMI1	Rabbit Polyclonal	Imgenex	IMG-6362A	1:400
BMI1	Mouse	Abcam	Ab14389	1:400
SOX2	Rabbit Polyclonal	Imgenex	IMG-6507A	1:400
Nestin	Rabbit Polyclonal	Imgenex	IMG-6492A	1:400
Anti-gamma H2A.X (phospho S139)	Rabbit	Abcam	ab11174	1:500
Phospho-histone H3	Mouse	Cell Signaling	9706S	1:100
Alpha-beta tubulin	Rabbit Polyclonal	Cell Signaling	2148S	1:50
Gamma tubulin	Rabbit	Sigma	T3559	1:1000
KU70	Mouse	BD	611892	1:100
pCHEK1	Rabbit	Cell Signaling	2348S	1:100

APPENDIX C: LIST OF ANTIBODIES USED FOR FLOW CYTOMETRY

Antibody	Type	Company	Catalog No.	Dilution
CD44	Mouse monoclonal FITC	BD	555478	1:100
CD133/1 (AC133)-PE	Mouse IgG1 Monoclonal	Miltenyi Biotec	130-098-826	1:10

APPENDIX D: ABBREVIATIONS

AT - Ataxia telangiectasia

ATM – Ataxia telangiectasia mutated

ATR - Ataxia telangiectasia and Rad3-related

ATRIP - ATR interacting protein

BER - Base excision repair

BFB - breakage-fusion-bridge

CIN – Chromosomal instability

CSC - Cancer stem cell

CSD - Chromosomal segregation defects

CSLC – Cancer stem-like cell

DDR - DNA damage response

DFS – Disease-free survival

DSB - Double-strand break

EGFR - Epidermal growth factor receptor

ELDA – Extreme limiting dilution analysis

EMT – Epithelial-mesenchymal transition

EOD – Every other day

ESC - Embryonic stem cells

FACS – Flow cytometry cell sorting

FGF - Fibroblast growth factor

HNSCC – Head and neck squamous cell carcinoma

HR - Homologous recombination

IF – Immunofluorescence

IHC – Immunohistochemistry

IR – Ionizing radiation

MC - Mitotic catastrophe

MMR - Mismatch repair

MRN - MRE11A-RAD50-NBN

MSC - Mesenchymal stem cell

MTOR - Mammalian target of rapamycin

NER - Nucleotide excision repair

NHEJ - Non-homologous end joining

NSCLC – Non-small cell lung carcinoma

OS – Overall survival

OSCC – Oral squamous cell carcinoma

PARP - Poly (ADP-ribose) polymerase

PBS - Phosphate buffered saline

PRKDC - Protein kinase, DNA-activated, catalytic polypeptide

RPA - Replication protein A

RT - Room temperature

SC - Stem cell

SCC - Squamous cell carcinoma

SFE - Spheroid forming efficiency

ShRNA - Short hairpin RNA

siRNA - Small interfering RNA

SMG1 - Suppressor of morphogenesis in genitalia-1

SMI - Small molecule inhibitor

SOX2 - Sex-determining region Y [SRY]-box

SP – Side population

SSB – Single-strand break

TRRAP - Transformation/transcription domain-associated protein

UT - Untreated

UV - Ultraviolet light

BIBLIOGRAPHY

Abraham RT. 2004. PI 3-kinase related kinases: 'big' players in stress-induced signaling pathways. DNA Repair (Amst) 3(8-9):883-887.

Al-Hajj M, Wicha MS, Benito-Hernandez A, Morrison SJ, Clarke MF. 2003. Prospective identification of tumorigenic breast cancer cells. Proc Natl Acad Sci U S A 100(7):3983-3988.

Albertson DG. 2006. Gene amplification in cancer. Trends Genet 22(8):447-455.

Ang KK, Berkey BA, Tu X, Zhang HZ, Katz R, Hammond EH, Fu KK, Milas L. 2002. Impact of epidermal growth factor receptor expression on survival and pattern of relapse in patients with advanced head and neck carcinoma. Cancer Res 62(24):7350-7356.

Bakhoum SF, Kabeche L, Wood MD, Laucius CD, Qu D, Laughney AM, Reynolds GE, Louie RJ, Phillips J, Chan DA, Zaki BI, Murnane JP, Petritsch C, Compton DA. 2015. Numerical chromosomal instability mediates susceptibility to radiation treatment. Nat Commun 6:5990.

Bao S, Wu Q, McLendon RE, Hao Y, Shi Q, Hjelmeland AB, Dewhirst MW, Bigner DD, Rich JN. 2006. Glioma stem cells promote radioresistance by preferential activation of the DNA damage response. Nature 444(7120):756-760.

Bartek J, Lukas J. 2003. Chk1 and Chk2 kinases in checkpoint control and cancer. Cancer Cell 3(5):421-429.

Bartkova J, Rezaei N, Liontos M, Karakaidos P, Kletsas D, Issaeva N, Vassiliou LV, Kolettas E, Niforou K, Zoumpourlis VC, Takaoka M, Nakagawa H, Tort F, Fugger K, Johansson F, Sehested M, Andersen CL, Dyrskjot L, Orntoft T, Lukas J, Kittas C, Helleday T, Halazonetis TD, Bartek J, Gorgoulis VG. 2006. Oncogene-induced senescence is part of the tumorigenesis barrier imposed by DNA damage checkpoints. Nature 444(7119):633-637.

Bartucci M, Svensson S, Romania P, Dattilo R, Patrizii M, Signore M, Navarra S, Lotti F, Biffoni M, Pilozzi E, Duranti E, Martinelli S, Rinaldo C, Zeuner A, Maugeri-Sacca M, Eramo A, De Maria R. 2012. Therapeutic targeting of Chk1 in NSCLC stem cells during chemotherapy. Cell Death Differ 19(5):768-778.

Bassing CH, Suh H, Ferguson DO, Chua KF, Manis J, Eckersdorff M, Gleason M, Bronson R, Lee C, Alt FW. 2003. Histone H2AX: a dosage-dependent suppressor of oncogenic translocations and tumors. Cell 114(3):359-370.

Basu D, Montone KT, Wang LP, Gimotty PA, Hammond R, Diehl JA, Rustgi AK, Lee JT, Rasanen K, Weinstein GS, Herlyn M. 2011. Detecting and targeting mesenchymal-like subpopulations within squamous cell carcinomas. Cell Cycle 10(12):2008-2016.

Baumann M, Krause M, Hill R. 2008. Exploring the role of cancer stem cells in radioresistance. Nat Rev Cancer 8(7):545-554.

Beckmann J, Scheitza S, Wernet P, Fischer JC, Giebel B. 2007. Asymmetric cell division within the human hematopoietic stem and progenitor cell compartment: identification of asymmetrically segregating proteins. Blood 109(12):5494-5501.

Betschinger J, Knoblich JA. 2004. Dare to be different: asymmetric cell division in Drosophila, C. elegans and vertebrates. Curr Biol 14(16):R674-685.

Bhaijee F, Pepper DJ, Pitman KT, Bell D. 2012. Cancer stem cells in head and neck squamous cell carcinoma: a review of current knowledge and future applications. Head Neck 34(6):894-899.

Blagosklonny MV. 2007. Cancer stem cell and cancer stemloids: from biology to therapy. Cancer Biol Ther 6(11):1684-1690.

Blasina A, Hallin J, Chen E, Arango ME, Kraynov E, Register J, Grant S, Ninkovic S, Chen P, Nichols T, O'Connor P, Anderes K. 2008. Breaching the DNA damage checkpoint via PF-00477736, a novel small-molecule inhibitor of checkpoint kinase 1. Mol Cancer Ther 7(8):2394-2404.

Bonner JA, Harari PM, Giralt J, Cohen RB, Jones CU, Sur RK, Raben D, Baselga J, Spencer SA, Zhu J, Youssoufian H, Rowinsky EK, Ang KK. 2010. Radiotherapy plus cetuximab for locoregionally advanced head and neck cancer: 5-year survival data from a phase 3 randomised trial, and relation between cetuximab-induced rash and survival. Lancet Oncol 11(1):21-28.

Bonnet D, Dick JE. 1997. Human acute myeloid leukemia is organized as a hierarchy that originates from a primitive hematopoietic cell. Nat Med 3(7):730-737.

Borst GR, McLaughlin M, Kyula JN, Neijenhuis S, Khan A, Good J, Zaidi S, Powell NG, Meier P, Collins I, Garrett MD, Verheij M, Harrington KJ. 2013. Targeted radiosensitization by the Chk1 inhibitor SAR-020106. Int J Radiat Oncol Biol Phys 85(4):1110-1118.

Branzei D, Foiani M. 2008. Regulation of DNA repair throughout the cell cycle. Nat Rev Mol Cell Biol 9(4):297-308.

Bryant HE, Schultz N, Thomas HD, Parker KM, Flower D, Lopez E, Kyle S, Meuth M, Curtin NJ, Helleday T. 2005. Specific killing of BRCA2-deficient tumours with inhibitors of poly(ADP-ribose) polymerase. Nature 434(7035):913-917.

Bucher N, Britten CD. 2008. G2 checkpoint abrogation and checkpoint kinase-1 targeting in the treatment of cancer. Br J Cancer 98(3):523-528.

Bunger S, Barow M, Thorns C, Freitag-Wolf S, Danner S, Tiede S, Pries R, Gorg S, Bruch HP, Roblick UJ, Kruse C, Habermann JK. 2012. Pancreatic carcinoma cell lines reflect frequency and variability of cancer stem cell markers in clinical tissue. Eur Surg Res 49(2):88-98.

Byun TS, Pacek M, Yee MC, Walter JC, Cimprich KA. 2005. Functional uncoupling of MCM helicase and DNA polymerase activities activates the ATR-dependent checkpoint. Genes Dev 19(9):1040-1052.

Califano J, Westra WH, Meininger G, Corio R, Koch WM, Sidransky D. 2000. Genetic progression and clonal relationship of recurrent premalignant head and neck lesions. Clin Cancer Res 6(2):347-352.

Casper AM, Nghiem P, Arlt MF, Glover TW. 2002. ATR regulates fragile site stability. Cell 111(6):779-789.

Caussinus E, Gonzalez C. 2005. Induction of tumor growth by altered stem-cell asymmetric division in Drosophila melanogaster. Nat Genet 37(10):1125-1129.

Chang WW, Hu FW, Yu CC, Wang HH, Feng HP, Lan C, Tsai LL, Chang YC. 2013. Quercetin in elimination of tumor initiating stem-like and mesenchymal transformation property in head and neck cancer. Head Neck 35(3):413-419.

Chen H, Zhou L, Dou T, Wan G, Tang H, Tian J. 2011a. BMI1'S maintenance of the proliferative capacity of laryngeal cancer stem cells. Head Neck 33(8):1115-1125.

Chen SF, Chang YC, Nieh S, Liu CL, Yang CY, Lin YS. 2012. Nonadhesive culture system as a model of rapid sphere formation with cancer stem cell properties. PLoS One 7(2):e31864.

Chen YC, Chen YW, Hsu HS, Tseng LM, Huang PI, Lu KH, Chen DT, Tai LK, Yung MC, Chang SC, Ku HH, Chiou SH, Lo WL. 2009. Aldehyde dehydrogenase 1 is a putative marker for cancer stem cells in head and neck squamous cancer. Biochem Biophys Res Commun 385(3):307-313.

Chen YS, Wu MJ, Huang CY, Lin SC, Chuang TH, Yu CC, Lo JF. 2011b. CD133/Src axis mediates tumor initiating property and epithelial-mesenchymal transition of head and neck cancer. PLoS One 6(11):e28053.

Chen YW, Chen KH, Huang PI, Chen YC, Chiou GY, Lo WL, Tseng LM, Hsu HS, Chang KW, Chiou SH. 2010. Cucurbitacin I suppressed stem-like property and enhanced radiation-induced apoptosis in head and neck squamous carcinoma--derived CD44(+)ALDH1(+) cells. Mol Cancer Ther 9(11):2879-2892.

Chinn SB, Darr OA, Owen JH, Bellile E, McHugh JB, Spector ME, Papagerakis SM, Chepeha DB, Bradford CR, Carey TE, Prince MEP. 2015. Cancer stem cells: Mediators of tumorigenesis and metastasis in head and neck squamous cell carcinoma. Head Neck 37(3):317-326.

Chiou SH, Yu CC, Huang CY, Lin SC, Liu CJ, Tsai TH, Chou SH, Chien CS, Ku HH, Lo JF. 2008. Positive correlations of Oct-4 and Nanog in oral cancer stem-like cells and high-grade oral squamous cell carcinoma. Clin Cancer Res 14(13):4085-4095.

Cho YM, Kim YS, Kang MJ, Farrar WL, Hurt EM. 2012. Long-term recovery of irradiated prostate cancer increases cancer stem cells. Prostate 72(16):1746-1756.

Chou MY, Hu FW, Yu CH, Yu CC. 2015. Sox2 expression involvement in the oncogenicity and radiochemoresistance of oral cancer stem cells. Oral Oncol 51(1):31-39.

Chung CH, Parker JS, Karaca G, Wu J, Funkhouser WK, Moore D, Butterfoss D, Xiang D, Zanation A, Yin X, Shockley WW, Weissler MC, Dressler LG, Shores CG, Yarbrough WG, Perou CM. 2004. Molecular classification of head and neck squamous cell carcinomas using patterns of gene expression. Cancer Cell 5(5):489-500.

Clarke MF, Dick JE, Dirks PB, Eaves CJ, Jamieson CH, Jones DL, Visvader J, Weissman IL, Wahl GM. 2006. Cancer stem cells--perspectives on current status and future directions: AACR Workshop on cancer stem cells. Cancer Res 66(19):9339-9344.

Clay MR, Tabor M, Owen JH, Carey TE, Bradford CR, Wolf GT, Wicha MS, Prince ME. 2010. Single-marker identification of head and neck squamous cell carcinoma cancer stem cells with aldehyde dehydrogenase. Head Neck 32(9):1195-1201.

Clevers H. 2005. Stem cells, asymmetric division and cancer. Nat Genet 37(10):1027-1028.

Collins AT, Berry PA, Hyde C, Stower MJ, Maitland NJ. 2005. Prospective identification of tumorigenic prostate cancer stem cells. Cancer Res 65(23):10946-10951.

Croker AK, Goodale D, Chu J, Postenka C, Hedley BD, Hess DA, Allan AL. 2009. High aldehyde dehydrogenase and expression of cancer stem cell markers selects for breast cancer cells with enhanced malignant and metastatic ability. J Cell Mol Med 13(8B):2236-2252.

Dai Y, Grant S. 2010. New insights into checkpoint kinase 1 in the DNA damage response signaling network. Clin Cancer Res 16(2):376-383.

Dalerba P, Dylla SJ, Park IK, Liu R, Wang X, Cho RW, Hoey T, Gurney A, Huang EH, Simeone DM, Shelton AA, Parmiani G, Castelli C, Clarke MF. 2007. Phenotypic characterization of human colorectal cancer stem cells. Proc Natl Acad Sci U S A 104(24):10158-10163.

Damek-Poprawa M, Volgina A, Korostoff J, Sollecito TP, Brose MS, O'Malley BW, Jr., Akintoye SO, DiRienzo JM. 2011. Targeted inhibition of CD133+ cells in oral cancer cell lines. J Dent Res 90(5):638-645.

Dickson MA, Hahn WC, Ino Y, Ronfard V, Wu JY, Weinberg RA, Louis DN, Li FP, Rheinwald JG. 2000. Human keratinocytes that express hTERT and also bypass a p16(INK4a)-enforced mechanism that limits life span become immortal yet retain normal growth and differentiation characteristics. Mol Cell Biol 20(4):1436-1447.

Draviam VM, Xie S, Sorger PK. 2004. Chromosome segregation and genomic stability. Curr Opin Genet Dev 14(2):120-125.

Druker BJ, Tamura S, Buchdunger E, Ohno S, Segal GM, Fanning S, Zimmermann J, Lydon NB. 1996. Effects of a selective inhibitor of the Abl tyrosine kinase on the growth of Bcr-Abl positive cells. Nat Med 2(5):561-566.

Fang DD, Cao J, Jani JP, Tsaparikos K, Blasina A, Kornmann J, Lira ME, Wang J, Jirout Z, Bingham J, Zhu Z, Gu Y, Los G, Hostomsky Z, Vanarsdale T. 2013. Combined gemcitabine and CHK1 inhibitor treatment induces apoptosis resistance in cancer stem cell-like cells enriched with tumor spheroids from a non-small cell lung cancer cell line. Front Med 7(4):462-476.

Fargeas CA, Corbeil D, Huttner WB. 2003. AC133 antigen, CD133, prominin-1, prominin-2, etc.: prominin family gene products in need of a rational nomenclature. Stem Cells 21(4):506-508.

Farmer H, McCabe N, Lord CJ, Tutt AN, Johnson DA, Richardson TB, Santarosa M, Dillon KJ, Hickson I, Knights C, Martin NM, Jackson SP, Smith GC, Ashworth A. 2005. Targeting the DNA repair defect in BRCA mutant cells as a therapeutic strategy. Nature 434(7035):917-921.

Fenech M, Kirsch-Volders M, Natarajan AT, Surralles J, Crott JW, Parry J, Norppa H, Eastmond DA, Tucker JD, Thomas P. 2011. Molecular mechanisms of micronucleus, nucleoplasmic bridge and nuclear bud formation in mammalian and human cells. Mutagenesis 26(1):125-132.

Ferrari E, Lucca C, Foiani M. 2010. A lethal combination for cancer cells: synthetic lethality screenings for drug discovery. Eur J Cancer 46(16):2889-2895.

Foty R. 2011. A simple hanging drop cell culture protocol for generation of 3D spheroids. J Vis Exp(51).

Fouillade C, Monet-Lepretre M, Baron-Menguy C, Joutel A. 2012. Notch signalling in smooth muscle cells during development and disease. Cardiovasc Res 95(2):138-146.

Francipane MG, Lagasse E. 2013. Selective targeting of human colon cancer stem-like cells by the mTOR inhibitor Torin-1. Oncotarget 4(11):1948-1962.

Freier K, Knoepfle K, Flechtenmacher C, Pungs S, Devens F, Toedt G, Hofele C, Joos S, Lichter P, Radlwimmer B. 2010. Recurrent copy number gain of transcription factor SOX2 and corresponding high protein expression in oral squamous cell carcinoma. Genes Chromosomes Cancer 49(1):9-16.

Friedrich J, Seidel C, Ebner R, Kunz-Schughart LA. 2009. Spheroid-based drug screen: considerations and practical approach. Nat Protoc 4(3):309-324.

Fujii H, Honoki K, Tsujiuchi T, Kido A, Yoshitani K, Takakura Y. 2009. Sphere-forming stem-like cell populations with drug resistance in human sarcoma cell lines. Int J Oncol 34(5):1381-1386.

Fukusumi T, Ishii H, Konno M, Yasui T, Nakahara S, Takenaka Y, Yamamoto Y, Nishikawa S, Kano Y, Ogawa H, Hasegawa S, Hamabe A, Haraguchi N, Doki Y, Mori M, Inohara H. 2014. CD10 as a novel marker of therapeutic resistance and cancer stem cells in head and neck squamous cell carcinoma. Br J Cancer 111(3):506-514.

Gallmeier E, Hermann PC, Mueller MT, Machado JG, Ziesch A, De Toni EN, Palagyi A, Eisen C, Ellwart JW, Rivera J, Rubio-Viqueira B, Hidalgo M, Bunz F, Goke B, Heeschen C. 2011. Inhibition of ataxia telangiectasia- and Rad3-related function abrogates the in vitro and in vivo tumorigenicity of human colon cancer cells through depletion of the CD133(+) tumor-initiating cell fraction. Stem Cells 29(3):418-429.

Garcia SB, Novelli M, Wright NA. 2000. The clonal origin and clonal evolution of epithelial tumours. Int J Exp Pathol 81(2):89-116.

Garon EB, Finn RS, Hosmer W, Dering J, Ginther C, Adhami S, Kamranpour N, Pitts S, Desai A, Elashoff D, French T, Smith P, Slamon DJ. 2010. Identification of common predictive markers of in vitro response to the Mek inhibitor selumetinib (AZD6244; ARRY-142886) in human breast cancer and non-small cell lung cancer cell lines. Mol Cancer Ther 9(7):1985-1994.

Gaykalova DA, Mambo E, Choudhary A, Houghton J, Buddavarapu K, Sanford T, Darden W, Adai A, Hadd A, Latham G, Danilova LV, Bishop J, Li RJ, Westra WH, Hennessey P, Koch WM, Ochs MF, Califano JA, Sun W. 2014. Novel insight into mutational landscape of head and neck squamous cell carcinoma. PLoS One 9(3):e93102.

Ghisolfi L, Keates AC, Hu X, Lee DK, Li CJ. 2012. Ionizing radiation induces stemness in cancer cells. PLoS One 7(8):e43628.

Giudice FS, Pinto DS, Jr., Nor JE, Squarize CH, Castilho RM. 2013. Inhibition of histone deacetylase impacts cancer stem cells and induces epithelial-mesenchyme transition of head and neck cancer. PLoS One 8(3):e58672.

Gollin SM. 2005. Mechanisms leading to chromosomal instability. Semin Cancer Biol 15(1):33-42.

Gollin SM. 2014. Cytogenetic alterations and their molecular genetic correlates in head and neck squamous cell carcinoma: A next generation window to the biology of disease. Genes Chromosomes Cancer 53(12):972-990.

Goodell MA, Brose K, Paradis G, Conner AS, Mulligan RC. 1996. Isolation and functional properties of murine hematopoietic stem cells that are replicating in vivo. J Exp Med 183(4):1797-1806.

Graham SM, Jorgensen HG, Allan E, Pearson C, Alcorn MJ, Richmond L, Holyoake TL. 2002. Primitive, quiescent, Philadelphia-positive stem cells from patients with chronic myeloid leukemia are insensitive to STI571 in vitro. Blood 99(1):319-325.

Grimshaw MJ, Cooper L, Papazisis K, Coleman JA, Bohnenkamp HR, Chiapero-Stanke L, Taylor-Papadimitriou J, Burchell JM. 2008. Mammosphere culture of metastatic breast cancer cells enriches for tumorigenic breast cancer cells. Breast Cancer Res 10(3):R52.

Groth C, Fortini ME. 2012. Therapeutic approaches to modulating Notch signaling: current challenges and future prospects. Semin Cell Dev Biol 23(4):465-472.

Guo C, Liu H, Zhang BH, Cadaneanu RM, Mayle AM, Garraway IP. 2012. Epcam, CD44, and CD49f distinguish sphere-forming human prostate basal cells from a subpopulation with predominant tubule initiation capability. PLoS One 7(4):e34219.
Ha PK, Califano JA, 3rd. 2002. The molecular biology of laryngeal cancer. Otolaryngol Clin North Am 35(5):993-1012.
Han JS, Crowe DL. 2009. Tumor initiating cancer stem cells from human breast cancer cell lines. Int J Oncol 34(5):1449-1453.
Hanahan D, Weinberg RA. 2000. The hallmarks of cancer. Cell 100(1):57-70.
Hanahan D, Weinberg RA. 2011. Hallmarks of cancer: the next generation. Cell 144(5):646-674.
Hannon GJ. 2002. RNA interference. Nature 418(6894):244-251.
Harper LJ, Costea DE, Gammon L, Fazil B, Biddle A, Mackenzie IC. 2010. Normal and malignant epithelial cells with stem-like properties have an extended G2 cell cycle phase that is associated with apoptotic resistance. BMC Cancer 10:166.
Harper LJ, Piper K, Common J, Fortune F, Mackenzie IC. 2007. Stem cell patterns in cell lines derived from head and neck squamous cell carcinoma. J Oral Pathol Med 36(10):594-603.
He KF, Zhang L, Huang CF, Ma SR, Wang YF, Wang WM, Zhao ZL, Liu B, Zhao YF, Zhang WF, Sun ZJ. 2014. CD163+ tumor-associated macrophages correlated with poor prognosis and cancer stem cells in oral squamous cell carcinoma. Biomed Res Int 2014:838632.
Helt CE, Cliby WA, Keng PC, Bambara RA, O'Reilly MA. 2005. Ataxia telangiectasia mutated (ATM) and ATM and Rad3-related protein exhibit selective target specificities in response to different forms of DNA damage. J Biol Chem 280(2):1186-1192.
Hermann PC, Bhaskar S, Cioffi M, Heeschen C. 2010. Cancer stem cells in solid tumors. Semin Cancer Biol 20(2):77-84.
Ho WY, Yeap SK, Ho CL, Rahim RA, Alitheen NB. 2012. Development of multicellular tumor spheroid (MCTS) culture from breast cancer cell and a high throughput screening method using the MTT assay. PLoS One 7(9):e44640.
Hosoya N, Miyagawa K. 2014. Targeting DNA damage response in cancer therapy. Cancer Sci 105(4):370-388.
Hu Y, Smyth GK. 2009. ELDA: extreme limiting dilution analysis for comparing depleted and enriched populations in stem cell and other assays. J Immunol Methods 347(1-2):70-78.
Huang CF, Xu XR, Wu TF, Sun ZJ, Zhang WF. 2014. Correlation of ALDH1, CD44, OCT4 and SOX2 in tongue squamous cell carcinoma and their association with disease progression and prognosis. J Oral Pathol Med 43(7):492-498.
Huang X, Godfrey TE, Gooding WE, McCarty KS, Jr., Gollin SM. 2006. Comprehensive genome and transcriptome analysis of the 11q13 amplicon in human oral cancer and synteny to the 7F5 amplicon in murine oral carcinoma. Genes Chromosomes Cancer 45(11):1058-1069.
Hueng DY, Sytwu HK, Huang SM, Chang C, Ma HI. 2011. Isolation and characterization of tumor stem-like cells from human meningiomas. J Neurooncol 104(1):45-53.
Humbert P, Russell S, Richardson H. 2003. Dlg, Scribble and Lgl in cell polarity, cell proliferation and cancer. Bioessays 25(6):542-553.
Izumi H, Kaneko Y. 2012. Evidence of asymmetric cell division and centrosome inheritance in human neuroblastoma cells. Proc Natl Acad Sci U S A 109(44):18048-18053.

Jiang H, Reinhardt HC, Bartkova J, Tommiska J, Blomqvist C, Nevanlinna H, Bartek J, Yaffe MB, Hemann MT. 2009. The combined status of ATM and p53 link tumor development with therapeutic response. Genes Dev 23(16):1895-1909.

Joshua B, Kaplan MJ, Doweck I, Pai R, Weissman IL, Prince ME, Ailles LE. 2012. Frequency of cells expressing CD44, a head and neck cancer stem cell marker: correlation with tumor aggressiveness. Head Neck 34(1):42-49.

Jung YS, Vermeer PD, Vermeer DW, Lee SJ, Goh AR, Ahn HJ, Lee JH. 2015. CD200: Association with cancer stem cell features and response to chemoradiation in head and neck squamous cell carcinoma. Head Neck 37(3):327-335.

Kaseb HO, Gollin SM. 2015. Concerning consequences of blocking Notch signaling in satellite muscle stem cells. Front Cell Dev Biol 3:11.

Khammanivong A, Gopalakrishnan R, Dickerson EB. 2014. SMURF1 silencing diminishes a CD44-high cancer stem cell-like population in head and neck squamous cell carcinoma. Mol Cancer 13(1).

Kiang A, Yu MA, Ongkeko WM. 2012. Progress and pitfalls in the identification of cancer stem cell-targeting therapies in head and neck squamous cell carcinoma. Curr Med Chem 19(35):6056-6064.

Kim SY, Rhee JG, Song X, Prochownik EV, Spitz DR, Lee YJ. 2012. Breast cancer stem cell-like cells are more sensitive to ionizing radiation than non-stem cells: role of ATM. PLoS One 7(11):e50423.

Knoblich JA. 2001. Asymmetric cell division during animal development. Nat Rev Mol Cell Biol 2(1):11-20.

Knoblich JA. 2010. Asymmetric cell division: recent developments and their implications for tumour biology. Nat Rev Mol Cell Biol 11(12):849-860.

Kokko LL, Hurme S, Maula SM, Alanen K, Grenman R, Kinnunen I, Ventela S. 2011. Significance of site-specific prognosis of cancer stem cell marker CD44 in head and neck squamous-cell carcinoma. Oral Oncol 47(6):510-516.

Krishnamurthy S, Dong Z, Vodopyanov D, Imai A, Helman JI, Prince ME, Wicha MS, Nor JE. 2010. Endothelial cell-initiated signaling promotes the survival and self-renewal of cancer stem cells. Cancer Res 70(23):9969-9978.

Lagadec C, Vlashi E, Della Donna L, Meng Y, Dekmezian C, Kim K, Pajonk F. 2010. Survival and self-renewing capacity of breast cancer initiating cells during fractionated radiation treatment. Breast Cancer Res 12(1):R13.

Lagasse E. 2008. Cancer stem cells with genetic instability: the best vehicle with the best engine for cancer. Gene Ther 15(2):136-142.

Lansdorp PM. 2007. Immortal strands? Give me a break. Cell 129(7):1244-1247.

Lathia JD, Hitomi M, Gallagher J, Gadani SP, Adkins J, Vasanji A, Liu L, Eyler CE, Heddleston JM, Wu Q, Minhas S, Soeda A, Hoeppner DJ, Ravin R, McKay RD, McLendon RE, Corbeil D, Chenn A, Hjelmeland AB, Park DM, Rich JN. 2011. Distribution of CD133 reveals glioma stem cells self-renew through symmetric and asymmetric cell divisions. Cell Death Dis 2:e200.

Lechner M, Frampton GM, Fenton T, Feber A, Palmer G, Jay A, Pillay N, Forster M, Cronin MT, Lipson D, Miller VA, Brennan TA, Henderson S, Vaz F, O'Flynn P, Kalavrezos N, Yelensky R, Beck S, Stephens PJ, Boshoff C. 2013. Targeted next-generation sequencing of head and neck squamous cell carcinoma identifies novel genetic alterations in HPV+ and HPV- tumors. Genome Med 5(5):49.

Lee SH, Oh SY, Do SI, Lee HJ, Kang HJ, Rho YS, Bae WJ, Lim YC. 2014. SOX2 regulates self-renewal and tumorigenicity of stem-like cells of head and neck squamous cell carcinoma. Br J Cancer 111(11):2122-2130.

Leemans CR, Braakhuis BJ, Brakenhoff RH. 2011. The molecular biology of head and neck cancer. Nat Rev Cancer 11(1):9-22.

Li J, Luthra S, Wang XH, Chandran UR, Sobol RW. 2012. Transcriptional profiling reveals elevated Sox2 in DNA polymerase ss null mouse embryonic fibroblasts. Am J Cancer Res 2(6):699-713.

Li T, Su Y, Mei Y, Leng Q, Leng B, Liu Z, Stass SA, Jiang F. 2010. ALDH1A1 is a marker for malignant prostate stem cells and predictor of prostate cancer patients' outcome. Lab Invest 90(2):234-244.

Li W, Li B, Wang R, Huang D, Jin W, Yang S. 2014. SOX2 as prognostic factor in head and neck cancer: a systematic review and meta-analysis. Acta Otolaryngol 134(11):1101-1108.

Lim YC, Oh SY, Cha YY, Kim SH, Jin X, Kim H. 2011. Cancer stem cell traits in squamospheres derived from primary head and neck squamous cell carcinomas. Oral Oncol 47(2):83-91.

Lim YC, Oh SY, Kim H. 2012. Cellular characteristics of head and neck cancer stem cells in type IV collagen-coated adherent cultures. Exp Cell Res 318(10):1104-1111.

Lindquist D, Ahrlund-Richter A, Tarjan M, Tot T, Dalianis T. 2012. Intense CD44 expression is a negative prognostic factor in tonsillar and base of tongue cancer. Anticancer Res 32(1):153-161.

Lingala S, Cui YY, Chen X, Ruebner BH, Qian XF, Zern MA, Wu J. 2010. Immunohistochemical staining of cancer stem cell markers in hepatocellular carcinoma. Exp Mol Pathol 89(1):27-35.

Liu W, Feng JQ, Shen XM, Wang HY, Liu Y, Zhou ZT. 2012. Two stem cell markers, ATP-binding cassette, G2 subfamily (ABCG2) and BMI-1, predict the transformation of oral leukoplakia to cancer: a long-term follow-up study. Cancer 118(6):1693-1700.

Liu W, Jeganathan G, Amiri S, Morgan KM, Ryan BM, Pine SR. 2013. Asymmetric segregation of template DNA strands in basal-like human breast cancer cell lines. Mol Cancer 12(1):139.

Lo WL, Chien Y, Chiou GY, Tseng LM, Hsu HS, Chang YL, Lu KH, Chien CS, Wang ML, Chen YW, Huang PI, Hu FW, Yu CC, Chu PY, Chiou SH. 2012. Nuclear localization signal-enhanced RNA interference of EZH2 and Oct4 in the eradication of head and neck squamous cell carcinoma-derived cancer stem cells. Biomaterials 33(14):3693-3709.

Lo WL, Yu CC, Chiou GY, Chen YW, Huang PI, Chien CS, Tseng LM, Chu PY, Lu KH, Chang KW, Kao SY, Chiou SH. 2011. MicroRNA-200c attenuates tumour growth and metastasis of presumptive head and neck squamous cell carcinoma stem cells. J Pathol 223(4):482-495.

Locke M, Heywood M, Fawell S, Mackenzie IC. 2005. Retention of intrinsic stem cell hierarchies in carcinoma-derived cell lines. Cancer Res 65(19):8944-8950.

Lord CJ, Ashworth A. 2012. The DNA damage response and cancer therapy. Nature 481(7381):287-294.

Lundholm L, Haag P, Zong D, Juntti T, Mork B, Lewensohn R, Viktorsson K. 2013. Resistance to DNA-damaging treatment in non-small cell lung cancer tumor-initiating cells involves

reduced DNA-PK/ATM activation and diminished cell cycle arrest. Cell Death Dis 4:e478.
Ma Z, Yao G, Zhou B, Fan Y, Gao S, Feng X. 2012. The Chk1 inhibitor AZD7762 sensitises p53 mutant breast cancer cells to radiation in vitro and in vivo. Mol Med Rep 6(4):897-903.
Mack B, Gires O. 2008. CD44s and CD44v6 expression in head and neck epithelia. PLoS One 3(10):e3360.
Mao P, Joshi K, Li J, Kim SH, Li P, Santana-Santos L, Luthra S, Chandran UR, Benos PV, Smith L, Wang M, Hu B, Cheng SY, Sobol RW, Nakano I. 2013. Mesenchymal glioma stem cells are maintained by activated glycolytic metabolism involving aldehyde dehydrogenase 1A3. Proc Natl Acad Sci U S A 110(21):8644-8649.
Martin CL, Reshmi SC, Ried T, Gottberg W, Wilson JW, Reddy JK, Khanna P, Johnson JT, Myers EN, Gollin SM. 2008. Chromosomal imbalances in oral squamous cell carcinoma: examination of 31 cell lines and review of the literature. Oral Oncol 44(4):369-382.
Martinez Arias A, Zecchini V, Brennan K. 2002. CSL-independent Notch signalling: a checkpoint in cell fate decisions during development? Curr Opin Genet Dev 12(5):524-533.
Massague J. 2004. G1 cell-cycle control and cancer. Nature 432(7015):298-306.
Michalides RJ, van de Brekel M, Balm F. 2002. Defects in G1-S cell cycle control in head and neck cancer: a review. Head Neck 24(7):694-704.
Michifuri Y, Hirohashi Y, Torigoe T, Miyazaki A, Kobayashi J, Sasaki T, Fujino J, Asanuma H, Tamura Y, Nakamori K, Hasegawa T, Hiratsuka H, Sato N. 2012. High expression of ALDH1 and SOX2 diffuse staining pattern of oral squamous cell carcinomas correlates to lymph node metastasis. Pathol Int 62(10):684-689.
Minhas KM, Singh B, Jiang WW, Sidransky D, Califano JA. 2003. Spindle assembly checkpoint defects and chromosomal instability in head and neck squamous cell carcinoma. Int J Cancer 107(1):46-52.
Mitchell C, Park M, Eulitt P, Yang C, Yacoub A, Dent P. 2010. Poly(ADP-ribose) polymerase 1 modulates the lethality of CHK1 inhibitors in carcinoma cells. Mol Pharmacol 78(5):909-917.
Mitelman F, Johansson B, Mertens F. 2007. The impact of translocations and gene fusions on cancer causation. Nat Rev Cancer 7(4):233-245.
Mitelman F, Johansson B, Mertens F, editors. 2014. Mitelman Database of Chromosome Aberrations and Gene Fusions in Cancer Available at: http://cgap.nci.nih.gov/Chromosomes/Mitelman.
Mizrak D, Brittan M, Alison M. 2008. CD133: molecule of the moment. J Pathol 214(1):3-9.
Molofsky AV, Pardal R, Iwashita T, Park IK, Clarke MF, Morrison SJ. 2003. Bmi-1 dependence distinguishes neural stem cell self-renewal from progenitor proliferation. Nature 425(6961):962-967.
Momcilovic O, Knobloch L, Fornsaglio J, Varum S, Easley C, Schatten G. 2010. DNA damage responses in human induced pluripotent stem cells and embryonic stem cells. PLoS One 5(10):e13410.
Monzani E, Facchetti F, Galmozzi E, Corsini E, Benetti A, Cavazzin C, Gritti A, Piccinini A, Porro D, Santinami M, Invernici G, Parati E, Alessandri G, La Porta CA. 2007. Melanoma contains CD133 and ABCG2 positive cells with enhanced tumourigenic potential. Eur J Cancer 43(5):935-946.

Morimoto K, Kim SJ, Tanei T, Shimazu K, Tanji Y, Taguchi T, Tamaki Y, Terada N, Noguchi S. 2009. Stem cell marker aldehyde dehydrogenase 1-positive breast cancers are characterized by negative estrogen receptor, positive human epidermal growth factor receptor type 2, and high Ki67 expression. Cancer Sci 100(6):1062-1068.

Morrison SJ, Kimble J. 2006. Asymmetric and symmetric stem-cell divisions in development and cancer. Nature 441(7097):1068-1074.

Mourikis P, Sambasivan R, Castel D, Rocheteau P, Bizzarro V, Tajbakhsh S. 2012. A critical requirement for notch signaling in maintenance of the quiescent skeletal muscle stem cell state. Stem Cells 30(2):243-252.

Moynahan ME, Jasin M. 2010. Mitotic homologous recombination maintains genomic stability and suppresses tumorigenesis. Nat Rev Mol Cell Biol 11(3):196-207.

Murillo-Sauca O, Chung MK, Shin JH, Karamboulas C, Kwok S, Jung YH, Oakley R, Tysome JR, Farnebo LO, Kaplan MJ, Sirjani D, Divi V, Holsinger FC, Tomeh C, Nichols A, Le QT, Colevas AD, Kong CS, Uppaluri R, Lewis JS, Jr., Ailles LE, Sunwoo JB. 2014. CD271 is a functional and targetable marker of tumor-initiating cells in head and neck squamous cell carcinoma. Oncotarget 5(16):6854-6866.

Narasimhan K, Pillay S, Bin Ahmad NR, Bikadi Z, Hazai E, Yan L, Kolatkar PR, Pervushin K, Jauch R. 2011. Identification of a polyoxometalate inhibitor of the DNA binding activity of Sox2. ACS Chem Biol 6(6):573-581.

Nghiem P, Park PK, Kim Y, Vaziri C, Schreiber SL. 2001. ATR inhibition selectively sensitizes G1 checkpoint-deficient cells to lethal premature chromatin condensation. Proc Natl Acad Sci U S A 98(16):9092-9097.

Noutomi Y, Oga A, Uchida K, Okafuji M, Ita M, Kawauchi S, Furuya T, Ueyama Y, Sasaki K. 2006. Comparative genomic hybridization reveals genetic progression of oral squamous cell carcinoma from dysplasia via two different tumourigenic pathways. J Pathol 210(1):67-74.

Odoux C, Fohrer H, Hoppo T, Guzik L, Stolz DB, Lewis DW, Gollin SM, Gamblin TC, Geller DA, Lagasse E. 2008. A stochastic model for cancer stem cell origin in metastatic colon cancer. Cancer Res 68(17):6932-6941.

Oh SY, Kang HJ, Kim YS, Kim H, Lim YC. 2013. CD44-negative cells in head and neck squamous carcinoma also have stem-cell like traits. Eur J Cancer 49(1):272-280.

Okamoto A, Chikamatsu K, Sakakura K, Hatsushika K, Takahashi G, Masuyama K. 2009. Expansion and characterization of cancer stem-like cells in squamous cell carcinoma of the head and neck. Oral Oncol 45(7):633-639.

Okubo T, Clark C, Hogan BL. 2009. Cell lineage mapping of taste bud cells and keratinocytes in the mouse tongue and soft palate. Stem Cells 27(2):442-450.

Okumura-Nakanishi S, Saito M, Niwa H, Ishikawa F. 2005. Oct-3/4 and Sox2 regulate Oct-3/4 gene in embryonic stem cells. J Biol Chem 280(7):5307-5317.

Origanti S, Cai SR, Munir AZ, White LS, Piwnica-Worms H. 2013. Synthetic lethality of Chk1 inhibition combined with p53 and/or p21 loss during a DNA damage response in normal and tumor cells. Oncogene 32(5):577-588.

Parikh RA, Appleman LJ, Bauman JE, Sankunny M, Lewis DW, Vlad A, Gollin SM. 2013. Upregulation of the ATR-CHEK1 pathway in oral squamous cell carcinomas. Genes Chromosomes Cancer 53(1):25-37.

Parikh RA, White JS, Huang X, Schoppy DW, Baysal BE, Baskaran R, Bakkenist CJ, Saunders WS, Hsu LC, Romkes M, Gollin SM. 2007. Loss of distal 11q is associated with DNA

repair deficiency and reduced sensitivity to ionizing radiation in head and neck squamous cell carcinoma. Genes Chromosomes Cancer 46(8):761-775.

Pastrana E, Silva-Vargas V, Doetsch F. 2011. Eyes wide open: a critical review of sphere-formation as an assay for stem cells. Cell Stem Cell 8(5):486-498.

Pece S, Serresi M, Santolini E, Capra M, Hulleman E, Galimberti V, Zurrida S, Maisonneuve P, Viale G, Di Fiore PP. 2004. Loss of negative regulation by Numb over Notch is relevant to human breast carcinogenesis. J Cell Biol 167(2):215-221.

Peddibhotla S, Lam MH, Gonzalez-Rimbau M, Rosen JM. 2009. The DNA-damage effector checkpoint kinase 1 is essential for chromosome segregation and cytokinesis. Proc Natl Acad Sci U S A 106(13):5159-5164.

Penno MB, August JT, Baylin SB, Mabry M, Linnoila RI, Lee VS, Croteau D, Yang XL, Rosada C. 1994. Expression of CD44 in human lung tumors. Cancer Res 54(5):1381-1387.

Perego M, Alison MR, Mariani L, Rivoltini L, Castelli C. 2011. Spheres of influence in cancer stem cell biology. J Invest Dermatol 131(2):546-547.

Piao LS, Hur W, Kim TK, Hong SW, Kim SW, Choi JE, Sung PS, Song MJ, Lee BC, Hwang D, Yoon SK. 2012. CD133+ liver cancer stem cells modulate radioresistance in human hepatocellular carcinoma. Cancer Lett 315(2):129-137.

Pickering CR, Zhang J, Yoo SY, Bengtsson L, Moorthy S, Neskey DM, Zhao M, Ortega Alves MV, Chang K, Drummond J, Cortez E, Xie TX, Zhang D, Chung W, Issa JP, Zweidler-McKay PA, Wu X, El-Naggar AK, Weinstein JN, Wang J, Muzny DM, Gibbs RA, Wheeler DA, Myers JN, Frederick MJ. 2013. Integrative genomic characterization of oral squamous cell carcinoma identifies frequent somatic drivers. Cancer Discov 3(7):770-781.

Pine SR, Ryan BM, Varticovski L, Robles AI, Harris CC. 2010. Microenvironmental modulation of asymmetric cell division in human lung cancer cells. Proc Natl Acad Sci U S A 107(5):2195-2200.

Ponti D, Costa A, Zaffaroni N, Pratesi G, Petrangolini G, Coradini D, Pilotti S, Pierotti MA, Daidone MG. 2005. Isolation and in vitro propagation of tumorigenic breast cancer cells with stem/progenitor cell properties. Cancer Res 65(13):5506-5511.

Prince ME, Sivanandan R, Kaczorowski A, Wolf GT, Kaplan MJ, Dalerba P, Weissman IL, Clarke MF, Ailles LE. 2007. Identification of a subpopulation of cells with cancer stem cell properties in head and neck squamous cell carcinoma. Proc Natl Acad Sci U S A 104(3):973-978.

Pruitt KD, Brown GR, Hiatt SM, Thibaud-Nissen F, Astashyn A, Ermolaeva O, Farrell CM, Hart J, Landrum MJ, McGarvey KM, Murphy MR, O'Leary NA, Pujar S, Rajput B, Rangwala SH, Riddick LD, Shkeda A, Sun H, Tamez P, Tully RE, Wallin C, Webb D, Weber J, Wu W, DiCuccio M, Kitts P, Maglott DR, Murphy TD, Ostell JM. 2014. RefSeq: an update on mammalian reference sequences. Nucleic Acids Res 42(Database issue):D756-763.

Rajarajan A, Stokes A, Bloor BK, Ceder R, Desai H, Grafstrom RC, Odell EW. 2012. CD44 expression in oro-pharyngeal carcinoma tissues and cell lines. PLoS One 7(1):e28776.

Reing JE, Gollin SM, Saunders WS. 2004. The occurrence of chromosome segregational defects is an intrinsic and heritable property of oral squamous cell carcinoma cell lines. Cancer Genet Cytogenet 150(1):57-61.

Reshmi SC, Roychoudhury S, Yu Z, Feingold E, Potter D, Saunders WS, Gollin SM. 2007. Inverted duplication pattern in anaphase bridges confirms the breakage-fusion-bridge (BFB) cycle model for 11q13 amplification. Cytogenet Genome Res 116(1-2):46-52.

Reshmi SC, Saunders WS, Kudla DM, Ragin CR, Gollin SM. 2004. Chromosomal instability and marker chromosome evolution in oral squamous cell carcinoma. Genes Chromosomes Cancer 41(1):38-46.

Ricci-Vitiani L, Lombardi DG, Pilozzi E, Biffoni M, Todaro M, Peschle C, De Maria R. 2007. Identification and expansion of human colon-cancer-initiating cells. Nature 445(7123):111-115.

Riesterer O, Matsumoto F, Wang L, Pickett J, Molkentine D, Giri U, Milas L, Raju U. 2011. A novel Chk inhibitor, XL-844, increases human cancer cell radiosensitivity through promotion of mitotic catastrophe. Invest New Drugs 29(3):514-522.

Rietbergen MM, Martens-de Kemp SR, Bloemena E, Witte BI, Brink A, Baatenburg de Jong RJ, Leemans CR, Braakhuis BJ, Brakenhoff RH. 2014. Cancer stem cell enrichment marker CD98: a prognostic factor for survival in patients with human papillomavirus-positive oropharyngeal cancer. Eur J Cancer 50(4):765-773.

Salahshourifar I, Vincent-Chong VK, Kallarakkal TG, Zain RB. 2014. Genomic DNA copy number alterations from precursor oral lesions to oral squamous cell carcinoma. Oral Oncol 50(5):404-412.

Salnikov AV, Kusumawidjaja G, Rausch V, Bruns H, Gross W, Khamidjanov A, Ryschich E, Gebhard MM, Moldenhauer G, Buchler MW, Schemmer P, Herr I. 2009. Cancer stem cell marker expression in hepatocellular carcinoma and liver metastases is not sufficient as single prognostic parameter. Cancer Lett 275(2):185-193.

Sankunny M, Parikh RA, Lewis DW, Gooding WE, Saunders WS, Gollin SM. 2014. Targeted inhibition of ATR or CHEK1 reverses radioresistance in oral squamous cell carcinoma cells with distal chromosome arm 11q loss. Genes Chromosomes Cancer 53(2):129-143.

Sarkar A, Hochedlinger K. 2013. The sox family of transcription factors: versatile regulators of stem and progenitor cell fate. Cell Stem Cell 12(1):15-30.

Saunders WS, Shuster M, Huang X, Gharaibeh B, Enyenihi AH, Petersen I, Gollin SM. 2000. Chromosomal instability and cytoskeletal defects in oral cancer cells. Proc Natl Acad Sci U S A 97(1):303-308.

Sayed SI, Dwivedi RC, Katna R, Garg A, Pathak KA, Nutting CM, Rhys-Evans P, Harrington KJ, Kazi R. 2011. Implications of understanding cancer stem cell (CSC) biology in head and neck squamous cell cancer. Oral Oncol 47(4):237-243.

Schuuring E. 1995. The involvement of the chromosome 11q13 region in human malignancies: cyclin D1 and EMS1 are two new candidate oncogenes--a review. Gene 159(1):83-96.

Schuuring E, van Damme H, Schuuring-Scholtes E, Verhoeven E, Michalides R, Geelen E, de Boer C, Brok H, van Buuren V, Kluin P. 1998. Characterization of the EMS1 gene and its product, human Cortactin. Cell Adhes Commun 6(2-3):185-209.

SEER. 2015. Surveillance, Epidemiology, and End Results (SEER) Program Populations (1969-2013) (www.seer.cancer.gov/popdata). National Cancer Institute, DCCPS, Surveillance Research Program, Surveillance Systems Branch released January 2015.

Shaheen M, Allen C, Nickoloff JA, Hromas R. 2011. Synthetic lethality: exploiting the addiction of cancer to DNA repair. Blood 117(23):6074-6082.

Shahriyari L, Komarova NL. 2013. Symmetric vs. asymmetric stem cell divisions: an adaptation against cancer? PLoS One 8(10):e76195.

Sheng X, Li Z, Wang DL, Li WB, Luo Z, Chen KH, Cao JJ, Yu C, Liu WJ. 2013. Isolation and enrichment of PC-3 prostate cancer stem-like cells using MACS and serum-free medium. Oncol Lett 5(3):787-792.

Shiloh Y. 2003. ATM and related protein kinases: safeguarding genome integrity. Nat Rev Cancer 3(3):155-168.
Shiloh Y. 2006. The ATM-mediated DNA-damage response: taking shape. Trends Biochem Sci 31(7):402-410.
Shiloh Y. 2014. ATM: expanding roles as a chief guardian of genome stability. Exp Cell Res 329(1):154-161.
Shinin V, Gayraud-Morel B, Gomes D, Tajbakhsh S. 2006. Asymmetric division and cosegregation of template DNA strands in adult muscle satellite cells. Nat Cell Biol 8(7):677-687.
Shrivastava S, Steele R, Sowadski M, Crawford SE, Varvares M, Ray RB. 2015. Identification of molecular signature of head and neck cancer stem-like cells. Sci Rep 5:7819.
Sidi S, Sanda T, Kennedy RD, Hagen AT, Jette CA, Hoffmans R, Pascual J, Imamura S, Kishi S, Amatruda JF, Kanki JP, Green DR, D'Andrea AA, Look AT. 2008. Chk1 suppresses a caspase-2 apoptotic response to DNA damage that bypasses p53, Bcl-2, and caspase-3. Cell 133(5):864-877.
Siebers TJ, Bergshoeff VE, Otte-Holler I, Kremer B, Speel EJ, van der Laak JA, Merkx MA, Slootweg PJ. 2013. Chromosome instability predicts the progression of premalignant oral lesions. Oral Oncol 49(12):1121-1128.
Siegel R, Ma J, Zou Z, Jemal A. 2014. Cancer statistics, 2014. CA Cancer J Clin 64(1):9-29.
Siegel RL, Miller KD, Jemal A. 2015. Cancer statistics, 2015. CA Cancer J Clin 65(1):5-29.
Simpson DR, Mell LK, Cohen EE. 2015. Targeting the PI3K/AKT/mTOR pathway in squamous cell carcinoma of the head and neck. Oral Oncol 51(4):291-298.
Singec I, Knoth R, Meyer RP, Maciaczyk J, Volk B, Nikkhah G, Frotscher M, Snyder EY. 2006. Defining the actual sensitivity and specificity of the neurosphere assay in stem cell biology. Nat Methods 3(10):801-806.
Solit DB, Garraway LA, Pratilas CA, Sawai A, Getz G, Basso A, Ye Q, Lobo JM, She Y, Osman I, Golub TR, Sebolt-Leopold J, Sellers WR, Rosen N. 2006. BRAF mutation predicts sensitivity to MEK inhibition. Nature 439(7074):358-362.
Sorensen CS, Syljuasen RG, Falck J, Schroeder T, Ronnstrand L, Khanna KK, Zhou BB, Bartek J, Lukas J. 2003. Chk1 regulates the S phase checkpoint by coupling the physiological turnover and ionizing radiation-induced accelerated proteolysis of Cdc25A. Cancer Cell 3(3):247-258.
Stolzenburg S, Rots MG, Beltran AS, Rivenbark AG, Yuan X, Qian H, Strahl BD, Blancafort P. 2012. Targeted silencing of the oncogenic transcription factor SOX2 in breast cancer. Nucleic Acids Res 40(14):6725-6740.
Stransky N, Egloff AM, Tward AD, Kostic AD, Cibulskis K, Sivachenko A, Kryukov GV, Lawrence MS, Sougnez C, McKenna A, Shefler E, Ramos AH, Stojanov P, Carter SL, Voet D, Cortes ML, Auclair D, Berger MF, Saksena G, Guiducci C, Onofrio RC, Parkin M, Romkes M, Weissfeld JL, Seethala RR, Wang L, Rangel-Escareno C, Fernandez-Lopez JC, Hidalgo-Miranda A, Melendez-Zajgla J, Winckler W, Ardlie K, Gabriel SB, Meyerson M, Lander ES, Getz G, Golub TR, Garraway LA, Grandis JR. 2011. The mutational landscape of head and neck squamous cell carcinoma. Science 333(6046):1157-1160.
Strojan P, Corry J, Eisbruch A, Vermorken JB, Mendenhall WM, Lee AW, Haigentz M, Jr., Beitler JJ, de Bree R, Takes RP, Paleri V, Kelly CG, Genden EM, Bradford CR, Harrison

LB, Rinaldo A, Ferlito A. 2015. Recurrent and second primary squamous cell carcinoma of the head and neck: When and how to reirradiate. Head Neck 37(1):134-150.
Stucki M, Clapperton JA, Mohammad D, Yaffe MB, Smerdon SJ, Jackson SP. 2005. MDC1 directly binds phosphorylated histone H2AX to regulate cellular responses to DNA double-strand breaks. Cell 123(7):1213-1226.
Su J, Xu XH, Huang Q, Lu MQ, Li DJ, Xue F, Yi F, Ren JH, Wu YP. 2011. Identification of cancer stem-like CD44+ cells in human nasopharyngeal carcinoma cell line. Arch Med Res 42(1):15-21.
Su Y, Qiu Q, Zhang X, Jiang Z, Leng Q, Liu Z, Stass SA, Jiang F. 2010. Aldehyde dehydrogenase 1 A1-positive cell population is enriched in tumor-initiating cells and associated with progression of bladder cancer. Cancer Epidemiol Biomarkers Prev 19(2):327-337.
Sun Y, Pollard S, Conti L, Toselli M, Biella G, Parkin G, Willatt L, Falk A, Cattaneo E, Smith A. 2008. Long-term tripotent differentiation capacity of human neural stem (NS) cells in adherent culture. Mol Cell Neurosci 38(2):245-258.
Tabor MH, Clay MR, Owen JH, Bradford CR, Carey TE, Wolf GT, Prince ME. 2011. Head and neck cancer stem cells: the side population. Laryngoscope 121(3):527-533.
Takahashi-Yanaga F, Kahn M. 2010. Targeting Wnt signaling: can we safely eradicate cancer stem cells? Clin Cancer Res 16(12):3153-3162.
Takahashi K, Tanabe K, Ohnuki M, Narita M, Ichisaka T, Tomoda K, Yamanaka S. 2007. Induction of pluripotent stem cells from adult human fibroblasts by defined factors. Cell 131(5):861-872.
Tan L, Sui X, Deng H, Ding M. 2011. Holoclone forming cells from pancreatic cancer cells enrich tumor initiating cells and represent a novel model for study of cancer stem cells. PLoS One 6(8):e23383.
Telmer CA, An J, Malehorn DE, Zeng X, Gollin SM, Ishwad CS, Jarvik JW. 2003. Detection and assignment of TP53 mutations in tumor DNA using peptide mass signature genotyping. Hum Mutat 22(2):158-165.
Tian T, Zhang Y, Wang S, Zhou J, Xu S. 2012. Sox2 enhances the tumorigenicity and chemoresistance of cancer stem-like cells derived from gastric cancer. J Biomed Res 26(5):336-345.
Tijink BM, Buter J, de Bree R, Giaccone G, Lang MS, Staab A, Leemans CR, van Dongen GA. 2006. A phase I dose escalation study with anti-CD44v6 bivatuzumab mertansine in patients with incurable squamous cell carcinoma of the head and neck or esophagus. Clin Cancer Res 12(20 Pt 1):6064-6072.
Timmons L. 2006. Delivery methods for RNA interference in C. elegans. Methods Mol Biol 351:119-125.
Tirino V, Desiderio V, d'Aquino R, De Francesco F, Pirozzi G, Graziano A, Galderisi U, Cavaliere C, De Rosa A, Papaccio G, Giordano A. 2008. Detection and characterization of CD133+ cancer stem cells in human solid tumours. PLoS One 3(10):e3469.
Tomasetti C, Vogelstein B. 2015. Cancer etiology. Variation in cancer risk among tissues can be explained by the number of stem cell divisions. Science 347(6217):78-81.
Tong AH, Evangelista M, Parsons AB, Xu H, Bader GD, Page N, Robinson M, Raghibizadeh S, Hogue CW, Bussey H, Andrews B, Tyers M, Boone C. 2001. Systematic genetic analysis with ordered arrays of yeast deletion mutants. Science 294(5550):2364-2368.

Tosoni D, Di Fiore PP, Pece S. 2012. Functional purification of human and mouse mammary stem cells. Methods Mol Biol 916:59-79.
Trapasso S, Allegra E. 2012. Role of CD44 as a marker of cancer stem cells in head and neck cancer. Biologics 6:379-383.
Tsai LL, Hu FW, Lee SS, Yu CH, Yu CC, Chang YC. 2014. Oct4 mediates tumor initiating properties in oral squamous cell carcinomas through the regulation of epithelial-mesenchymal transition. PLoS One 9(1):e87207.
Uchida N, Buck DW, He D, Reitsma MJ, Masek M, Phan TV, Tsukamoto AS, Gage FH, Weissman IL. 2000. Direct isolation of human central nervous system stem cells. Proc Natl Acad Sci U S A 97(26):14720-14725.
Vermorken JB, Mesia R, Rivera F, Remenar E, Kawecki A, Rottey S, Erfan J, Zabolotnyy D, Kienzer HR, Cupissol D, Peyrade F, Benasso M, Vynnychenko I, De Raucourt D, Bokemeyer C, Schueler A, Amellal N, Hitt R. 2008. Platinum-based chemotherapy plus cetuximab in head and neck cancer. N Engl J Med 359(11):1116-1127.
Vinci M, Box C, Zimmermann M, Eccles SA. 2013. Tumor spheroid-based migration assays for evaluation of therapeutic agents. Methods Mol Biol 986:253-266.
Visus C, Wang Y, Lozano-Leon A, Ferris RL, Silver S, Szczepanski MJ, Brand RE, Ferrone CR, Whiteside TL, Ferrone S, DeLeo AB, Wang X. 2011. Targeting ALDH(bright) human carcinoma-initiating cells with ALDH1A1-specific CD8(+) T cells. Clin Cancer Res 17(19):6174-6184.
Visvader JE. 2011. Cells of origin in cancer. Nature 469(7330):314-322.
Vunjak-Novakovic G, Scadden DT. 2011. Biomimetic platforms for human stem cell research. Cell Stem Cell 8(3):252-261.
Walter V, Yin X, Wilkerson MD, Cabanski CR, Zhao N, Du Y, Ang MK, Hayward MC, Salazar AH, Hoadley KA, Fritchie K, Sailey CJ, Weissler MC, Shockley WW, Zanation AM, Hackman T, Thorne LB, Funkhouser WD, Muldrew KL, Olshan AF, Randell SH, Wright FA, Shores CG, Hayes DN. 2013. Molecular subtypes in head and neck cancer exhibit distinct patterns of chromosomal gain and loss of canonical cancer genes. PLoS One 8(2):e56823.
Wan G, Zhou L, Xie M, Chen H, Tian J. 2010. Characterization of side population cells from laryngeal cancer cell lines. Head Neck 32(10):1302-1309.
Wang H, Ouyang Y, Somers WG, Chia W, Lu B. 2007. Polo inhibits progenitor self-renewal and regulates Numb asymmetry by phosphorylating Pon. Nature 449(7158):96-100.
Wang J, Sakariassen PO, Tsinkalovsky O, Immervoll H, Boe SO, Svendsen A, Prestegarden L, Rosland G, Thorsen F, Stuhr L, Molven A, Bjerkvig R, Enger PO. 2008. CD133 negative glioma cells form tumors in nude rats and give rise to CD133 positive cells. Int J Cancer 122(4):761-768.
Wang P, Gao Q, Suo Z, Munthe E, Solberg S, Ma L, Wang M, Westerdaal NA, Kvalheim G, Gaudernack G. 2013. Identification and characterization of cells with cancer stem cell properties in human primary lung cancer cell lines. PLoS One 8(3):e57020.
Wang Y, Zhe H, Ding Z, Gao P, Zhang N, Li G. 2012. Cancer stem cell marker Bmi-1 expression is associated with basal-like phenotype and poor survival in breast cancer. World J Surg 36(5):1189-1194.
Warmerdam DO, Kanaar R. 2010. Dealing with DNA damage: relationships between checkpoint and repair pathways. Mutat Res 704(1-3):2-11.

Warrier S, Bhuvanalakshmi G, Arfuso F, Rajan G, Millward M, Dharmarajan A. 2014. Cancer stem-like cells from head and neck cancers are chemosensitized by the Wnt antagonist, sFRP4, by inducing apoptosis, decreasing stemness, drug resistance and epithelial to mesenchymal transition. Cancer Gene Ther 21(9):381-388.

Wei X, Wang J, He J, Ma B, Chen J. 2014. Biological characteristics of CD133(+) cancer stem cells derived from human laryngeal carcinoma cell line. Int J Clin Exp Med 7(9):2453-2462.

Wei XD, Zhou L, Cheng L, Tian J, Jiang JJ, Maccallum J. 2009. In vivo investigation of CD133 as a putative marker of cancer stem cells in Hep-2 cell line. Head Neck 31(1):94-101.

White JS, Weissfeld JL, Ragin CC, Rossie KM, Martin CL, Shuster M, Ishwad CS, Law JC, Myers EN, Johnson JT, Gollin SM. 2007. The influence of clinical and demographic risk factors on the establishment of head and neck squamous cell carcinoma cell lines. Oral Oncol 43(7):701-712.

Wilkerson PM, Reis-Filho JS. 2013. The 11q13-q14 amplicon: clinicopathological correlations and potential drivers. Genes Chromosomes Cancer 52(4):333-355.

Wilson GD, Marples B, Galoforo S, Geddes TJ, Thibodeau BJ, Grenman R, Akervall J. 2013. Isolation and genomic characterization of stem cells in head and neck cancer. Head Neck 35(11):1573-1582.

Woolard K, Fine HA. 2009. Glioma stem cells: better flat than round. Cell Stem Cell 4(6):466-467.

Wu Y, Cain-Hom C, Choy L, Hagenbeek TJ, de Leon GP, Chen Y, Finkle D, Venook R, Wu X, Ridgway J, Schahin-Reed D, Dow GJ, Shelton A, Stawicki S, Watts RJ, Zhang J, Choy R, Howard P, Kadyk L, Yan M, Zha J, Callahan CA, Hymowitz SG, Siebel CW. 2010. Therapeutic antibody targeting of individual Notch receptors. Nature 464(7291):1052-1057.

Xiao W, Graham PH, Power CA, Hao J, Kearsley JH, Li Y. 2012. CD44 is a biomarker associated with human prostate cancer radiation sensitivity. Clin Exp Metastasis 29(1):1-9.

Yan M, Yang X, Wang L, Clark D, Zuo H, Ye D, Chen W, Zhang P. 2013. Plasma membrane proteomics of tumor spheres identify CD166 as a novel marker for cancer stem-like cells in head and neck squamous cell carcinoma. Mol Cell Proteomics 12(11):3271-3284.

Yin S, Li J, Hu C, Chen X, Yao M, Yan M, Jiang G, Ge C, Xie H, Wan D, Yang S, Zheng S, Gu J. 2007. CD133 positive hepatocellular carcinoma cells possess high capacity for tumorigenicity. Int J Cancer 120(7):1444-1450.

Yu CC, Hu FW, Ph DC, Chou MY. 2014. Targeting CD133 in the enhancement of chemosensitivity in oral squamous cell carcinomas-derived side population cancer stem cells. Head Neck [PMID:25545959].

Yu J, Vodyanik MA, Smuga-Otto K, Antosiewicz-Bourget J, Frane JL, Tian S, Nie J, Jonsdottir GA, Ruotti V, Stewart R, Slukvin, II, Thomson JA. 2007. Induced pluripotent stem cell lines derived from human somatic cells. Science 318(5858):1917-1920.

Yu S, Zhang R, Liu F, Wang H, Wu J, Wang Y. 2012. Notch inhibition suppresses nasopharyngeal carcinoma by depleting cancer stem-like side population cells. Oncol Rep 28(2):561-566.

Zhang Q, Shi S, Yen Y, Brown J, Ta JQ, Le AD. 2010. A subpopulation of CD133(+) cancer stem-like cells characterized in human oral squamous cell carcinoma confer resistance to chemotherapy. Cancer Lett 289(2):151-160.

Zhao R, Quaroni L, Casson AG. 2012. Identification and characterization of stemlike cells in human esophageal adenocarcinoma and normal epithelial cell lines. J Thorac Cardiovasc Surg 144(5):1192-1199.

Zheng S, Franzmann EJ. 2013. Comments on 'CD44-negative cells in head and neck squamous carcinoma also have stem-cell like traits', Se-Yeong Oh et al., European Journal of Cancer, published online 6 July 2012. Eur J Cancer 49(15):3380-3381.

Zhou C, Sun B. 2014. The prognostic role of the cancer stem cell marker aldehyde dehydrogenase 1 in head and neck squamous cell carcinomas: A meta-analysis. Oral Oncol 50(12):1144-1148.